Green Chemistry

CRITICAL REVIEW

View Article Online
View Journal

Cite this: DOI: 10.1039/d6gc00426a

Deep eutectic solvents in lignocellulosic biorefineries: a comprehensive review of mechanistic insights, molecular modeling, and artificial intelligence

Kaixuan Huang,*†[a,b] Mood Mohan,*†[c] Kaiyue Su,[a] Chang Gao,[a] Yufeng Chen,[a] Xiaoran Xu,[a] Yanping Cai,[a] Jianming Guo,[b,d] Yong Xu,[b,d] Xin Zhou[b,d] and Jeremy C. Smith[c,e]

Deep eutectic solvents (DESs) have gained significant attention as solvents and catalysts in a wide range of research applications owing to their attractive properties, ease of preparation, low cost, and environmental friendliness. In recent years, the application of DESs in lignocellulosic biomass pretreatment has been growing rapidly, driven by the ability to tailor DES compositions to meet the specific processing needs of different biomass components. Despite the recent progress, biomass pretreatment using DESs still lacks a comprehensive understanding of the intermolecular interactions and designing principles. Here we review emerging strategies that combine experimental approaches, computational chemistry, and machine learning (ML) techniques to develop DESs with improved pretreatment efficiency. We summarize studies that investigate the effects of DES pretreatment on lignocellulosic biomass and what is known about the underlying mechanisms. The role of quantum chemical calculations and molecular dynamics simulations in revealing molecular-level interactions and plausible depolymerization mechanism is discussed. The implementation, challenges and limitations of ML are discussed in DES-based biomass pretreatment together with DES recovery methods aimed at reducing pretreatment costs on the economic feasibility and life-cycle environmental impacts of DES-based processes. Finally, we outline future research directions for advancing DES applications in lignocellulosic biomass pretreatment.

Received 21st January 2026,
Accepted 14th May 2026

DOI: 10.1039/d6gc00426a

rsc.li/greenchem

Green foundation

1. The article discusses the development of deep eutectic solvents (DESs) as sustainable, biodegradable, and low-toxicity alternatives to traditional solvents. Key advances include ternary DES formulations that enhance lignin removal and cellulose retention, and the integration of machine learning (ML) and computational chemistry to transition from trial-and-error to precise, data-driven solvent design.
2. This research is of wider interest due to its role in advancing circular bioeconomy. By enabling efficient fractionation of lignocellulosic biomass-the most abundant renewable resource-it facilitates the production of biofuels, biochemicals, and high-value materials while reducing reliance on petrochemicals.
3. Future research will focus on scaling up DES recovery and using ML to optimize pretreatment protocols. This review helps shape green chemistry by providing a systematic theoretical framework for understanding solvent–biomass interactions, guiding the industry toward scalable, eco-conscious biorefinery practices.

[a]College of Marine and Bio-engineering, Yancheng Teachers University, Yancheng, Jiangsu 224007, China. E-mail: huangkx@yctu.edu.cn
[b]International Innovation Center for Forest Chemicals and Materials, Nanjing Forestry University, Nanjing 210037, China
[c]Biosciences Division and Center for Molecular Biophysics, Oak Ridge National Laboratory, Oak Ridge, Tennessee 37831, USA. E-mail: moodm@ornl.gov
[d]State Key Laboratory for Development and Utilization of Forest Food Resources, Nanjing Forestry University, Nanjing 210037, China
[e]Department of Biochemistry and Cellular and Molecular Biology, University of Tennessee, Knoxville, Tennessee 37996, USA
†K. Huang and M. Mohan contributed equally to the manuscript.

1. Introduction

In recent years, deep eutectic solvents (DESs) have been widely recognized as a novel class of sustainable and environmentally friendly solvents. A DES consists of a hydrogen bond donor (HBD) and a hydrogen bond acceptor (HBA) and these can be mixed at a specific molar ratio.[1] Fig. 1 shows typical chemical structures of HBAs and HBDs. The eutectic temperature (or melting point, T_m) of DESs is significantly lower than the melting points of their individual components. DESs consist

of large, asymmetric ions that exhibit low lattice energy,[2] and also form strong hydrogen bonding networks between HBA and HBD resulting in the low melting points.[3] The result is a highly disordered network with increased configurational entropy and structural disorder, hindering efficient packing and stabilizing the liquid relative to the solid. DESs exhibit several attractive properties such as non-volatility, low toxicity, good chemical and thermal stability, bio-degradability, ease of preparation, and high selectivity.[4] In 2003, Abbott *et al.*[5] conducted a pioneering study in which they prepared various DESs by combining quaternary ammonium salts with several HBDs at specific molar ratios and measured the melting temperatures (T_m) of the resulting mixtures. They observed that the lowest T_m of 12 °C, was obtained when choline chloride ([Ch]Cl) (T_m = 302 °C) was mixed with urea (T_m = 133 °C) at 1 : 2 molar ratio. This initial work laid the foundation for the development of a broad range of liquids formed from eutectic mixtures of salts and HBDs. The term DES specifically refers to liquids prepared near the eutectic composition, *i.e.*, at the molar ratio of components that yields the lowest melting point. DESs hold significant promise in a wide variety of research and industrial applications, such as CO_2 capture, biomass processing, rechargeable batteries, nanotechnology, separation processes, electrochemistry, catalysts, *etc.*[2,6] Over the years, DESs have been explored as potential solvents for deconstructing lignocellulosic biomass and selectively cleaving unstable ether bonds between lignin phenyl propane units, resulting in the depolymerization of lignin and its separation from biomass.[7–15]

Lignocellulosic biomass which is composed of cellulose, hemicellulose, and lignin, represents the most abundant renewable resource on Earth[16] and is of particular interest as an alternative to petrochemical resources, providing a critical raw material for green and sustainable development of global industry. Fig. 2 and 3 show chemical structures of cellulose, hemicellulose, and lignin and their potential application in various industries. In bioenergy production from cellulose, lignocellulosic biomass is recalcitrant to deconstruction and the accessibility of cellulose to cellulase enzymes during enzymatic hydrolysis is limited.[17–20] The presence of lignin interferes with the effective adsorption of cellulases, reducing the hydrolysis rate and thereby constraining the development and utilization of lignocellulosic biomass. Therefore, the efficient deconstruction of lignocellulose is a prerequisite for achieving the high-value utilization of these polysaccharides as well as the lignin. Research on the separation and extraction of lignocellulosic materials generally focuses on two main categories: herbaceous plants and woody plants, reflecting distinct properties of each group.[21–28] Herbaceous plants are characterized by rapid growth cycles (annual or perennial) and high biomass

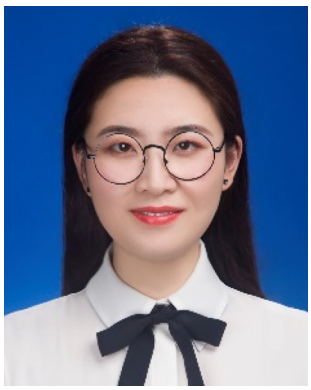

Kaixuan Huang

Dr Kaixuan Huang is a lecturer at the College of Marine and Bioengineering, Yancheng Teachers University. Dr Huang received her PhD in Chemical Processing Engineering of Forest Products in Nanjing Forestry University, China. During her PhD, she also completed a joint doctoral training program at the Joint BioEnergy Institute (JBEI), which is led by Lawrence Berkeley National Laboratory, USA. Her research primarily involves the high-value utilization of agricultural and forestry biomass, with a focus on the structural interpretation of lignocellulose and the mechanisms of components (hemicellulose, cellulose and lignin) separation. She is also active in the production of prebiotics (e.g. xylo-oligosaccharides), platform chemicals and bio-based materials.

Mood Mohan

Dr Mohan Mood is an Associate R&D Staff Scientist in the Biosciences Division at Oak Ridge National Laboratory. His research focuses on integrating computational chemistry (molecular dynamics simulations, quantum chemical calculations, and COSMO-RS thermodynamic modeling), artificial intelligence, and high-performance computing for the discovery and design of sustainable materials, solvents, and chemical processes. Prior to joining ORNL, he was a Postdoctoral Research Associate at Sandia National Laboratories, Livermore, USA. He received his Ph.D. in Chemical Engineering from Indian Institute of Technology Guwahati from India. His primary research interests include the design and discovery of green and designer solvents, including ionic liquids, deep eutectic solvents, and bio-derived solvents, for applications in lignocellulosic biomass processing, plastic upcycling, carbon capture, and sustainable chemical manufacturing. Dr Mood has published over 49 peer-reviewed articles, received more than 2000 citations with the h-index of 30, and has contributed to several patent applications.

productivity. Agricultural residues from herbaceous plants, such as wheat straw and rice husks are produced in massive quantities globally, offering low-cost and underutilized feedstock. Woody plants (*e.g.*, trees, shrubs, and bamboo) are widely distributed across forests, plantations, and agroforestry systems. Fast-growing species such as poplar, willow, eucalyptus can be sustainably harvested within 5–15 years, ensuring a steady supply of timber, fiber, and biomass. Both herbaceous and woody plants are among the most abundant and renewable biological resources on Earth, providing a sustainable alternative to finite fossil fuels and mineral resources. In general, the cellulose content of lignocellulosic biomass ranges from 35% to 50%, hemicellulose from 25% to 50%, and lignin from 10% to 30%.[29–33] However, the composition varies significantly depending on the biomass type, age, and soil conditions. Table 1 summarizes the composition of several common feedstocks.

Pretreatment of biomass is applied to ease solubilization and fractionation and significantly modifies the 3D structures involved, making the cellulose more accessible to subsequent enzymatic hydrolysis.[34] A comparison of various pretreatment methods is presented in Table 2 along with their energy consumption, solvent recovery rate, and total sugar yields. Herbaceous biomass typically contains relatively low lignin content and higher proportions of cellulose and hemicellulose; its degradation characteristics align with the principle of "cellulose priority" or "hemicellulose priority".[34] As a result, previous studies on lignocellulose conversion using DESs have primarily focused on herbaceous plants.[35–37] However, the potential applications of lignin have gained increasing attention, leading to a growing interest in its value-added utilization in recent years.[38,39] Consequently, achieving efficient separation of lignocellulose while preserving lignin in a relatively intact and ordered form for later valorization has become a key scientific focus.[40–42] Compared to herbaceous plants, woody plants offer a higher lignin content, making them a promising target for lignin valorization. Woody biomass can be further classified into hardwoods (broadleaf species) and softwoods (conifers), with lignin contents typically ranging from 18% to 25% in hardwoods and 27% to 33% in softwoods.[43,44] The same intermolecular features of DESs that depress their eutectic points make them also effective for biomass pretreatment. The strong, dynamic and flexible hydrogen-bonding networks preventing crystallization can also form hydrogen bonds with the heterogeneous polymer matrix of lignocellulose biomass components and DESs can solvate lignin through aromatic, ionic, and hydrogen-bonding interactions. The result is disrupted biomass and solubilized biomass components.

As shown in Fig. 4, research on lignocellulosic biomass deconstruction using DESs has steadily increased over the years. Compared to traditional lignin separation processes, DESs offer several advantages, including low cost, high efficiency, and renewability.[7,45] However, despite this rapid progress, there are still critical gaps, and in-depth studies on DES applications in biomass processing remain limited. Recent reviews by Zhou *et al.*,[12] Zhang *et al.*,[45] Loow *et al.*,[46] Xu *et al.*,[47] have summarized the pretreatment of lignocellulosic biomass and lignin solubility in DESs. These reviews highlight the fact that mechanistic understanding of how specific DES–biomass interactions influence pretreatment efficiency and selectivity is limited, and that lack of quantitative performance comparisons across various DES formulations. In addition, the integration of computational tools and predictive models to design DES remains underdeveloped, providing significant opportunities for systematic, data-driven optimization strategies. In this context, the most significant contribution of this review is the transition from "fragmented research summaries" to "systematic theoretical construction", addressing specific critical research gaps by the following:

Kaiyue Su

Kaiyue Su is an undergraduate at the College of Marine and Bioengineering, Yancheng Teachers University. He is a research member of the Laboratory for Green Catalytic Conversion of Biomass. His research focuses on the valorization of lignocellulosic biomass and natural product fermentation. He is experienced in data analysis, manuscript writing and patent drafting. He is proficient in lignocellulose pretreatment, enzymatic hydrolysis, natural product purification and material characterization, with solid expertise in eco-friendly biomass valorization and catalytic transformation.

Chang Gao

Chang Gao graduated with a bachelor's degree from the College of Marine and Biological Engineering of Yancheng Teachers University and is now a junior high school biology teacher. Her research activities mainly involve using environmentally friendly methods to decompose and utilize natural biomass. Her current research involves separating lignin from biomass using deep eutectic solvents aiming to improve the efficiency of biomass industrial production and reduce resource waste.

(1) establishing a quantitative understanding of DES–biomass interactions, rather than merely offering descriptive summaries.

(2) providing a standardized comparison framework for the performance of different DES formulations, resolving the issue of data fragmentation.

(3) comprehending a computationally and AI/ML-driven DES design methodology, advancing DES development from the "trial-and-error phase" into the "era of precise design".

This systematic study not only deepens the understanding of the mechanisms underlying DES-based pretreatment but also provides practical technical guidance for the biomass refining industry. Further, methods for DES recovery, as well as techno-economic and life-cycle analysis are also discussed. This review not only advances the scientific understanding of DES–biomass interactions but also paves the way for scalable, eco-conscious biorefinery practices, aligning with the broader principles of green chemistry and circular bioeconomy development.

2. Composition of DES systems

DESs are categorized into different types based on their dissociation constant (pK_a), the number of components (binary or ternary), and the specific combinations of HBAs and HBDs.[48]

2.1 Dissociation constant (pK_a)

Based on the pK_a, DESs were classified into three categories: acidic, alkaline, and neutral.[12] For example, DESs composed of organic acids and salts (*e.g.*, [Ch]Cl) are classified as acidic and the DESs formed from amines or amides and salts are considered as alkaline; while alcohol-based systems with [Ch]Cl are regarded as neutral.[12] DESs are particularly useful in biomass delignification.[12] However, under similar experimental conditions, the efficiency of lignin separation varies greatly depending on the type and nature of the DES used.[49,50] Generally, acidic DESs have demonstrated superior performance in removing both lignin and hemicellulose compared to their alkaline and neutral counterparts.[51,52] The performance of acidic-based DESs in biomass pretreatment can be attributed to their ability to synergistically cleave lignin–carbohydrate complexes (LCC) linkages and solubilize lignin.[12,53] Acidic DESs promote protonation of ether bonds, particularly the labile β-O-4 linkages in lignin, facilitating their cleavage under relatively mild conditions.[54,55] Moreover, the acidic environment enhances hydrogen bonding interactions between DES components and the hydroxyl groups of polysaccharides, further weakening intermolecular networks within the biomass.[56] The combined effect of selective bond cleavage and effective solvation of lignin fragments lead to enhanced delignification and hemicellulose removal. In contrast, neutral or alkaline DESs predominantly act through physical swelling and hydrogen-bond disruption, with comparatively limited capacity for covalent bond cleavage.[57,58]

2.2 Number of components

DES can be further classified according to the number of components present in the system. Initially, DESs were prepared as binary mixtures of an HBA and an HBD component. Among these, a system comprising [Ch]Cl (HBA) and lactic acid (HBD) is one of the most commonly used in poplar pretreatment.[59] and indeed this mixture has been shown to be effective in a wide range of applications.[51,60,61]

As the development of DESs continues to advance, several studies have demonstrated that incorporating additional components into binary DES systems may substantially enhance biomass pretreatment efficacy.[62,63] This has motivated the exploration of more complex solvent formulations, particularly ternary deep eutectic solvents (TDESs). TDESs represent a versatile class of solvents typically composed of one or more HBAs and HBDs. The addition of a third component provides


Yufeng Chen

Yufeng Chen is an undergraduate majoring in Biological Science (Teacher Education) at the College of Marine and Bioengineering, Yancheng Teachers University. He is a research member of the Laboratory for Green Catalytic Conversion of Biomass. His main research focuses on lignocellulosic biomass pretreatment and biomass catalytic conversion. Since June 2023, he has been actively doing research in the laboratory for green catalytic conversion of biomass, where he has conducted experiments on organic acid pretreatment of lignocellulose and biomass catalytic conversion.


Xiaoran Xu

Xiaoran Xu is an undergraduate at the College of Marine and Bioengineering, Yancheng Teachers University. She is a research member of the Laboratory for Green Catalytic Conversion of Biomass. Her research focuses on the reuse of lignocellulosic wastes, specifically the design of novel systems using organic acids and biochemical catalysis. This work addresses the growing demand for eco-friendly, cost-effective materials.

greater flexibility in solvent design, enabling fine-tuning of key physicochemical properties such as polarity, acidity, and viscosity to meet specific application demands.[64] Compared to binary DESs, TDESs exhibits unique physicochemical properties, including lower viscosities, lower melting points, higher thermal stabilities, and enhanced solvation capabilities. These characteristics facilitate better mass transfer and reaction kinetics, making TDESs particularly attractive for biomass pretreatment applications.[64] For example, Xia *et al.* introduced $AlCl_3{\cdot}6H_2O$ into a binary DES system with [Ch]Cl as an HBA and glycerol as an HBD, and this increased lignin fractionation efficiency from 3.61% to 95.46%.[65] Similarly, Han *et al.* employed a TDES composed of maleic acid (MA), [Ch]Cl, and ethylene glycol (EG) for poplar wood pretreatment, achieving cellulose retention and lignin removal rates of 94% and 98%, respectively.[66] This approach reduced lignin condensation, a common side reaction during acidic biomass pretreatment, primarily caused by the formation of benzylic carbocations that undergo electrophilic substitution with aromatic rings in lignin, resulting in properties comparable to groundwood pulp, and the DES exhibited good recyclability.[66] Panyamao *et al.* employed a ternary DES consisting of [Ch]Cl, oxalic acid, and water at a molar ratio of 2 : 2 : 1, combined with a two-step alkaline hydrogen peroxide (AHP) process, to pretreat coffee parchment under microwave heating at 130 °C for 15 minutes. The removal rates of hemicellulose and lignin achieved were 99.6% and 97.7%, respectively, while the retained cellulose content was 86.1%, with a highly crystalline structure and excellent thermal stability of cellulose.[67] It has thus been reported that several ternary DESs have improved solubility for lignin while also offering other advantages, such as a higher cellulose retention rate and good recycling performance.[63,68]

2.3 HBA and HBD combinations

Besides the two basic classification methods described above, DESs are classified into five types based on the nature of the HBA and HBD combinations used. Table 3 presents these DESs types along with the general formulae for HBAs and HBDs. Type I DESs, formed from metal salts ($zMCl_x$) and quaternary ammonium salts ($Cat^+ X^-$), are analogous to the well-studied metal halide/imidazolium salt systems. The range of non-hydrated metal halides which have a low melting point so as to form type I DESs is limited. However, the scope can be expanded by using hydrated metal halides and [Ch]Cl, resulting in type II DESs. Type III DESs, consisting of quaternary halides (HBAs) and nonionic HBDs, have attracted significant interest due to their ability to solvate a broad range of species, including transition metal complexes[5,69] as well as lignocellulosic biomass,[70] and are also promising for carbon capture applications.[71]

Most ionic liquids (ILs) are indeed liquid at room temperature and are composed of organic cations paired with organic/inorganic anions.[72,73] Inorganic cations, on the other hand, generally do not form low-melting-point solvents because of their high charge density. However, it has been demonstrated that certain inorganic salts can form eutectic mixtures with melting points below 150 °C when combined with HBDs such as urea.[74] Abbott *et al.*[75] showed that different metal salts can be turned into room temperature eutectics, which are thus classified as type IV DESs. For example, $ZnCl_2$ has been found to form eutectic mixtures with urea, acetamide, ethylene glycol, and 1,6-hexanediol. Finally, more recently type V DESs have also been explored, and these are composed of non-ionic compounds (Table 3).[76] For instance, DL-menthol and thymol form a eutectic solvent at room temperature in a 1 : 2 molar ratio. Notably, type V DESs typically exhibit lower viscosities than other types of DESs, making them attractive for various applications.[76,77]

DESs are widely promoted as green and sustainable alternatives to conventional organic solvents and ILs, this classification requires critical re-examination, particularly for metal-containing Type I, Type II, and Type IV DESs. As shown in Table 3 and Fig. 1, several DES formulations incorporate heavy

Yanping Cai

Yanping Cai is an undergraduate at the College of Marine and Bioengineering, Yancheng Teachers University. She is a research member of the Laboratory for Green Catalytic Conversion of Biomass. Her research focuses on the pretreatment of lignocellulosic biomass and its catalytic conversion into high-value bio-based products. She is experienced in experimental operations and data analysis. Her technical skills include lignocellulose pretreatment, enzymatic hydrolysis and natural product extraction.

Jianming Guo

Jianming Guo is a PhD candidate at the College of Chemical Engineering, Nanjing Forestry University, China. Her current main research activities focus on the biorefining of lignocellulosic feedstocks. Her research primarily involves the degradation of lignin using acidic hydrogen peroxide, the production of functional xylo-oligosaccharides, and the investigation of mechanisms to enhance enzymatic cellulose saccharification.

metal chlorides, such as $ZnCl_3$, $CuCl_2$, $CrCl_3$, and $FeCl_3$, as HBAs or key components.[78] Type I and II DESs containing $ZnCl_2$, $CuCl_2$, or $CrCl_3$ exhibit superior delignification efficiency due to their strong Lewis acidity and coordination with lignin hydroxyl groups, they present significant environmental hazards.[78] Taking $ZnCl_2$ as a specific example, Juneidi *et al.* systematically evaluated cholinium-based DESs and reported that [Ch]Cl : $ZnCl_2$ exhibited the largest inhibition zone diameters against fungal growth (*Aspergillus niger*, *Phanerochaete chrysosporium*) among all tested formulations, with toxicity levels significantly exceeding those of Type III DESs.[79] In addition, the LC_{50} values on *Cyprinus carpio* ranged from practically harmless ([Ch]Cl : EG) to highly toxic (ethanolamine chloride : $ZnCl_2$), directly correlating with the presence of leachable metal ions.[80]

DES classification is not only structural but also closely related to their environmental impact and functional performance. Importantly, this classification based on HBA–HBD combinations is not merely structural but also fundamentally governs the physicochemical behavior of DES systems. Variations in the chemical structures of HBAs and HBDs across different DES types lead to different intermolecular interaction networks, including hydrogen bonding, electrostatic and vdW interactions, and steric effects. These interactions directly influence key physicochemical properties such as viscosity, polarity, conductivity, and melting point. Consequently, understanding DES classification provides a critical foundation for rationalizing how different DES systems exhibit varying performance in lignocellulosic biomass pretreatment.

3. DES properties

The physicochemical properties of DESs discussed in this section are intrinsically linked to their classification and composition, as outlined in section 2.3. A key advantage of DES over conventional solvents is their chemical diversity, allowing for the selection and tuning of HBAs, HBDs, and molar ratios to achieve desired properties and phase behavior.[81] Further, the type of DES and the nature of HBA–HBD combinations dictate the strength and organization of intermolecular interactions within the solvent system. These interactions govern macroscopic properties such as viscosity, polarity, density, and conductivity, which play a decisive role in biomass fractionation processes.[82,83] Therefore, establishing a clear structure–property relationship is essential for understanding and predicting the performance of different DES types in lignocellulosic biomass pretreatment. This section explores six key properties of DESs: conductivity, density, melting point, polarity, surface tension, and viscosity, and establishes their structure–property relationships (see Table 4).[47,84–87]

3.1 Conductivity

Conductivity describes how well electric charge is carried by ions moves through the liquid. The conductivity of DESs has

Xin Zhou

Dr Xin Zhou is an Associate Professor at the College of Chemical Engineering, Nanjing Forestry University, China. His main research activities are related to the resource utilization of plant fibers, with particular emphasis on the utilization and functionalization of cellulose and hemicellulose-based polysaccharide fractions, as well as the biocatalytic conversion of carbohydrates. And he mainly focuses on the production of bio-based materials, xylo-oligosaccharides, xylonic acid and gluconic acid.

Jeremy C. Smith

Prof. Jeremy C. Smith specializes in computational molecular biophysics, with an emphasis on the simulation of biological molecules. A native of England, after postdoctoral work with Martin Karplus at Harvard in 1989 he set up a group in biomolecular simulation at the French Atomic Energy Commission in Saclay. In 1998 he moved to the University of Heidelberg, Germany, where he held a Chair in Computational Biology. In 2006, he became the first Governor's Chair at the University of Tennessee in a joint position with Oak Ridge National Laboratory where he is director of the Center for Molecular Biophysics. He researches in a wide range of topics, including theoretical and computational methods for studying biomacromolecules, bioenergy, drug discovery, vaccine design, neutron scattering, supercomputing, AI, bioenergy and biomaterials. He has published >500 articles, has been cited >80 000 times and has supervised >140 graduate students and postdoctoral fellows. He is a Fellow of the Royal Society of Chemistry and Associate Editor of Biophysical Journal.

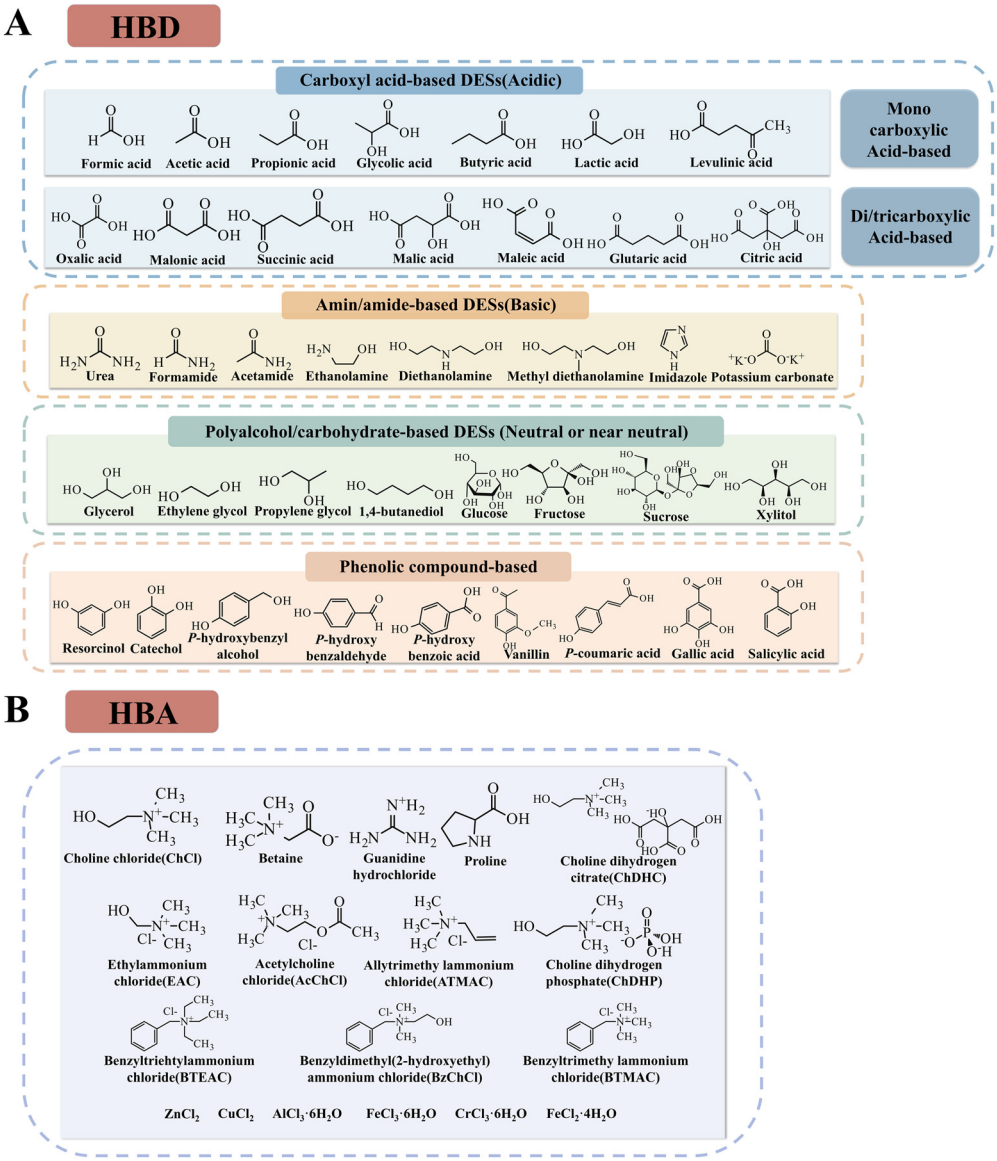

Fig. 1 Chemical structures of (A) hydrogen bond donors (HBDs) and (B) hydrogen bond acceptors (HBAs) in deep eutectic solvents. Redrawn based on a figure from ref. 12.

attracted significant research interest, especially for power applications such as in advanced electrolytes in redox-flow batteries. DESs typically show lower conductivity than molten salts and ionic liquids.[88–90] For instance, the conductivity of [Ch]Cl–urea is 0.199 mS cm^{-1} at 20 °C,[91] while the molten salt $BiCl_3$ shows a conductivity of 350 mS cm^{-1} at 200 °C and 1-ethyl-3-methylimidazolium tetrafluoroborate has a conductivity of 13.05 mS cm^{-1} at 20 °C.[89,90,92] The significant difference in conductivity can be attributed due to the molecular size, shape, and viscosity, which are related to hole theory – ion mobility depending on the number, size and dynamics of free holes.[93] Glycol-type DESs exhibit higher electrical conductivity than acid-type DESs.[94,95]

DES conductivity is governed by multiple factors. Higher ionic mobility results in better charge transport.[91] Conductivity is inversely proportional to viscosity, as higher viscosity slows down ion movement.[94] Temperature also has a strong effect: as temperature increases, the conductivity increases due to lower viscosity. Molecular size plays a critical role, as smaller molecular size species typically exhibit higher ionic mobility, resulting in higher electrical conductivity. The conductivity of DESs also strongly depends on the choice of HBA and HBD, as well as their molar ratios. DESs prepared with polar HBDs (*e.g.*, organic acids, amines, alcohols, *etc.*) show higher conductivity than those with less polar components.[96,97] For example, when using the same HBA [Ch]Cl at a 1 : 2 molar ratio with different HBDs, the conductivity of [Ch]Cl–ethylene glycol at 20 °C is 7.61 mS cm^{-1}, while that of [Ch]Cl–glycerol at 20 °C is 1.05 mS cm^{-1}. This difference is due to the higher viscosity and larger molecular size of [Ch]Cl–

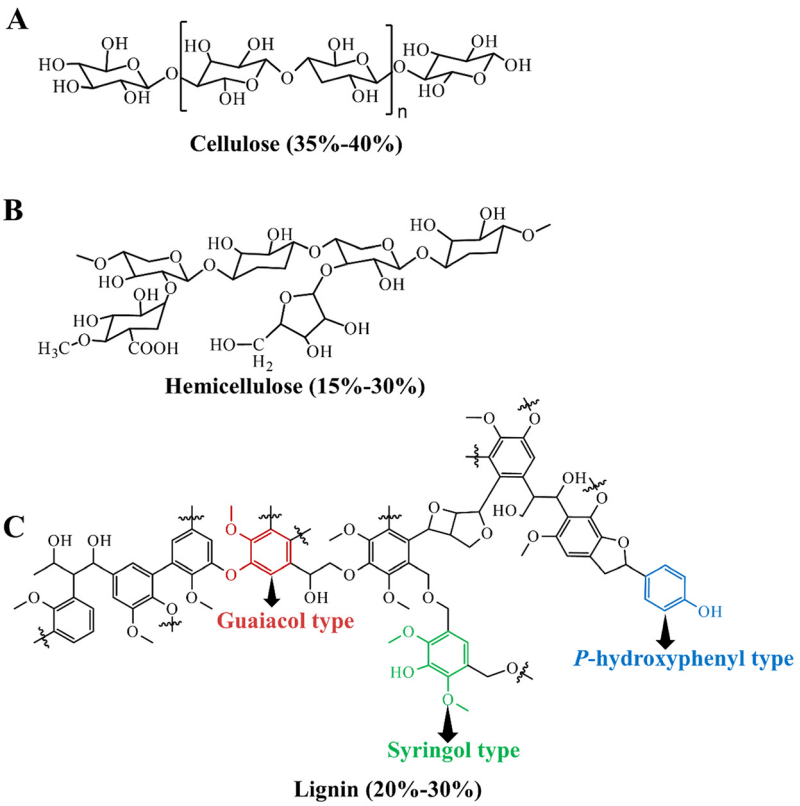

Fig. 2 Chemical structures of lignocellulosic biomass components: (A) cellulose (B) hemicellulose and (C) lignin.

glycerol compared to [Ch]Cl–ethylene glycol. Similarly, the conductivities of acetylcholine chloride–urea (1 : 2) and triethylammonium chloride–urea (1 : 1.5) at 40 °C are 0.017 mS cm^{-1} and 0.348 mS cm^{-1}, respectively.[98]

Theoretical predictions suggest that high conductivity facilitates the breakdown of LCCs by accelerating charge transfer.[12] This process is crucial for biomass pretreatment since the disintegration of the recalcitrant LCC matrix is a key determinant for achieving good fractionation and solubilization as well as high enzymatic saccharification yields of the carbohydrate fractions.[99] Conductivity serves as a critical parameter in DES-mediated biomass pretreatment. Through rational selection of HBA/HBD pairs and optimization of their molar ratios, ionic mobility can be precisely modulated. This enables the DES solvent to efficiently disrupt lignin–carbohydrate complexes, accelerate mass transfer processes, and consequently enhance enzymatic saccharification efficiency.[99,100] The above demonstrates that conductivity can be tuned by adjusting the HBA, HBD, and their molar ratios. In ternary natural DESs, conductivity shows a non-monotonic trend with increasing water content: it first increases at low water concentration and then decreases at higher water concentration, a behavior consistent with Gaussian theory.[100,101] Gaussian theory describes how a property can reach a maximum at an optimal composition where viscosity is sufficiently reduced to facilitate ion motion, but the ionic network is not yet disrupted. The temperature dependence of DES conductivity is described by the Arrhenius equation; however, the Vogel–Fulcher–Tammann (VFT) equation usually provides a better fit, indicating that ion transport follows the cooperative, glass-like dynamics characteristic of supercooled liquids rather than a simple single-barrier process.[102]

3.2 Density

Density is an important property of a chemical compound that can provide insight into intermolecular interactions in a DES and significantly influence separation performance. DESs generally have higher densities than that of water; for example, [Ch]Cl–ethylene glycol (1 : 2 molar ratio) has a density of 1.14 g cm^{-3} and [Ch]Cl–glycerol (1 : 2 molar ratio) has a density of 1.19 g cm^{-3} at 20 °C.[103] The HBD strongly affects the density differences observed among various DES formulations. For instance, HBDs with increased hydroxyl densities such as glycerol, ethylene glycol, and acids show higher mass densities due to stronger intermolecular interactions.[104–107] In contrast, aromatic moieties (*e.g.*, phenol) introduce steric effects that reduce density due to the weaker arrangement of molecular unit cell packing.[95,108,109] In diacid-based DESs, the density decreases as the carbon chain length increases, following the trend: oxalic acid > malonic acid > glutaric acid.[96,110,111] Furthermore, experimental data at 20–60 °C show different density ranges depending on the halide: 1.1215–1.4971 g cm^{-3} for mixtures of ethylene glycol (EG) with NaCl (16 : 1), NaBr (6 : 1), and NaI (4 : 1), reflecting the combined effects of ionic

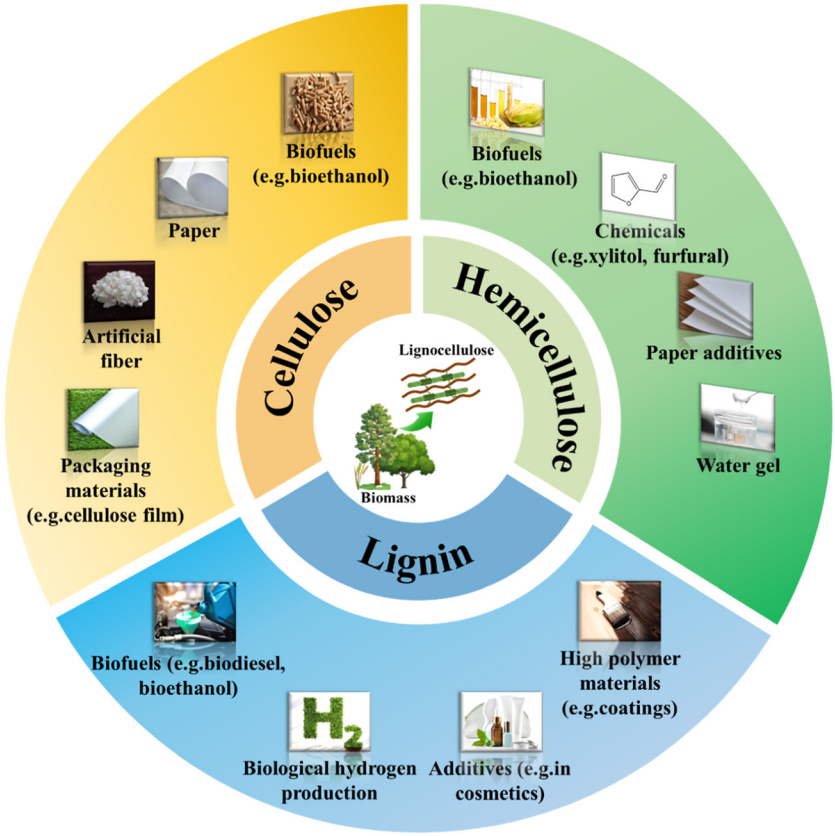

Fig. 3 Industrial applications of lignocellulosic biomass derived components cellulose, hemicellulose, and lignin.

nature and stoichiometry.[112] High-density systems (*e.g.*, [Ch]Cl/glycerol) have been shown to enhance hemicellulose solubility by increasing permeability.[46,113]

The molar ratio of HBA to HBD also plays a significant role in determining the density of eutectic mixtures. Studies have shown that increasing the concentration of the salt (HBA) generally decreases the density of DESs, whereas increasing the HBD fraction leads to higher density.[114] At the molecular level, adding more HBA alters the balance between ion–ion, ion–HBD, and HBD–HBD interactions and disrupts the extended hydrogen-bonded network formed by the HBD. This leads to less efficient packing and an increase in free volume, which manifests as a lower macroscopic density. In contrast, higher HBD content strengthens the hydrogen-bond network and promotes more compact molecular packing, reducing free volume and thus increasing density. These trends are consistently supported by independent experimental measurements and molecular simulations, which show that increasing the HBA fraction enlarges free volume and reduces density, whereas increasing the HBD fraction enhances hydrogen bonding, compacts the liquid structure, and increases density.[114,115]

Further, either substitution of the HBD or increasing its molar concentrations results in stronger interactions between HBD molecules. As discussed, DESs are classified into five types. Type IV DES containing transition metals show substantially higher densities (1.30–1.63 g cm^{-3}) compared to other DES types.[15,76] This is attributed to differences in molecular packing, which can be explained by the hole theory describing vacancy distributions in molten ionic systems.[2,108,116] As expected, DES density decreases with increasing temperature because of greater molecular motion, expansion of molar volume, and reduced packing efficiency, resulting in thermal expansion.[117]

3.3 Melting point

The eutectic temperature (or melting point, T_m) of DESs is usually much lower than that of their individual components. This arises because mixing an HBA with an HBD generates strong, heterogeneous interactions that disrupt the regular crystal lattices of the pure components. The interactions clearly involve extensive hydrogen bonding but also, in many cases, ionic or charge-delocalized complexes, both of which stabilize the liquid relative to the solid. The result is a highly disordered network with increased configurational entropy and structural disorder, hindering efficient packing.

The same intermolecular features that depress the melting point of DESs also make them potentially effective for biomass pretreatment. The strong and flexible hydrogen-bonding networks, charge delocalization, and molecular complexity that prevent crystallization also enable DESs to interact intimately with the heterogeneous polymer matrix of lignocellulose. They can form hydrogen bonds with cellulose and hemicellulose,

Table 1 The chemical composition of lignocellulosic biomass with different categories

Lignocellulosic biomass	Specific types	Cellulose (%)	Hemicellulose (%)	Lignin (%)	Ref.
Herbaceous	Corncob	37.1	31.7	16.1	176
	Wheat straw	35.6	25.9	19.4	330
	Barley straw	39.2	41.0	18.5	331
	Switchgrass	34.5	23.3	20.4	115
	Sugarcane bagasse	34.5	28.6	23.6	164
	Hybrid *pennisetum*	41.5	29.7	23.8	170
	Corn straw	40.9	19.8	22.3	332
	Rice straw	41.1	21.5	16.6	333
	Moso bamboo	41.1	12.8	31.0	334
	Cenchrus purpureus	34.9	20.2	25.6	16
	Miscanthus	45.9	18.5	24.8	335
	Sisal Fiber	67.0–78.0	10.0–14.2	8.0–11.0	336
	Jute Fiber	67.0–71.5	13.6–20.4	12.0–13.0	336
	Cyperus esculentus L.	47.2	13.0	29.3	337
	Furcraea Foetida fibers	70.7	18.6	9.8	338
	Lemongrass leaves	35.4	19.5	8.3	339
	Kenaf	66.5	19.4	6.8	340
	Boehmeria nivea stalks	34.5	22.5	21.5	341
Hardwood	Poplar	49.9	28.8	19.1	342
	Eucalyptus	46.4	27.9	25.7	220
	Willow	49.0	17.3	19.8	182
	Acacia dealbata	47.4	16.5	22.2	343
	Eucalyptus globulus	46.6	30.2	22.2	344
	Almond	22.3	11.1	20.0	345
	Walnut	26.5	10.6	20.0	345
	Fagus crenata	49.9	29.3	23.0	344
	Paraserianthes falcataria	52.5	21.0	26.5	344
	Birch	35.2	28.0	26.1	346
	Olive tree	38.0	28.0	21.0	347
Softwood	Spruce sawdust	37.7	20.3	27.9	192
	Douglas fir	48.0	16.8	27.7	58
	Radiata pine	44.8	23.7	27.3	193
	Bleached softwood kraft pulp	79.1	15.2	<0.1	348
	Pine	33.0	14.0	27.4	345
	Cryptomeria japonica	47.8	20.3	31.0	344
	Spruce	39.3	30.5	28.1	346
	Oil palm rachis	38.0	21.0	16.0	24
	Picea abies	47.0	23.0	27.0	349

Table 2 The comparison of various pretreatment methods

Type	Specific methods	Advantages	Disadvantages	Energy consumption (MJ kg^{-1})	Solvent recovery rate (%)	Total sugar yield (%)	Ref.
Physical methods	Steam explosion	Little environmental pollution	Professional equipment required	2–4	N/A	70–85	350–352
Chemical methods	Dilute acid	Efficient removal of hemicellulose	Equipment corrosion	2–18	70–90	~85	352–354
	Caustic pretreating	Mild action conditions	Producing a lot of waste liquid	2–35	N/A	65–75	351, 352 and 355
	Ionic liquid	Easy to prepare	High cost and high viscous	25–40	>97	>75	354 and 356–358
	Deep eutectic solvent	Easy to prepare, green environmental protection	Difficult extraction	15–40	>90	>90	207, 351 and 359–361
Biological methods	Biological enzyme	High efficiency and no pollution	Long time	0.5–2	N/A	30–60	362 and 363

disrupt the extensive cellulose hydrogen-bond network, and solvate lignin through aromatic, ionic, and hydrogen-bonding interactions. For instance, a 1 : 2 molar ratio of [Ch]Cl (HBA, T_m = 302 °C) and urea (HBD, T_m = 131 °C) forms a DES with a melting point of 12 °C,[97] which is significantly lower than either pure component owing to charge delocalization and strong hydrogen bonding networks (Fig. 5).[104]

In binary eutectic mixtures, the difference between the eutectic melting point and that of an ideal mixture is related to the interaction strength between the components.[118] Most

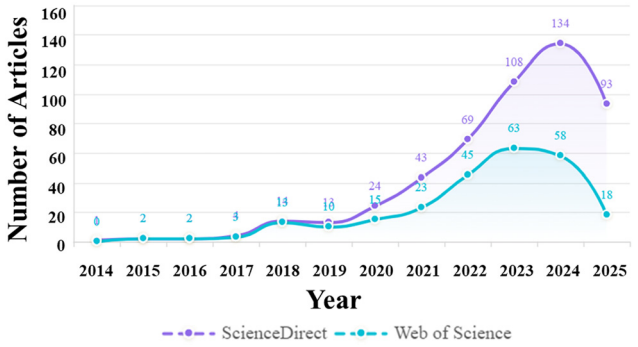

Fig. 4 Trends in research publications on deep eutectic solvent (DES) pretreatment of lignocellulosic biomass from 2014 to 2025 based on ScienceDirect and Web of Science databases.

DESs have melting points below 150 °C,[119,120] but DESs with a T_m lower than 50 °C are more attractive because they can serve as low-cost and safe solvents for various applications.[91] The choice of HBD is important for preparing low-melting-point DESs. For example, among the HBDs, urea and 2,2,2-trifluoroacetamide interact strongly with [Ch]Cl, tend to form DESs that are liquid at room temperature.[2,120] Other factors that affect the melting points of DESs include the type of organic salt, the molar ratio of DESs, and the anion in choline-based salts.[121] DESs formed from urea and various ammonium salts at a 2 : 1 molar ratio have melting points ranging from 38 °C to 131 °C.[122] Moreover, DESs prepared from choline-based salts and urea, the melting points follow the trend: $F^- > NO_3^- > Cl^- > BF_4^-$.[97,120] This melting point reduction is again explained by enhanced charge delocalization due to hydrogen bonding between HBA and HBD.[123]

The eutectic point of DESs can be calculated using thermodynamic models such as COSMO-RS (Conductor-like Screening Model for Realistic Solvation) and PC-SAFT (perturbed-chain statistical associating fluid theory).[76,124,125] The COSMO-RS model is a widely used computational method that predicts the eutectic composition of DESs based on the solid–liquid equilibrium and the phase transition properties of the HBA and HBD.[124] In addition to these models, machine learning (ML) approaches have also shown high accuracy in predicting the eutectic composition of DESs.[126–128] For biomass pretreatment and other industrial applications,[127–129] DESs with low melting points and a wide chemical stability window are more attractive and promising.

3.4 Polarity

Polarity is a multi-dimensional concept and key property of DESs, determining their ability to dissolve both charged and neutral species. As a quantitative measure of solvent strength, polarity is generally related to the strength of intermolecular interactions.[130] However, it is difficult to measure polarity accurately because no single macroscopic parameter can fully capture the complex associated interactions between solutes and solvents at the molecular scale.[131] Common methods for approximating DES polarity include solvatochromic measurements (*i.e.*, Kamlet–Taft parameters) using UV-Vis absorbance and fluorescence probes.[132] In addition, the polarity of a solvent can be assessed using the Dimroth and Reichardt E_T (30) polarity scale, which is based on the electronic transition energy of a probe dye, such as Reichardt's Dye 30, dissolved in the solvent.[133] Recently, studies found an inverse relationship between the polarity and pH of some PEG-based DESs, suggesting that pH could also serve as an indicator of polarity.[134–136] Further, we developed a ML model to predict

Table 3 Classification and general formulae of deep eutectic solvents[151]

DES type	General formula	Terms
I	$Cat^+ X^- + zMCl_x$ (quaternary halide + metal chloride)	M = Zn, Sn, Al, Ga, In X = Cl, Br
II	$Cat^+ X^- + zMCl_x{\cdot}yH_2O$ (quaternary halide + metal chloride hydrate)	M = Cr, Co, Cu, Fe, Ni X = Cl, Br
III	$Cat^+ X^- + zRZ$ (quaternary halide + nonionic hydrogen bond donor)	Z = $CONH_2$, COOH, OH X = Cl, Br
IV	$zMCl_x + RZ$ (metal chloride + nonionic hydrogen bond donor)	M = Al, Zn Z = $CONH_2$, OH
V	$RZ_1 + RZ_2$ (non-ionic compounds)	Z_1 and Z_2 = COOH, OH

Table 4 Property comparisons of different types of deep eutectic solvents[2,12,15,76,97,108,110,111,132,140,364–371]

DES type	Density (g cm^{-3})	Viscosity (mPa s)	Melting point (°C)	Conductivity (mS cm^{-1})	Surface tension (mN m^{-1})	Polarity (E_T(30) kcal mol^{-1})
I	1.10–1.40	200–20 000	<100	<2	40–60	52–59
II	1.15–1.45	100–15 000	<70	<2	45–65	50–58
III	1.00–1.35	50–20 000	<70	<2	35–55	45–60
IV	1.20–1.50	100–30 000	<100	<2	50–70	48–55
V	0.90–1.10	10–500	<50	<2	25–45	35–50

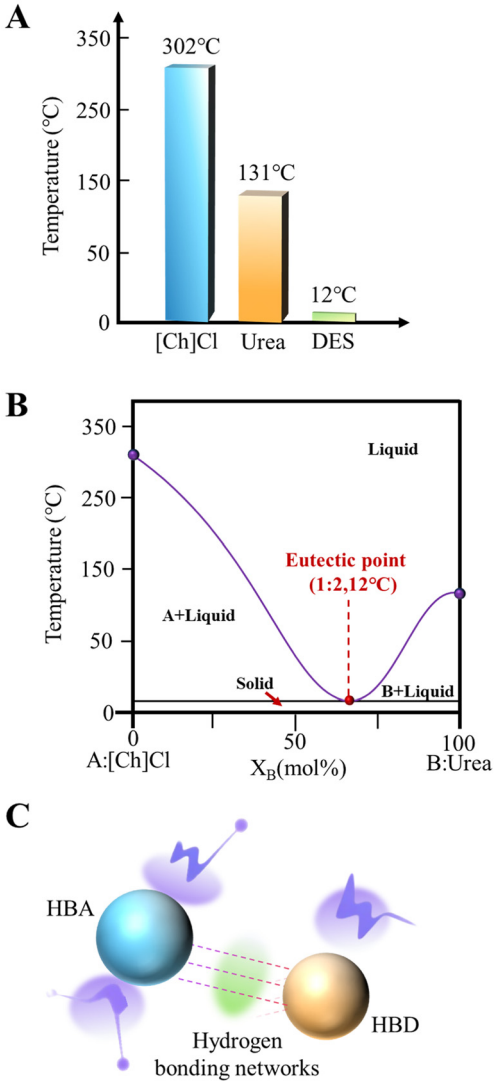

Fig. 5 Schematic diagram of the melting point reduction phenomenon in deep eutectic systems. (A) Melting point comparison. (B) Phase diagram. Adapted with permission from ref. 326. Copyright 2019, Elsevier. (C) Molecular interactions.

the polarity of DESs (Kamlet–Taft parameters (α, β, and π^*)) using the COSMO-RS-derived input features, and further correlated with lignin removal and carbon capture applications.[133]

In contrast to conventional ionic liquids which tend to maintain high polarity regardless of cation or anion structure, DES polarity depends heavily on the HBA and HBD.[132] In general, DESs prepared with acidic HBDs tend to have greater polarity than those containing amides or ammonium salts, mainly due to the presence of polar carboxyl groups in acids.[135,136] Furthermore, the DESs contain amines and hydroxyl groups tend to show higher polarity and stronger hydrogen bonding accepting capabilities.[133] Water content strongly affects DES polarity. For instance, adding 25% water to [Ch]Cl/triethylene glycol and [Ch]Cl/PEG 200 increases their polarity and molar transition energies.[96,100]

3.5 Surface tension

Surface tension, which reflects the energy required to increase a liquid's surface area, is an important property for determining DES performance in industrial processes such as fluid flow, multiphase mixing, and separation.[137–139] This property largely controls how suitable DESs are for operations involving mass transfer at interfaces. Surface tension decreases as temperature increases because higher temperatures weaken intermolecular forces.[140]

The surface tension of DESs is fundamentally governed by the strength and organization of intermolecular interactions, and size of the molecules. In DES systems, these interactions arise primarily from hydrogen bonding, ionic interactions, and van der Waals (vdW) forces between HBA and HBD components. Strong, polar, smaller size, and highly coordinated hydrogen-bond networks increase cohesive energy density, leading to higher surface tension, whereas weaker, large size, or more disrupted networks exhibit lower surface tension.[138,141] The nature of HBA and HBD plays a critical role in determining DES surface tension. For instance, HBDs with extensive hydroxyl (–OH), carboxyl (–COOH), and amide functionality can enhance hydrogen bonding, increasing surface cohesion.[5] In contrast, bulky or less polar components reduce intermolecular packing efficiency and lower surface tension. Similarly, the size, charge distribution, and structure of the HBA influence ion–dipole interactions and the overall cohesion of the liquid.[120] Additives such as water further modulate surface tension by preferentially accumulating at the interface, where they disrupt the native DES hydrogen-bond network and reduce surface cohesive energy.[142] As a result, surface tension decreases with increasing water content. These compositional effects provide a direct means to tune interfacial properties, which are critical for mass transfer, wetting, and biomass penetration during pretreatment processes. Finally, the molar ratio of HBA to HBD provides an additional lever for tuning surface tension. By adjusting this ratio, one can modulate the density of hydrogen-bonding interactions within the solvent, which in turn alters the surface cohesive energy density and thus the measured surface tension.[143]

Notably, ammonium-based DESs, such as those containing tetra-*n*-butylammonium bromide ([TBA]Br) or [Ch]Cl mixed with ethylene glycol (EG), show surface tension values similar to glycerol- and phosphonium/amine-based DESs.[140] Hence, ammonium-type DESs can deliver the same interfacial driving force needed for efficient wetting, lignin dissolution or nanoparticle dispersion without the high cost and toxicity constraints of phosphonium solvents, thereby reinforcing their practical appeal for large-scale biomass fractionation and other green-engineering applications.[140] Sugar-based DESs also show surface tension in a similar range as phosphonium-based DESs, *i.e.*, methyltriphenylphosphonium bromide [MTPP]Br–EG and benzyltriphenylphosphonium chloride [BzTPP]Cl–EG.[131,144,145] The presence of water in DESs tends to lower surface tension depending on the specific system.[135] Water exhibits the highest surface tension among common

liquids (≈72 mN m^{-1} at 25 °C), attributed to its robust three-dimensional hydrogen-bonding network.[131,146] When incorporated into DESs, water reduces the solvent's surface tension through the following mechanism: its small, strongly hydrogen-bonded molecules preferentially accumulate at the DESs surface, and this surface enrichment disrupts the cohesive hydrogen-bond network of bulk DESs. Consequently, the average surface cohesive energy density of DESs decreases, thereby lowering their surface energy and overall surface tension. This phenomenon has been experimentally validated for a broad range of DESs, including choline chloride-based, sugar-based, and phosphonium-based systems, and aligns with the "surface activity" of water observed in aqueous ionic liquid systems.[147,148] Recently, Lemaoui *et al.* developed artificial neural networks (ANN) to predict the surface tension of DESs at different temperature ranges, molar ratios, and HBA/HBD combinations.[149] This approach can accelerate the design of eutectic mixtures with optimal surface tension values for different research applications including biomass fractionation. Surface tension shows a negative correlation with sugar release from lignocellulosic biomass.[138] In lignocellulosic pretreatment systems, reducing the surface tension of DESs markedly enhances their wetting and penetration into biomass pores. This enhancement disrupts the LCC and exposes additional enzymatically accessible sites. Both experimental results and molecular simulations confirm a distinct negative correlation between DES surface tension and subsequent enzymatic sugar production, *i.e.*, lower surface tension correlates with higher enzymatic sugar yield. Consequently, surface tension should be prioritized as a key optimization parameter in DES design for biomass fractionation.[150]

3.6 Viscosity

Viscosity measures a fluid's resistance to flow when a force is applied.[107,151] It is a critical property in industrial applications and must be addressed. Notably, viscosity plays a critical role in biomass pretreatment: higher viscosity tends to reduce pretreatment efficiency.[45,63] Generally, liquids with lower viscosity flow easily, while those with higher viscosity restrict their flow and limit mass transfer rate. The viscosity of a DES is influenced by the identities of the HBA and HBD, the molar ratio, operating temperature, pressure, and water content.[84] In the literature [Ch]Cl-based HBAs are the most widely studied DES component, whereas EG-based HBDs are the most frequently investigated.[151] For [Ch]Cl-based DESs, viscosity depends strongly on the choice of HBD. [Ch]Cl/EG at a 1 : 4 molar ratio shows relatively low viscosity (19 cP at 20 °C), whereas the use of sugar derivatives (*e.g.*, xylitol, sorbitol) or carboxylic acids (*e.g.*, malonic acid) as HBDs shows much higher viscosities.[91] This is due to the stronger polar interactions between [Ch]Cl and sugars/carboxylic acids as compared to EG.[151]

Similar to ILs and organic solvents, the viscosity of DESs decreases with temperature, following Arrhenius-like behavior. The extensive strong hydrogen-bond network among DES components is often responsible for their high viscosity, which limits molecular mobility.[84,152,153] The hole theory – in which liquids are more viscous when holes in them are harder to create – provides a rational framework for designing low-viscosity DESs through strategic component selection. For instance, using small cations or fluorinated HBDs can lower viscosity effectively.[95,98] It has been interesting to mention that type III (quaternary halide + nonionic hydrogen bond donor) DESs exhibit a wider range of viscosity values (0.135 cP to 24 343 cP) than other types of DESs, owing to their unique composition: the only DES family composed of a quaternary halide salt and a neutral, non-ionic HBD.[154] Notably, the charge-neutral nature of the HBD enables nearly unrestricted modulation of its molecular weight, polarity, and hydroxyl/carboxyl group content—spanning from small-molecule ethylene glycol to bulky sugar alcohols or phenolic acids. Furthermore, their molar ratio can be tuned over a broad range without destabilizing the liquid phase. Each variation in HBD structure or molar ratio alters the density and lifetime of the anion–HBD hydrogen-bond network, thereby inducing a five-order-of-magnitude swing in viscosity.[2,3] Moreover, type III DESs are most studied in the literature.[151]

The application of ML methods for predicting DES properties has grown significantly.[107] Recently, empirical models based on a large dataset (553 measurements across 112 DES systems) were developed, showing good predictive accuracy.[155] In recent work, we employed a range of ML methods to predict viscosities using 697 different DESs and 4949 data points across various temperatures and molar ratios. The best of these models achieves an average absolute relative deviation (AARD) of 5.22%.

Optimal physicochemical properties of DESs make them promising solvents for many applications. However, to fully leverage their potential, a deeper understanding is needed of how composition and structure control their properties. ML models can bridge the gap by designing an optimal DES with desirable physicochemical properties. Overall, the physicochemical properties of DESs, particularly viscosity, polarity, and surface tension play a critical role in determining biomass pretreatment efficiency (see Table 5). Lower viscosity and surface tension enhance mass transfer and biomass penetration, whereas polarity matching between DES and lignin improves solubilization. These structure–property relationships provide key design principles for developing next-generation DES systems.

4. Pretreatment of lignocellulosic biomass using DESs

DESs have emerged as an effective class of solvents for the pretreatment of lignocellulosic biomass due to their ability to selectively disrupt the complex structure of plant cell walls. In a typical DES-based pretreatment process, biomass is mixed with a DES at elevated temperatures, where the solvent penetrates the biomass matrix and interacts with its components through hydrogen bonding, ionic interactions, and π–π inter-

Table 5 Summary of structure–property–performance relationships in DES-mediated biomass pretreatment

Property	Key factors	Trend	Impact on biomass pretreatment	Key insight
Conductivity	HBA/HBD type, viscosity, temperature	Increase with temp and decrease with viscosity	Enhances charge transfer, improves LCC disruption	Higher conductivity enhances charge transport and facilitates LCC disruption, improving delignification efficiency
Density	HBD type, molar ratio	Increase with stronger HBD interactions	Influences solvent penetration and packing	Correlates with interaction strength (system-dependent)
Melting point	Composition and H-bond strength of HBA/HBD	Decrease due to eutectic effects and intermolecular interactions (electrostatic and H-bonds)	Enables liquid-phase processing	Lower T_m improves processability and enables efficient operation under mild conditions
Polarity	HBA/HBD chemistry, water content	System dependent	Controls lignin solubility	Matching polarity between DES and lignin enhances solubilization and improves dissolution efficiency
Surface tension	HBA/HBD composition and water content	Decrease with temperature and water content	Improves wetting and penetration	Lower surface tension enhances biomass wetting and penetration, leading to improved sugar yields
Viscosity	HBA and HBD types, temperature	Decrease with temperature	Controls mass transfer and molecular diffusivity	Lower viscosity enhances mass transfer and improves pretreatment efficiency

actions and disrupting LCCs and promoting the solubilization of lignin and partial removal of hemicellulose, while largely preserving the cellulose fraction.[156] This process enhances biomass porosity and improves the accessibility of cellulose to subsequent enzymatic hydrolysis, thereby enabling more efficient conversion to sugars and downstream products.[157] As research progresses, there is growing interest in developing new DES formulations.[158,159] The characteristics of different lignocellulosic biomasses after DES pretreatment are summarized in Table 6. The following sections will discuss the effects of DES pretreatment on various biomass types, including herbaceous, hardwoods, and softwoods. Fig. 6 shows the structures of plant cell walls and LCCs.

4.1 Pretreatment of herbaceous plants

Herbaceous plants were among the first feedstocks used with biomass pretreatment with DESs, mainly due to their short growth cycles, fast regeneration, and high biomass yields.[160] Most agricultural crops are herbaceous. Large amounts of associated agricultural residues, such as rice straw, wheat straw, corncob, and bagasse, are produced annually.[161] These agricultural byproducts are an abundant and renewable source of lignocellulosic biomass. Efficient utilization of these residues using DES-based pretreatment offers a sustainable pathway for valorizing agricultural waste for biofuels, biochemicals, and biomaterials production.[162]

Some species of herbaceous plants naturally contain high cellulose content, such as bamboo (40–55%) and sugarcane bagasse (35–45%).[163–165] Many studies have focused on using carboxylic acids as key DES components, with the lactic acid/choline chloride system being one of the most widely studied for biomass pretreatment.[166–169] Wang *et al.* studied various Lewis acids in a [Ch]Cl–glycerol DES for pretreating hybrid *Pennsylvania* switchgrass.[170] They reported that adding Lewis acids significantly increased delignification efficiency, with ferric chloride boosting delignification to 91% and cellulose saccharification to over 95%. Further, the recovered lignin showed excellent antioxidant activity.[170] Li *et al.* prepared a ternary DES system comprising EG, [Ch]Cl, and lactic acid for the pretreatment of corn straw biomass.[171] After pretreatment, more than 93.5% of cellulose was retained and 65.5% of lignin was removed. These results indicate that the polyol-assisted ternary DES system demonstrated potential to selectively remove lignin and preserve carbohydrates.

Recent developments in DES design have demonstrated the potential of tailoring solvent components to enhance the pretreatment efficiency of lignocellulosic biomass. One notable approach involves the use of lignin-derived HBDs to prepare bio-based DESs for the fractionation of switchgrass.[172] DESs composed of [Ch]Cl and *p*-coumaric acid (PCA) demonstrated the highest pretreatment efficiency, dissolving 61% of lignin and 25.5% of cellulose, and achieving an 85% glucose yield after enzymatic saccharification. This is due to strong interaction between [Ch]Cl–PCA and biomass components and higher hydrogen bond basicity than other lignin-based DESs.

Building on these insights, subsequent studies explored various structural motifs in DES composition. For example, the systematic evaluation of monocarboxylic, dicarboxylic, and polyalcohol-based DESs revealed that a mixture of ethylene glycol and [Ch]Cl (in a 2 : 1 molar ratio) was highly efficient for corncob pretreatment.[173] Among all DES formulations for corncob pretreatment, the DES based on EG and [Ch]Cl (2 : 1 molar ratio) exhibited the best performance, removing 87.6% of lignin and achieving a high glucose yield of 96.4% after enzymatic hydrolysis. The high efficacy was attributed to favorable hydrogen bonding interactions and lower viscosity, which improved mass transfer. Further, structural analyses (XRD, FTIR, SEM) confirmed significant disruption of lignin and hemicellulose, enhancing cellulose accessibility. Extending this line of research, a nineteen [Ch]Cl-based DESs were screened for their effectiveness on wheat straw pretreatment.[174] These DESs were categorized into four groups based

Table 6 Characteristics of different types of lignocellulosic biomass after DESs pretreatment and the enzymatic efficiency of cellulose residue

Biomass	Specific types	DES	Reaction conditions	Cellulose retention (%)	Lignin removal (%)	Enzymatic efficiency (%)	Enzymatic efficiency of raw biomass (%)	Ref.
Herbaceous	Corn stover	[Ch]Cl : lactic acid : ethylene glycol	100 °C/6 h	93.5	65.5	75.9	~15.0	171
		[Ch]Cl : lactic acid	100 °C/6 h	~90.0	~65.0	49.5	~15.0	171
		[Ch]Cl : lactic acid : glycerol	100 °C/6 h	93.0	60.2	65.9	~15.0	171
		[Ch]Cl : lactic acid : PEG	100 °C/6 h	93.0	60.2	60.8	~15.0	171
		[Ch]Cl : ethylene glycol	160 °C/3 h	91.0	57.3	59.6	14.3	332
		[Ch]Cl : ethylene glycol + $NaHCO_3$	140 °C/3 h	82.8	90.3	97.5	14.3	332
		Lactic acid : betaine	140 °C/3 h	74.9	79.0	83.0	28.3	372
		[Ch]Cl : 1,4-butanediol + NaOH	100 °C/3 h	71.5	81.3	90.7	26.3	203
		[Ch]Cl : 1,4-butanediol + $AlCl_3$	100 °C/3 h	78.1	61.2	81.4	26.3	203
		[Ch]Cl : glycol + phosphotungstic acid	150 °C/3 h	~90.0	86.1	94.4	17.9	373
	Corn straw	[Ch]Cl : vanillin	140 °C/3 h	85.5	56.8	83.2	27.6	374
		Hydrated [Ch]Cl : vanillin	140 °C/3 h	—	61.4	85.0	27.6	374
		1-Ethyl-3-methylimidazolium acetate : 1,4-butanediol	121 °C/1 h	89.7	74.7	—	—	375
	Corncob	Benzyltrimethyl-ammonium chloride : lactic acid	140 °C/2 h	99.1	63.4	94.0	31.1	176
		Benzyltriethyl-ammonium chloride : lactic acid	140 °C/2 h	94.1	56.5	89.2	31.1	176
		[Ch]Cl : lactic acid	90 °C/24 h	48.2	77.9	83.5	22.1	173
		[Ch]Cl : glycolic acid	90 °C/24 h	50.5	56.4	67.3	22.1	173
		[Ch]Cl : levulinic acid	90 °C/24 h	71.2	43.0	62.0	22.1	173
		[Ch]Cl : malonic acid	90 °C/24 h	53.6	56.5	61.5	22.1	173
		[Ch]Cl : glutaric acid	90 °C/24 h	74.2	34.3	40.7	22.1	173
		[Ch]Cl : oxalic acid	90 °C/24 h	53.1	98.5	45.2	22.1	173
		[Ch]Cl : malic acid	90 °C/24 h	63.5	22.4	37.4	22.1	173
		[Ch]Cl : ethylene glycol	90 °C/24 h	73.4	87.6	85.3	22.1	173
		[Ch]Cl : glycerol	90 °C/24 h	71.2	71.3	96.4	22.1	173
	Wheat straw	[Ch]Cl : PEG-200 : boric acid	120 °C/4 h	91.0	88.4	59.3	26.0	330
		Triethylbenzyl ammonium chloride : lactic acid	273 K/10 h	76.2	79.7	89.1	25.8	376
		Glycerol : K_2CO_3 : PEG-200	120 °C/2 h	73.7	96.4	—	—	377
		[Ch]Cl : urea	120 °C/3 h	39.7	23.0	35.4	16.1	378
		[Ch]Cl : methylurea	120 °C/3 h	39.2	27.0	27.3	16.1	378
		[Ch]Cl : formamide	120 °C/3 h	36.5	32.0	38.5	16.1	378
		[Ch]Cl : glycerol	120 °C/3 h	40.0	36.0	46.7	16.1	378
		[Ch]Cl : acetic acid	120 °C/3 h	42.9	63.0	45.7	16.1	378
		[Ch]Cl : formic acid	120 °C/3 h	32.0	80.7	65.3	16.1	378
		[Ch]Cl : lactic acid	120 °C/3 h	33.5	78.1	65.3	16.1	378
		[Ch]Cl : malic acid	120 °C/3 h	37.0	76.0	58.8	16.1	378
		[Ch]Cl : itaconic acid	120 °C/3 h	36.5	80.5	62.4	16.1	378
		[Ch]Cl : levulinic acid	120 °C/3 h	37.2	65.0	58.8	16.1	378
		[Ch]Cl : glutaric acid	120 °C/3 h	38.6	70.0	45.7	16.1	378
		[Ch]Cl : propionic acid	120 °C/3 h	39.0	60.0	50.2	16.1	378
		[Ch]Cl : glycerol : $FeCl_3$	120 °C/3 h	32.5	81.1	50.5	16.1	378
		[Ch]Cl : lactic acid : $FeCl_3$	120 °C/3 h	35.8	78.0	55.3	16.1	378
		[Ch]Cl : formamide : $FeCl_3$	120 °C/3 h	38.3	32.0	35.7	16.1	378
	Reed straw	Benzyltriethylammonium chloride : formic acid	130 °C/3 h	88.6	94.1	76.6	14.6	175
		[Ch]Cl : oxalic acid : 1,2-butanediol	120 °C/24 h	90.1	74.7	91.6	<5.0	40
	Switchgrass	[Ch]Cl : 4-hydroxybenzyl alcohol	160 °C/3 h	93.5	0.4	32.0	<10.0	172
		[Ch]Cl : catechol	160 °C/3 h	95.3	49.0	77.0	<10.0	172
		[Ch]Cl : vanillin	160 °C/3 h	87.5	52.5	79.8	<10.0	172
		[Ch]Cl : *p*-coumaric acid	160 °C/3 h	74.5	60.8	85.7	<10.0	172

Table 6 *(Contd.)*

Biomass	Specific types	DES	Reaction conditions	Cellulose retention (%)	Lignin removal (%)	Enzymatic efficiency (%)	Enzymatic efficiency of raw biomass (%)	Ref.
	Miscanthus	[Ch]Cl : acetic acid	150 °C/2 h 52 min	87.0	61.7	64.1	—	335
		[Ch]Cl : lactic acid	120 °C/6 h	86.7	71.2	83.0	20.0	187
	Moso bamboo	[Ch]Cl : 1,4-butanediol : $AlCl_3$	110 °C/1 h	96.7	69.7	100	12.5	334
		Butanediol : $AlCl_3$	110 °C/1 h	98.7	63.1	94.8	12.5	334
	Hybrid *Pennisetum*	[Ch]Cl : glycerol : $FeCl_3$	120 °C/6 h	—	91%	>95.0	—	170
	Oil palm empty fruit bunches	[Ch]Cl : lactic acid	3 min	75.4	78.9	—	—	379
		[Ch]Cl : oxalic acid : ethylene glycol	3 min	71.7	73.9	—	—	379
	Sugarcane bagasse	[Ch]Cl : analog-VFAs	150 °C/3 h	—	74.1	—	—	380
	Rapeseed straw	Tetradecyltrimethylammonium bromide : lactic acid : Fe^{3+}	162.5 °C/ 61.7 min	79.8	89.2	92.5	20.1	381
	Tea stem	PEG-200 : oxalic acid	140 °C/4 h	82.0	70.9	—	—	382
Hardwood	Poplar	[Ch]Cl : *p*-hydroxybenzoic acid	160 °C/3 h	69.2	69.0	90.8	15.5	181
		[Ch]Cl : *p*-coumaric acid	160 °C/3 h	47.4	15.5	26.0	15.5	181
		[Ch]Cl : 4-hydroxybenzaldehyde	160 °C/3 h	54.0	30.7	26.0	15.5	181
		Monoethanolamine hydrochloride : monoethanolamine	110 °C/3 h	86.0–92.0	74.9	90.4	13.9	383
		[Ch]Cl : lactic acid	140 °C/2 h	>75.0	80.0	—	—	384
		$AlCl_3{\cdot}6H_2O$: formic acid : H_2O	120 °C/3 h	91.3	94.7	97.9	5.7	385
	Eucalyptus	[Ch]Cl : citric acid monohydrate	150 °C/10 min	72.5	72.7	94.3	22.1	184
		[Ch]Cl : lactic acid : PEG-400	140 °C/30 min	~100.0	89.7	—	—	220
		[Ch]Cl : lactic acid	110 °C/6 h	85.0	80.3	94.3	9.6	386
		[Ch]Cl : mannitol : *p*-TsOH	120 °C/1 h	84.5	95.7	87.1	10.1	387
	Eucalyptus grandis × *E. urophylla*	[Ch]Cl : maleic acid : glycerol	140 °C/20 min	87.5	90.9	82.5	21.5	388
	Acacia dealbata	[Ch]Cl : levulinic acid	160 °C/4 h	96.1	95.8	—	—	343
		[Ch]Cl : imidazole	160 °C/4 h	69.3	58.7	—	—	343
	Willow	$ZnCl_2$: ethylene glycol : malic acid	130 °C/1.5 h	86.0	90.1	96.0	6.8	182
		Lactic acid : betaine	140 °C/3 h	67.2	52.9	~65.0	14.8	372
	Oil palm fronds	[Ch]Cl : $CaCl_2{\cdot}6H_2O$	125 °C/4.5 h	95.4	46.5	59.3	39.1	87
		[Ch]Cl : $MgCl_2{\cdot}6H_2O$	125 °C/4.5 h	89.6	36.7	52.7	39.1	87
		[Ch]Cl : urea	120 °C/4 h	97.8	11.6	44.0	39.1	87
Softwood	Radiata pine	Benzyltrimethylammonium chloride : formic acid	150 °C/2 h	88.3	72.9	92.4	20.7	193
	Douglas fir	[Ch]Cl : levulinic acid	145 °C/9 h	~90.0	~50.0	—	—	58
	Chinese fir	Triethylbenzylammonium chloride : lactic acid	150 °C/1.5 h	95.8	97.4	97.1	8.2	389
	Spruce and pine	[Ch]Cl : lactic acid	80 °C/24 h	—	77.7	—	—	390
	Pinus insignis	[Ch]Cl : formic acid	140 °C/14 min	93.5	90.1	—	—	391

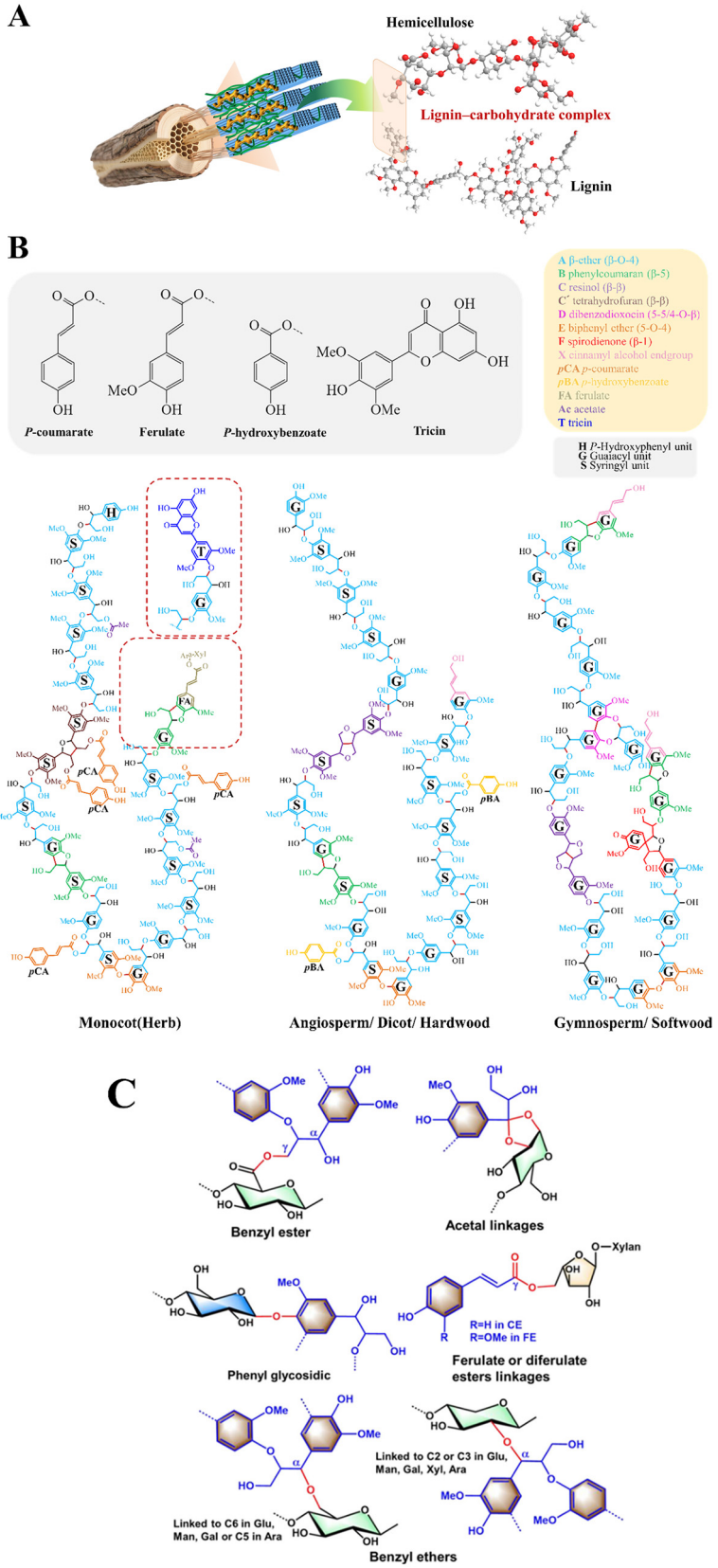

Fig. 6 (A) Three-dimensional representation of the lignin–carbohydrate complex (LCCs) in the wood cell wall. Redrawn based on a figure from ref. 328. (B) Representative lignin structures for three major plant classes. Adapted with permission from ref. 206. Copyright 2019, Elsevier. (C) Five chemical structures that have existed for lignin–carbohydrate linkages in wood and grass; Glu, glucose; Man, mannose; Gal, galactosyl; Xyl, xylan; Ara, arabinose. Reproduced with permission from ref. 327. Copyright 2023, Elsevier.

on their HBDs such as amide-based, polyol-based, acid-based, and ternary DESs, which offered valuable insights into structural–property relationships. Acid-based DESs showed higher efficacy in removing lignin and hemicellulose than amide and polyol-based DESs. By measuring the physicochemical properties of these nineteen DESs, correlations were drawn between pretreatment performance and DES properties. These findings demonstrated that the strengths of hydrogen bond donors and acceptors play critical roles in tuning DES systems for efficient biomass fractionation (delignification and xylan removal positively correlated with the Kamlet–Taft (K–T) parameters α and α–β).

Formulations of novel DES continue to emerge. Zhang *et al.* introduced a novel DES composed of benzyltriethylammonium chloride ([BTEA]Cl) and formic acid (FA) to deconstruct reed straw.[175] The associated pretreatment was performed under optimized conditions: a DES molar ratio of 1 : 6, a temperature of 130 °C, and a duration of 3 h with a solid-to-liquid ratio of 1 : 10. This process resulted in a significant delignification of 94.1% and enabled a high enzymatic glucose yield of 76.6% from the cellulose-rich residue. The recovered lignin showed desirable properties such as high purity, low molecular weight, and low polydispersity, making it suitable for further production of value-added chemicals. Guo *et al.* evaluated the pretreatment effects of two novel DESs on corncobs: benzyltrimethylammonium chloride ([BTMA]Cl)/lactic acid (LA) and benzyltriethylammonium chloride ([BTEA]Cl)/LA at a molar ratio of 1 : 2.[176] The DES [BTMA]Cl/LA showed better performance of the two, achieving 94.0% cellulose hydrolysis and 63.4% biomass delignification. Further, the recovered lignin demonstrated better structural properties, and the DES maintained excellent performance even after five reuse cycles, which is effective in reducing process costs. This work demonstrates an efficient approach for improving sugar yields from corncob biomass and producing valuable lignin coproducts. Chen *et al.* used a [Ch]Cl and EG DES at high solid loadings to pretreat switchgrass and subsequently convert it into platform chemicals such as furfural and 2,3-butanediol.[115] After pretreatment, enzymatic hydrolysis at 25% solids achieved 86.2% cellulose conversion within 48 h. The process produced furfural with a yield of 84.6% and a high titer of 90.2 g L^{-1} 2,3-butanediol without further need of sugar concentration. These results show that [Ch]Cl/EG DES pretreatment under high solids not only effectively fractionates biomass but also enables the industrial production of sugar-rich hydrolysates and valuable chemicals such as furfural and 2,3-butanediol.

4.2 Pretreatment of woody biomass

4.2.1 Hardwood. Hardwood biomasses have a higher cellulose content compared to many other lignocellulosic feedstocks, which makes them particularly attractive for biorefinery applications.[177,178] The use of DESs for hardwood biomass fractionation largely focused on the efficient extraction and utilization of cellulose.[179] Among woody feedstocks, hardwoods have been widely studied, with poplar receiving the most attention.[180]

Wang *et al.* conducted an experiment using lignin-based DES that are composed of *p*-hydroxybenzoic acid (PBA) and [Ch]Cl for the pretreatment of poplar biomass.[181] Their results showed that lignin-derived DES effectively fractionated poplar at relatively mild operating conditions, achieving a lignin removal of 69% and a cellulose enzymatic hydrolysis efficiency of over 90%. Similarly, Zhao *et al.* were the first to propose a ternary DES prepared from zinc chloride ($ZnCl_2$), EG, and malic acid (MA) to pretreat willow.[182] This ternary DES significantly improved biomass fractionation and conversion efficiency, with lignin removal reaching 90.1% and enzymatic hydrolysis efficiency achieving 96.0% under optimal conditions (130 °C, 1.5 h). Moreover, the recovered lignin exhibited uniform nanoparticle morphology and good antioxidant properties, demonstrating the potential of the $ZnCl_2$/EG/MA system to efficiently utilize lignocellulose under mild conditions. These studies demonstrate how modifying solvent compositions can improve DES performance. Other researchers have also tailored DES systems by adding auxiliary components.[62] Zhang *et al.* prepared a DES composed of [Ch]Cl/glycerol which is highly viscous. As discussed, the viscosity of the solvent plays an important role in biomass pretreatment. High-viscosity solvents limit the mass transfer rate of DESs, thereby reducing the pretreatment efficacy.[7] The viscosity was reduced by adding water to improve the pretreatment efficiency and achieve a high mass transfer rate.[183] When the water content was between 10% and 15%, the removal of lignin exceeded 77% and cellulose hydrolysis efficiency achieved 95%. The addition of water improved the biomass fractionation and purity of recovered lignin, supporting its use in lignin-derived biomaterials. These findings suggest that water is a promising auxiliary solvent in DES-based pretreatment.

Sun *et al.* introduced a biphasic system combining a water-soluble DES with cyclopentyl methyl ether (CPME) for the integrated production of furfural, lignin extraction, and enhanced enzymatic saccharification of eucalyptus.[184] In their study, the authors used a mixture of citric acid monohydrate, [Ch]Cl, 30 wt% of water, 2.5 wt% of $SnCl_4{\cdot}5H_2O$, and CPME. This approach increased furfural yield to 80.6%, while achieving 72.7% lignin removal and 94.3% glucose yield under pretreatment optimal conditions (150 °C and 10 min reaction time). The extracted lignin had a low molecular weight and uniform distribution, which is favorable for further valorization. This study demonstrated a one-step fractionation strategy for co-producing furfural, lignin, and fermentable sugars, providing a new approach for efficient biorefining. Ma *et al.* proposed a scalable method for nanocellulose production using hydrated DES combined with ultrasonication to treat kraft pulp.[185] In this study, the authors synthesized [Ch]Cl and oxalate dihydrate DES, diluted it with water to create hydrated DES at various concentrations, and used it to pretreat poplar-derived kraft pulp. The hydrated DES exhibited high hydrogen ionization and polarizability, reducing pulp polymerization and enhancing cellulose accessibility, resulting in a cellulose retention rate above 90%. This method improves nanocellulose pro-

duction efficiency and offers commercial viability due to its cost-effectiveness. Further, Shen *et al.* combined hydrothermal pretreatment (HP) and DES pretreatment sequentially for poplar woodchips, enabling the co-production of xylo-oligosaccharides, fermentable sugars, and recovered lignin.[186] This process demonstrated an excellent processability and provides a valuable platform for the comprehensive utilization of cellulose, hemicellulose, and lignin in woody biomass.

4.2.2 Softwood. The growth rate of softwood biomasses such as pine and fir is slower than hardwood biomasses, which leads to higher lumber costs. Softwoods contain a higher amount of lignin compared to hardwoods, making them valuable for studies focused on lignin utilization.[187] However, softwood lignin contains a higher proportion of carbon–carbon (C–C) linkages, whereas hardwood and grass lignin predominantly feature ether (C–O–C) linkages.[188–190]

Recent studies have explored various methods for fractionating cork and other lignocellulosic materials.[191] Sirviö *et al.* reported the use of an aqueous acid–thiourea DES to pretreat spruce sawdust with approximately 50% dry matter under mild operating conditions.[192] This process achieved 90% lignin removal at 100 °C within 90 minutes, and the method effectively separated lignin and cellulose from the cork biomass. Alvarez-Vasco *et al.* investigated [Ch]Cl as an HBA, combining it with acetic acid, lactic acid, levulinic acid, and glycerol to synthesize four DESs at different molar ratios.[58] These synthesized DESs were used to pretreat two different woody biomass types: poplar (hardwood) and fir (softwood). The study showed that DES pretreatment could selectively extract lignin with high purity (~95%) from biomass. Under optimal conditions, 78% of lignin was extracted from poplar and 58% of lignin from fir, confirming that softwoods are more resistant to deconstruction. This is due to the softwood biomass containing a higher proportion of C–C linkages and being difficult to solvate.

Recently, Xie *et al.* proposed a DES composed of [BTMA]Cl/FA for the deconstruction of radiata pine.[193] With this DES, the authors reported that they preserved a high cellulose content (88.3–91.8%) and achieved up to 92.4% enzymatic hydrolysis efficiency. Additionally, high-purity lignin nanoparticles with moderate molecular weight and low polydispersity were recovered, suggesting that [BTMA]Cl-based DES offer an effective strategy for softwood biomass fractionation, enabling the co-production of fermentable sugars and value-added lignin products. Jiang *et al.* prepared an environmentally friendly acidic DES to pretreat thermomechanical pulp (TMP) derived from coniferous wood, which can serve as a precursor for producing lignocellulosic nanomaterials.[194] At 90 °C for 6 h, about 57% of the lignin was recovered and the study demonstrated that this green pretreatment method can convert lignin-rich biomass into lignin–nanocellulose composite materials with potential applications.

As global interest in sustainable materials grows, nanocellulose (NC) has attracted considerable attention for its renewable origin and unique properties.[195] Conventionally, harsh chemical pretreatments are required to remove lignin before NC can be isolated.[196] However, this process is energy-intensive and inefficient. To address this, researchers have started developing approaches that retain some lignin in the nanocellulose structure. This results in lignin–nanocellulose (LNC) composites, which exhibit enhanced mechanical strength, thermal stability, barrier properties, antioxidant activity, and surface hydrophobicity.[197] DESs are among the promising green solvents being explored for producing such nanomaterials.[198] In addition to the work by Xie and Jiang, Cheng *et al.* developed a polyol-based DES for the direct conversion of raw lignocellulose into lignin micro-/nano-particle (LMNPs).[199] The results showed that the authors achieved over 90% lignin recovery and produced uniformly spherical LMNPs. The DES showed high recyclability, maintaining its efficiency even after three cycles. The study demonstrated the possibility of one-pot fractionation of biomass, yielding both sugars and lignin nanoparticles under mild conditions, a critical step toward more efficient biorefinery processes.

5. Mechanism of DES dissolution of lignin

In the plant cell wall, lignin is a highly hetero-polymerized aromatic compound that strongly interacts and forms LCC linkage with cellulose and hemicellulose, making a compact and rigid structure.[200,201] Currently, cellulose and hemicellulose are widely utilized for bioethanol and biohydrogen production, showing significant progress in these areas.[202,203] As a result, industrial biomass conversion typically focuses on these two components, while lignin is often treated as a low-value byproduct, either discarded or burned for energy.[204] In recent years, however, research has begun to explore lignin's potential although industrial application remains limited. A major challenge is that lignin forms complex polyphenolic structures and is chemically linked to the polysaccharides *via* ester and ether bonds. These linkages hinder enzymatic access to cellulose and reduce the efficiency of biomass conversion.[205,206] DES has emerged as an effective pretreatment method to disrupt the lignocellulosic structure with relatively low energy input.[207] Much of the current research on DES-based lignin removal focuses on breaking the chemical bonds in LCCs. For example, Xu *et al.* developed a phenyl glycoside lignin–carbohydrate complex (PG-LCC) model and evaluated the mechanism using various DES types.[55] Their results showed that DES pretreatment led to the cleavage of β-O-4 ether linkages in lignin, forming phenolic compounds and disrupting glycosidic bonds. Ether bond cleavage is considered a key step in effectively extracting lignin from biomass without altering C–C bonds. Therefore, delignification through DES is widely accepted as a major mechanism of selective cleavage of ether linkages without breaking C–C backbone in lignin.[55,56]

The dissolution of lignin in DES involves complex chemical and physical interactions.[56,208] Lignin solubility depends on both the composition and physicochemical properties of the DES as well as the structure of the lignin.[209] Lignin can be

physically solubilized in DESs without covalent bond cleavage, with the driving force being extensive hydrogen-bonding, π–π, and van der Waals interactions established between DESs and the native polymer. These interactions competitively disrupt LCC and replace lignin–lignin self-associations. Hence, lignin solubilization in DESs under mild conditions is dominated by supramolecular compatibility.[124,210,211] The mechanisms of lignin dissolution vary under acidic and alkaline conditions, where distinct dissolution pathways and chemical reactions occur. In acidic DES systems, lignin solubilization occurs *via* three main mechanisms: (1) acidic DESs promote elimination reactions at ether bonds, forming enol ether intermediates that undergo hydrolysis to break *β*-O-4 bonds and generate mono- and diketones.[212] (2) *α*-Hydroxyl groups in lignin undergo protonation, forming stable benzyl carbocations, facilitating the removal of *γ*-CH_2OH groups and further ether bond cleavage.[213] (3) Oxidation of the *α*-hydroxyl group followed by acylation enhances the breakdown of ether bonds, resulting in deeper depolymerization of lignin (Fig. 7A).[214] In alkaline DES systems, two major pathways occur. (1) In aliphatic lignin units, *β*-O-4 bonds break slowly, often forming epoxide intermediates.[215] (2) In phenolic lignin units, quinone–methyl intermediates may form, which can undergo depolymerization and repolymerization, leading to changes in lignin structure.[216] Alkaline DESs also facilitate ether bond cleavage through deprotonation, aiding lignin solubilization (Fig. 7B).

A critical consideration often overlooked in the literature is that the role of DESs cannot be strictly categorized as either a solvent or a catalyst; rather, their function spans a continuum between non-reactive solvation and chemically reactive behavior. This distinction is crucial for interpreting reported delignification mechanisms and guiding DES design. Previous studies have shown that DESs can act simultaneously as solvents (enhancing miscibility), catalysts (providing tunable acidity), and reactive extractants that promote *in situ* transformations.[53,187] Under mild conditions, lignin dissolution is dominated by supramolecular interactions (hydrogen bonding, π–π stacking, and vdW forces), which disrupt lignin–lignin and lignin–carbohydrate associations without covalent bond cleavage. In this regime, DESs function primar-

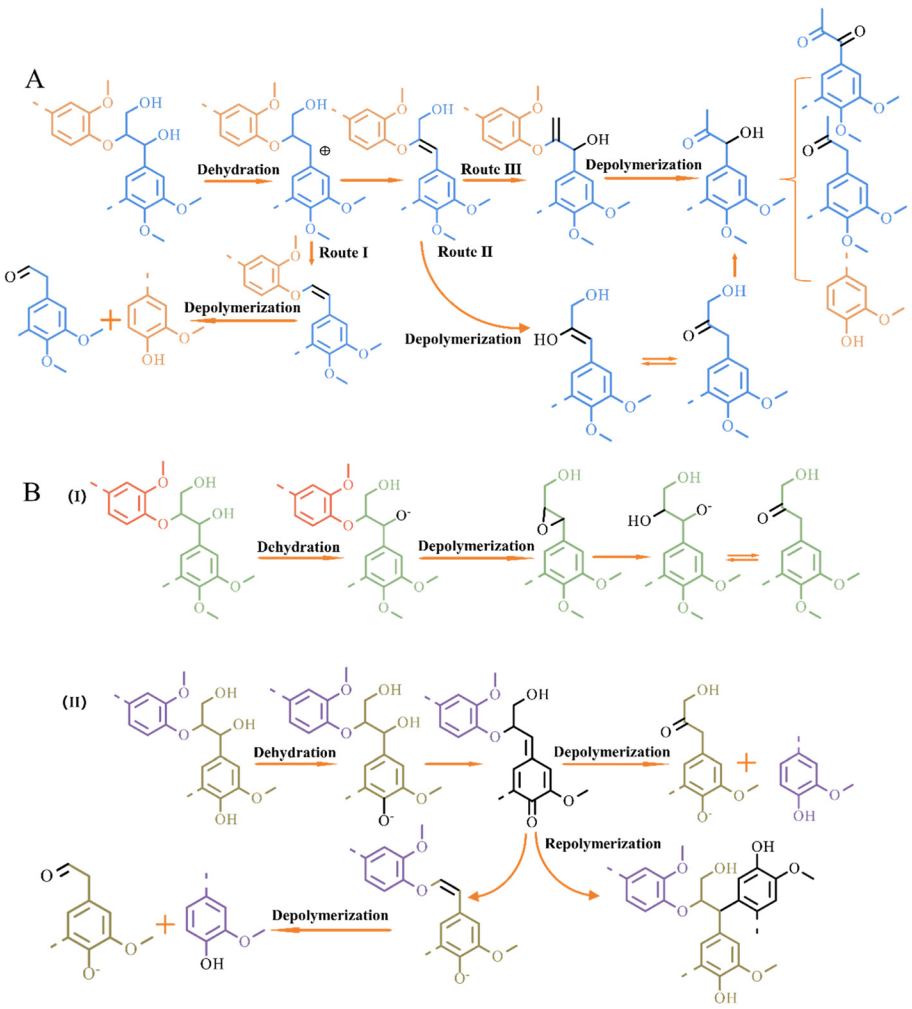

Fig. 7 Mechanism of lignin dissolution in DES. (A) Lignin solubilization occurs *via* three primary pathways in acidic DES. (B) Lignin solubilization follows two main pathways in alkaline DES. Adapted with permission from ref. 68. Copyright 2020, Royal Society of Chemistry.

ily as solvents, enabling lignin extraction while preserving structural integrity. In contrast, under more severe conditions, particularly in acidic DESs (Brønsted or Lewis acidic components) promote β-O-4 ether bond cleavage *via* elimination, carbocation formation, and hydrolysis pathways, indicating a transition to a reactive medium. This behavior is governed by DES composition, acidity, and operating conditions (*e.g.*, temperature, time, and water content), which determines whether solvation or chemical transformation dominates. For example, van Erven *et al.*[187] showed that DES components can covalently incorporate into lignin during pulping, confirming their active role in lignin modification. Thus, distinguishing between solvation-dominated and reaction-driven regimes provides a practical framework for DES design: weaker, interaction-driven systems favor lignin extraction, whereas more acidic or catalytic DESs enable targeted depolymerization.

Taking [Ch]Cl/LA DES as an example, its mechanism for biomass fractionation likely involves hydrogen bonding between chloride ions (Cl^-) in [Ch]Cl and hydroxyl groups (–OH) in LCC.[217] This weakens the LCC structure. The acidic protons from the hydrogen bond donor then help cleave ester bonds, selectively removing lignin.[164] This mechanism has been supported by several studies,[65,218,219] including recent work by Liu *et al.*[220] and He *et al.*[221] In addition, Liu and colleagues also developed a ternary DES by adding polyethylene glycol 400 (PEG 400) to the [Ch]Cl/LA DES system to pretreat eucalyptus wood, and this ternary DES achieved a delignification efficiency of 89.7%, which was significantly higher than the binary system.[220] Further analysis showed that the hydroxyl groups of PEG 400 formed hydrogen bonds with lignin, and the good miscibility of PEG with [Ch]Cl/LA allowed for additional hydrogen bond formation. PEG 400 thus acted as a molecular bridge between lignin and [Ch]Cl/LA, improving lignin solubilization and delignification efficiency.[222] This finding offers valuable insights into how ternary DESs enhance lignin removal. Wang *et al.* studied lignin solubility in DES using Hansen solubility parameters.[223] Their results showed that dispersion forces, polarity, and hydrogen bonding interactions all significantly influenced lignin dissolution. These findings emphasize the importance of intermolecular interactions, especially hydrogen bonding is effective in biomass fractionation. Moreover, the closer the solubility parameters of the DES and lignin, the solubility of lignin is higher.[124]

6. Methods for DES recovery

Currently, biomass fractionation using DES mainly focuses on dissolving lignin while preserving cellulose and hemicellulose for further use in enzymatic hydrolysis and value-added chemical production.[224,225] Efficient recovery of DES and separation of dissolved biomass components such as lignin remain critical challenges.[173,226,227] Given the diverse chemical properties of DESs and the wide variability of lignin-derived products, separation strategies must be carefully tailored to the specific system.[228] Several emerging techniques have been developed for DES recovery, including anti-solvent precipitation, liquid–liquid extraction, membrane separation, electrodialysis, and freeze-drying. Each method offers distinct mass transfer characteristics and opportunities for process intensification.[229,230]

6.1 Antisolvent method

The antisolvent method is one of the simplest and effective techniques for recovering DESs. Antisolvents can change the properties of DESs by breaking the hydrogen bond network between HBA and HBD, which leads to the precipitation of dissolved lignocellulosic components.[57] After separating the solid residue, the DES can be recovered from the antisolvent by performing evaporation or distillation.[156] Water, ethanol and acetone are the most common antisolvents. Thermodynamics models such as COSMO-RS can be employed to screen suitable anti-solvents for DES and biomass component separation. Mohan *et al.* performed COSMO-RS calculations to screen antisolvents for the separation of ionic liquids and carbohydrates.[231] Further, they performed molecular dynamics (MD) simulations and quantum chemistry (QC) calculations to understand the interactions between antisolvents and IL, and antisolvents and carbohydrate. It is also important to note that the recovered DESs may contain impurities or degradation products from lignocellulosic biomass, resulting in lower purity.[230,232,233] Adding water to a DES–lignin mixture decreases lignin solubility and promotes its precipitation. For instance, Cheng *et al.* reported that more than 90% of lignin could be recovered using aqueous antisolvent precipitation from a [Ch]Cl–BDO–$AlCl_3$ (25 : 50 : 1 molar ratio) DES across seven extraction cycles. However, the recovery efficiency decreases over repeated cycles due to the gradual loss of DES components through antisolvent carryover.[234] Further, Yan *et al.* showed that adding oxalic acid to ethanol-based recycled DES helped maintain its pretreatment performance for up to 10 cycles.[235] Despite its advantages, the antisolvent method requires significant volumes of solvent, which increases the energy cost for recovery and purification.

6.2 Extraction method

The extraction process is based on the principle of selective solubility, where one component dissolves more easily in the extractant. This method is used for the recovery of DESs or the separation of desired products from DESs.[236,237] Extraction methods are classified into liquid–liquid extraction and solid–liquid extraction.[238,239] Liquid–liquid extraction is a promising technique for separating lignin and recovering DESs, using an organic solvent that selectively dissolves lignin while keeping the DES components undissolved.[240] Recently, Naik *et al.*[241] and Verma *et al.*[125] used MD simulations to design extractants and study their interactions with DESs and target compounds. However, both liquid–liquid and solid–liquid extraction methods have inherent limitations in completely separating dissolved biomass and its degradation products.[242,243] As a result, the recovered DESs often contain impurities, which

reduce their effectiveness for reuse.[244–246] Additionally, these extraction processes typically require large amounts of solvents, further limiting their scalability and practicality.[247,248]

6.3 Membrane separation technologies

Membrane separation methods such as ultrafiltration (UF) and reverse osmosis (RO) are gaining interest due to their low energy use and solvent-free operation.[249] UF separates the lignin from DES based on size exclusion, while RO can efficiently reject specific molecules. Gholami *et al.* demonstrated that a polyethersulfone UF membrane with a 5000 Da molecular weight cutoff (MWCO) can effectively reject lignin (molecular weight >200 g mol^{-1}) with a rejection ratio of ~0.85–0.90, while allowing DES components (LA and [Ch]Cl) to pass through.[147] However, membrane fouling and flux decline were found, contingent on DES and lignin concentrations with elevated concentrations resulting in augmented filtration resistance.[147] Notwithstanding the challenges encountered, UF remains a viable option for the initial purification of DES solutions before subsequent processing.

Electrodialysis (ED) and bipolar membrane electrodialysis (BMED) have also been successfully applied for the selective recovery of DES constituents. Electrodialysis is a membrane separation process that uses ion-exchange membranes and an electric field to selectively transport ions, making it particularly effective for separating ionic components from DES. Liang *et al.* reported a membrane-based methodology combining UF and ED for the recovery of choline chloride ([Ch]Cl) and ethylene glycol (EG) from a DES used in biomass fractionation. The utilization of ED in conjunction with [Ch]Cl (an electrolyte) facilitated the efficient transfer of [Ch]Cl across ion-exchange membranes, while EG (a non-electrolyte) was retained, thereby achieving recovery ratios of 92% and 96%, respectively, with purities exceeding 98%.[250] In a similar manner, Liang and Guo utilized BMED for the divisional recovery of Ch^+ and Cl^- as choline hydroxide ([Ch][OH]) and hydrochloric acid (HCl), which were subsequently recombined to regenerate the DES.[251] This approach resulted in a DES recovery ratio of 97.4%, with a specific energy consumption of 6.0 kWh kg^{-1}, thereby demonstrating high efficiency and economic viability.[251] Liang *et al.*[252] investigated a process that combines UF with BMED to recover [Ch]Cl–urea (1 : 2 molar ratio) after pine biomass pretreatment. Their results showed that this system could maintain pretreatment efficiency for at least four reuse cycles. The operating cost of the UF-BMED process ranged from only 3% to 32.2% of the market price of the DES. Similarly, Zhang *et al.*[253] reported a 97.6% recovery of a carboxylic acid–polyalcohol-based DES using the same UF-BMED method, with consistent pretreatment performance after four reuse cycles. Whilst membrane-based techniques offer high recovery efficiency and selectivity, factors such as membrane cost, fouling mitigation, and energy consumption must be considered in order to ascertain their scalability and economic feasibility. It is recommended that future research efforts concentrate on the optimization of operating conditions, including but not limited to transmembrane pressure, feed flow rate, and membrane material.[254] This approach is expected to enhance long-term stability and concurrently reduce operational costs.

6.4 Other methods

In addition to the commonly used antisolvent method, other separation techniques for DES include rotary evaporation, nanofiltration,[147,255,256] lyophilization, *etc.* Lyophilization or freeze-drying involves rapid freezing of the DES–lignin mixture and then removing the solvent by sublimation under reduced pressure. This method is effective for recovering DES with high purity; however, its industrial application is limited due to the high energy consumption and long processing times.[257] Jeong *et al.*[258] demonstrated the effectiveness of lyophilization for recovering DES composed of glycerol, L-proline, and sucrose after saponin extraction. The freeze-dried DES retained 83% of its original extraction efficiency after three cycles, showing good recyclability.

Some studies have developed integrated separation systems that combine dialysis, membrane filtration, and vacuum distillation, showing promising results in isolating and purifying lignin from DESs.[109] However, these methods are more complex, time-consuming and expensive compared to antisolvent methods.[259]

Table 7 reports on the quantitative comparison of energy requirements for DES recovery methods.[147,230,251,257] From an energy perspective, significant differences exist among DES recovery methods due to their distinct driving forces. Antisolvent methods are constrained by the high latent heat of solvent evaporation.[230] Although membrane-based separations offer relatively low energy consumption, their large-scale implementation is challenged by membrane fouling, reduced flux, and limited selectivity in complex DES–biomass mixtures, which can increase operational costs and reduce long-term process stability.[147,260] In contrast, electrodialysis and freeze-drying provide high recovery purity at the expense of substantially higher energy inputs, potentially restricting their scalability for industrial applications.[251,257,258]

7. Techno-economic and life cycle assessment analysis

7.1 Techno-economic analysis of biomass pretreatment using DES

Techno-economic analysis (TEA) evaluates both the technical performance and economic feasibility of a chemical process.[261] Many studies have demonstrated that DESs are technically effective for pretreating lignocellulosic biomass, showing high delignification efficiency and improved enzymatic hydrolysis.[262] This section focuses on assessing the economic potential of DES-based pretreatment. Current research on the TEA of DESs pretreatment exhibits significant gaps, particularly in woody biomass applications. Generally, TEA analysis includes biomass characterization, DES compatibility analysis, process cost estimates, market potential evalu-

Table 7 Quantitative comparison of energy requirements for DES recovery methods

Recovery method	Primary energy driver	Typical energy consumption (MJ kg^{-1} DES)	Recovery efficiency (%)	Key energy-related challenges	Techno-economic viability	Ref.
Antisolvent (water/ethanol)	Solvent evaporation	15–40	80–90	High latent heat of water evaporation; antisolvent loss (5–15% per cycle)	Moderate: suitable for small-scale but energy-intensive for industrial scale	230 and 392
Membrane filtration (UF/NF)	Pumping (pressure gradient: 5–20 bar)	15–30	>90	Membrane fouling increasing pressure; cycles adding energy; membrane replacement	High: suitable for continuous operation	147 and 260
Electrodialysis (ED/BMED)	Electric field (ion migration)	10–60	>90	High electrical energy consumption; electrode cleaning; membrane degradation	Moderate: high energy cost offset by high purity recovery	251 and 252
Freeze-drying (lyophilization)	Sublimation (vacuum + low temperature)	>100	80–90	Extremely energy-intensive; long processing time (24–48 h); high capital cost	Low: unsuitable for industrial scale; limited to high-value products	257 and 258
Supercritical CO_2 extraction	Pressurization (70–300 bar) + cooling	10–40	80–95	High capital cost for high-pressure equipment; energy for compression and cooling	Moderate: emerging technology; promising for thermosensitive compounds	230 and 393

ation for bio-based products, and sensitivity and risk analyses.[263]

A comprehensive study conducted by Zang *et al.*, simulated DES pretreatment of switchgrass for the co-production of 2,3-butanediol (BDO), furfural, and industrial lignin.[264] Their TEA showed that the minimum selling price (MSP) of BDO was between \$1703 and \$1736 per ton, about half the market price, suggesting good commercial potential. Aspen Plus and Aspen Process Economic Analyzer were used for process modeling. When compared with dilute acid pretreatment for bioethanol production (MESP ranging from approximately \$2.15 per gal to \$2.54 per gal), DES-based BDO production exhibits promising economic viability, though direct comparison is hindered by the differing target products.[265] Similarly, Kumar *et al.* used the advanced interactive multidimensional modeling system (AIMMS) to simulate a biorefinery processing 1 ton per day of various lignin-rich feedstocks with a natural DES (NADES) composed of [Ch]Cl and lactic acid (LA).[266] Their model reported a net present value (NPV) of \$1.4 million, an internal rate of return (IRR) over 100%, and a payback period under two years, indicating excellent economic feasibility compared to traditional biorefineries. In comparison, an organosolv-based biorefinery processing 30 000 t per year of olive leaves achieved an NPV of \$47.9 million but a lower IRR of 27.8%, while an alkali pretreatment process for corncob residue demonstrated a shorter payback period of 0.96 years.[267] These comparisons suggest that, although DES-based systems can exhibit exceptionally high returns and rapid cost recovery, their economic performance is highly sensitive to factors such as feedstock characteristics, product distribution, and process scale, and therefore may not universally outperform conventional technologies.[267] Zhao *et al.*[268] employed SuperPro Designer, a leading process simulation software, to model an integrated biorefinery system for the co-production of lignin and 5-hydroxymethylfurfural (HMF) from corn stover *via* a two-stage DES ($ZnCl_2$/LA) and ionic liquid pretreatment.[268] The process achieved a 55% HMF yield and a minimum selling price (MSP) of \$16 453 per ton with a 10% IRR. Capital expenditure was reduced from \$659 million to \$613 million, demonstrating process optimization potential. When benchmarked against dilute acid pretreatment, which typically requires capital investments of a similar magnitude for corn stover-to-ethanol processes,[265,269] the reported reduction in capital expenditure emphasizes a key advantage of DES systems (the potential for milder operating conditions that lower equipment costs).

In addition, Huang *et al.* conducted a TEA on rice straw pretreatment using a [Ch]Cl/LA DES and achieved a total product yield of 75.7%.[270] The sugar production cost ranged from \$0.12 to \$0.17 per gram, suggesting competitive economic feasibility for the proposed biorefinery configuration. By comparison, a minimum sugar selling price of \$0.285 per pound (approximately \$0.00063 per gram) has been reported for an ammonium sulfite-based alkali pretreatment of corn stover; however, direct comparison is complicated by differences in sugar concentrations and purity requirements.[271] Peng *et al.* used Aspen Plus to evaluate the economic feasibility of rice straw pretreatment using two DESs of [Ch]Cl/urea and [Ch]Cl/LA for the production of bioethanol and lignin.[272] The MSP for bioethanol was \$3049.9 per ton with [Ch]Cl/urea and \$2128.1 per ton with [Ch]Cl/LA, respectively (Fig. 8). These studies collectively validate the commercial feasibility of DESs pretreatment technology for industrial-scale biorefineries and provide critical benchmarks for scaling up DES-based pretreatment processes, thereby facilitating the transition from laboratory-scale to commercial processing.

Despite these promising results, TEA studies focused on woody biomass remain limited. One critical factor affecting the economic feasibility of DES processes is the reusability of the solvent. For instance, He *et al.* developed a ternary DES

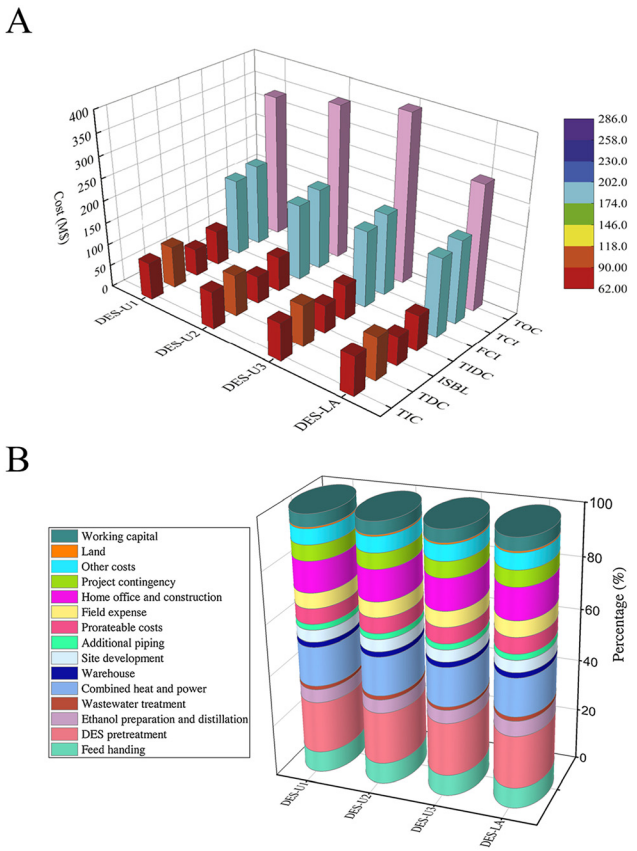

Fig. 8 (A) Total capital and operating cost of the process with integrated combined heat and power (CHP). (B) Cost distribution of total capital investment for four DES pretreatment processes. Reproduced with permission from ref. 272. Copyright 2021, Elsevier.

composed of [Ch]Cl/glycerol/sulfuric acid for efficient poplar biomass pretreatment and reused the solvent in red yeast fermentation for microbial oil production.[273] From 5 kg of biomass and 10 kg of DES, they obtained 693.2 g of ethanol and 1200 g of microbial lipids. Even after multiple reuse cycles, the DES maintained its pretreatment efficiency. Although delignification and hemicellulose removal decreased slightly, lignin yield and enzymatic hydrolysis efficiency remained high (78.3% after four cycles). Further, Analytical studies showed that [Ch]Cl remained stable and was not consumed by microbes, allowing it to be reused. This closed-loop strategy improves the economic and environmental sustainability of DES-based processes by reducing chemical costs. This breakthrough establishes a transformative pathway for addressing the longstanding challenge of high operational costs in lignocellulosic biomass valorization. Comparatively, solvent recovery is especially challenging in organosolv pretreatment, where regeneration drives costs. Dilute acid pretreatment, though using cheaper acids than DES, incurs significant costs from neutralization and waste treatment.[274] Consequently, DES reusability provides a clear economic advantage over both organosolv (energy-intensive distillation) and dilute acid (neutralization waste). Zhao *et al.*[268] also studied a ternary DES ($ZnCl_2$/EG/MA) and found that it maintained high performance over four cycles. After pretreating 100 g of willow biomass with 1000 g of DES, the system achieved 96.0% enzymatic hydrolysis and 85.6% delignification. Even in the fourth cycle, it retained over 70% delignification efficiency and 83.7% sugar yield, demonstrating strong recyclability and operational durability.[182] However, not all DES show good recycling performance. For example, the DES composed of PBA and [Ch]Cl showed a sharp decline in delignification efficiency from 69% to 49% in the second cycle.[181] This investigation establishes that DESs derived from phenolic compounds may need further optimization for repeated use. To optimize the potential circular economy of the system, further comprehensive research is required to characterize the physicochemical properties of recycled DES and elucidate its pretreatment performance mechanisms. Comparisons of key performance indicators, environmental metrics, economic considerations and durability data for DES-based biomass pretreatment are shown in Table 8.

Despite the impressive recyclability reported for certain DES systems, a more critical examination of overall process economics reveals that the solvent recovery bottleneck remains a formidable challenge to commercial viability.[230] In particular, the energy required to distill large volumes of antisolvents, such as water and ethanol from post-pretreatment streams is highly problematic. As critically assessed by Isci and Kaltschmitt,[230] the selection of an appropriate recovery method must account not only for DES properties and target product characteristics but also for energy consumption and associated equipment costs.[230] Energy analysis by Ntihuga *et al.*[275] further demonstrated that high thermal energy demand, primarily for steam used in solvent and ethanol recovery, dominates operational expenses, and that auxiliary material flows often remain substantial despite internal recycling. This mass-transfer and energy-balance limitation implies that even if a DES itself is cheap to synthesize, downstream separation costs can negate its initial economic advantage, positioning solvent recovery as the primary hurdle for the industrial-scale implementation of DES-based pretreatment processes.

Overall, these findings show that DESs offer promising economic advantages for biomass processing. More TEA studies, particularly for woody biomass, are required to identify optimal DES formulations and improve process design. The lack of a publicly available database of DES properties is a major barrier. Developing a comprehensive, large-scale DES property database would greatly support commercial viability assessments and risk analysis for future DES-based biorefineries.

7.2 Life cycle assessment of DES-based biomass pretreatment

Life cycle assessment (LCA) is a standardized method for quantitatively evaluating the environmental impacts of a product or process, and it is regulated by the International Organization for Standardization (ISO) under ISO 14040:2006

Table 8 Comparisons of key performance indicators, environmental metrics, economic considerations and durability data for DES-based biomass pretreatment

Biomass	DES system	Key performance indicators	Environmental metrics	Economic considerations	Durability data	Ref.
Corn stover	DES ($ZnCl_2$/LA) + IL([EMIM]Cl) + metal catalysts ($CuCl_2$–$CrCl_2$)	HMF yield: 55%	Environmentally benign reaction media	MSP of HMF: \$16 453 MT^{-1}; production capacity: 100 MT h^{-1}	$ZnCl_2$/LA recycling 5 times; $CuCl_2$–$CrCl_2$–[EMIM]Cl recycling 10 times	268
Rice straw	[Ch]Cl/urea, [Ch]Cl/LA	Bioethanol production: 0.21 t per t biomass ([Ch]Cl/LA)	Producing few toxic inhibitors and exhibiting high recovery rate	MSP of bioethanol: \$3049.9 per ton ([Ch]Cl/urea) and \$2128.1 per ton ([Ch]Cl/LA)	Recovery of 95% DES by multistage flash evaporation and distillation	272
Engineered poplar	[Ch]Cl/Gly	20.4 g ethanol per 100 g biomass	One-pot processing with biocompatible DESs with no water-washing, separation, or pH adjustment	—	Recovery of DES by evaporation or separation; thermally stable	394
Willow	$ZnCl_2$/EG/MA	Xylan removal: 91.7%; lignin removal: 90.2%; glucose yield: 96.0%	Green solvent	—	After 4 cycles: >70% of delignification; 83.7% of glucose yield	182
Poplar and *miscanthus*	*p*-TsOH/[Ch]Cl + NaOH	Near complete cellulose conversion and over 90% of delignification and xylan removal	Recyclable, low toxicity	—	—	161
Wheat straw	[Ch]Cl/oxalate dihydrate	Low-cost pellets with high heating value, durability and water stability	GWP: 0.05–0.08 kg CO_2-eq per MJ; AP: 0.2–0.4 g SO_2-eq per MJ	Low cost	Recovery of DES by heating the filtered liquid	279
Microalgae	DES-assisted hydrothermal disintegration	Increasing the energy output by 36.33%	GHG emissions: 26.04 g CO_2-eq per MJ; NER: 0.83	—	Low NER (0.58) for DES recovery *via* membrane filtration and recrystallization	280
Codfish skin waste	Urea/LA + water	Collagen type I extraction yield: 6%	Global warming: 1.03 kg CO_2-eq per 1 g of collagen; terrestrial acidification: 3.94 g SO_2-eq per 1 g of collagen	Lower cost compared to neat DES	—	80

LA: lactic acid. Gly: glycerol. EG: glycolic acid. MA: malic acid. MSP: minimum selling price. NPV: net present value. GWP: global warming potential. AP: acidification potential. GHG: greenhouse gas. NER: net energy ratio.

and ISO 14044:2006.[276] An LCA study typically involves four key stages: (1) defining objective and scope, (2) compiling a life cycle inventory, (3) conducting an impact assessment, and (4) interpretation of results. LCA quantifies the environmental impacts across the entire supply chain, from raw material extraction to manufacturing, use, and end-of-life disposal. Impact categories often include global warming potential, acidification, human toxicity, ozone depletion, and others. These indicators help assess the overall environmental sustainability of a process (see Fig. 9).

Compared to TEA, studies applying LCA to evaluate DES-based pretreatment of lignocellulosic biomass are still limited. However, LCA data of DESs in other domains are available and can provide valuable insights that can guide future biomass-related studies. Sun *et al.* conducted an LCA on DES pretreatment of woody biomass to traditional chlorite–alkaline hydrolysis.[277] Their analysis included categories such as climate change, human toxicity, and ecotoxicity in marine and freshwater environments. The results showed that the conventional method had 7.2 times more overall environmental impact than the DES-based approach. In another study, Zaib *et al.* evaluated the environmental performance of a widely used DES system ([Ch]Cl/urea), against common organic solvents such as methanol, ethanol, methylene chloride, and ethyl acetate.[278] The findings indicated that DESs had lower environmental impacts than methylene chloride and ethyl acetate but higher impacts compared to methanol and ethanol. Guo *et al.* investigated the use of a [Ch]Cl/oxalate dihydrate DES for partial dissolution of wheat straw to produce lignin-rich energy pellets and conducted a corresponding LCA.[279] The study used metrics such as global warming potential (GWP, in CO_2-equivalents), acidification potential (AP, in SO_2-equivalents), and cumulative energy demand (CED, in MJ). DES-treated pellets showed a GWP of 0.05–0.08 kg CO_2-eq per MJ, which was considerably lower than that of traditional lignin-based pellets. The AP values (0.2–0.4 g SO_2-eq per MJ) were similar. These results support the environmental advantages of using DES in pellet production. Moreover, the study found that most of the environmental burden originated from the DES itself, suggesting that improvements like reducing solvent dosage or increasing reuse cycles could further lower the impact.

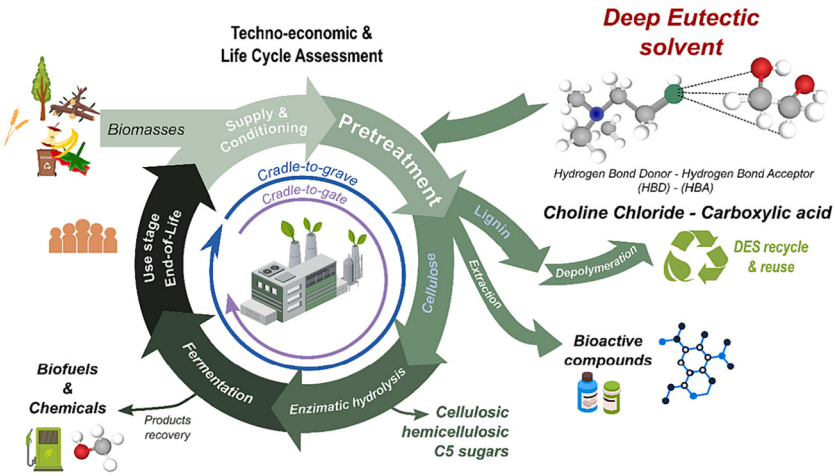

Fig. 9 General framework of an illustrative life cycle assessment for biomass valorization using deep eutectic solvents in the pretreatment stage. Reproduced with permission from ref. 156. Copyright 2023, Elsevier.

Apart from biomass applications, LCA studies in other research areas provide useful guidance. For instance, Song *et al.* performed a TEA on DES-based hydrothermal decomposition (HTD) of microalgae for biodiesel and biogas production.[280] They assessed the process using net energy ratio (NER) and greenhouse gas (GHG) emissions. Utilizing DES improved energy output, but it also significantly raised the energy input due to high synthesis demands, increasing NER from 0.65 to 0.83. GHG emissions rose from −25.53 to 26.04 g CO_2-eq per MJ. Bisht *et al.* carried out an LCA comparing various DES systems and acetic acid for collagen extraction from cod skin waste.[80] They used global warming, ozone formation, human health effects, acidification, and resource scarcity as performance metrics. Electricity consumption was the main contributor, accounting for 51–77% of the total environmental impact. The study emphasized that switching to renewable electricity sources, such as photovoltaic power, could reduce the carbon footprint by up to 69%. Reducing total electricity consumption was also identified as an effective strategy for lowering the overall environmental burden.

From an LCA perspective, the solvent recovery phase, specifically the energy-intensive distillation of antisolvents used to precipitate lignin and other value-added products, is a critical environmental hotspot. Wang *et al.*[281] conducted a prospective LCA of a scaled-up multicomponent DES pretreatment system and found that, while solvent recovery reduces environmental impacts by at least 67% across all midpoint categories compared to laboratory-scale operations, sensitivity analysis identified DES recovery efficiency as the key driver: increasing recovery from 50% to 90% cuts environmental impacts by approximately 70%. This finding underscores two interrelated points: (i) the environmental benefits of DES-based pretreatment are highly dependent on achieving high solvent recovery efficiencies, and (ii) the energy-intensive nature of antisolvent distillation, requiring the evaporation of large volumes of water or ethanol, can substantially offset the inherent sustainability advantages of DESs. Similarly, Putranto *et al.*[282] systematically reviewed LCA studies on DES-based nanocellulose production and concluded that pretreatment chemicals contribute substantially to global warming potential, and that maintaining DES recovery rates in the range of 80–95% is essential to minimize environmental burdens. Collectively, these critical assessments highlight that failing to address the energy burden of solvent recovery risks calling into question the environmental sustainability claims of DES-based biorefineries. Therefore, future process development must prioritize low-energy separation strategies, such as membrane-based technologies or electrodialysis, over conventional distillation approaches.

Many existing LCAs of DES-based pretreatment use cradle-to-gate system boundaries and do not clearly report allocation methods, especially for multifunctional DES systems and co-products.[263,283] In addition, different impact assessment methods (*e.g.*, ReCiPe *vs.* CML) can lead to variations in reported results. A consistent observation across studies is that electricity consumption is the main contributor to environmental impacts, mainly due to energy-intensive solvent recovery steps such as antisolvent distillation.[284,285] This suggests that the overall sustainability of DES-based processes depends strongly on reducing energy use. From a green chemistry perspective, this challenge also provides an opportunity for improved process design. DES-based systems can be made more sustainable by lowering energy demand through process intensification, operating under milder conditions, and adopting alternative recovery methods such as membrane separation or electrodialysis. In addition, the use of renewable energy sources can further reduce the environmental footprint.

Overall, there is still a significant research gap in implementing LCA to DES-based pretreatment of lignocellulosic biomass. In addition to TEA, LCA is a powerful tool for evaluating the environmental sustainability of these emerging processes. Implementing LCA early in the development of DES

systems allows for a quantitative understanding of environmental impacts and helps identify critical areas for improvement. This approach is essential for promoting the industrial adoption of greener and more sustainable biomass pretreatment technologies using DESs.

8. Computational studies for understanding lignocellulosic biomass pretreatment using deep eutectic solvents

Experimental studies provide useful conclusions for the dissolution and delignification of biomass; however, they lack a molecular-level understanding. Computational methods, such as density functional theory (DFT), Conductor-like Screening Model for Real Solvents (COSMO-RS), and molecular dynamics (MD) simulations, can provide structural details at the atomic and molecular level, and thus many results have been reported for dissolution and conversion mechanisms based on these techniques.[73,188,286–288]

The COSMO-RS model has been extensively utilized to screen solvents for cellulose dissolution as well as further conversion. In the COSMO-RS method, screening charge densities obtained from quantum chemical calculations are used to calculate the chemical potential of solutes. This method has been applied to predict the solubility of solutes in different solvent environments such as ILs and DESs. Recently, Zhou *et al.*[150] screened 260 DESs for lignin and biomass dissolution using the COSMO-RS model. In their study, the authors used four lignin dimers and four LCC structures as model compounds to screen DESs by calculating the logarithmic activity coefficients ($\ln(\gamma)$) of lignin/LCC in DESs. As per the solid–liquid equilibrium assumptions, the activity coefficient is inversely proportional to the solubility of the solute.[211] A low activity coefficient of lignin/LCC in DESs indicates high solubility of lignin/LCC. He *et al.*[289] calculated the $\ln(\gamma)$ and excess enthalpy of cellulose, hemicellulose, and lignin in seven DESs using the COSMO-RS model. Five monomeric units were used to construct cellulose and hemicellulose, whereas a trimer was used for lignin. K_2CO_3–EG was reported as an effective solvent for high lignin and hemicellulose dissolution. In another study, He *et al.*[290] screened tetramethylammonium hydroxide (TMAH)-based DESs for lignocellulosic biomass solubility. The calculations showed that TMAH-based DESs displayed good solubility for lignocellulose due to their lower $\ln(\gamma)$ and excess enthalpy, and strong hydrogen bonding forces (Fig. 10). A delignification rate of 63.33%–67.37% was achieved without compromising the carbohydrate recovery by using TMAH-based DESs at lower temperatures, and the cellulose and hemicellulose retention was over 90%. Several studies have screened different sets of DESs for lignocellulosic biomass solubility.[150,289,290] However, these investigations explored only a limited chemical space, evaluating just 260 DESs in total.

There have also been a few studies reporting the dissolution mechanism of cellulose, hemicellulose, and DESs using DFT and MD simulations. Wang *et al.*[211] performed multiscale molecular simulations (DFT and reactive MD) to elucidate the complex molecular interactions between lignin and [Ch]Cl-based DES. It has been reported that the chloride anion of HBA plays a major role in the solvation of lignin by forming strong hydrogen bonds with the hydroxyl groups of lignin (syringylglycerol-*β*-syringyl (SS) ether dimer as lignin model structure). In addition, Li *et al.*[56] showed that the ability of DESs to dissolve lignin strongly depends on hydrogen bonding between DES constituents and lignin. DESs based on [Ch]Cl with various HBDs such as formic acid, lactic acid, and ethylene glycol (EG) show distinct hydrogen bond patterns. EG preferentially forms H-bonds with α-OH groups, while lactic and formic acids target γ-OH groups of lignin. Also, Cl^- ions play an equivalent role to HBD in stabilizing interactions with lignin. Furthermore, MD simulations revealed how DES–lignin interactions are critical for separating lignin from cellulose. DESs with stronger H-bonding (*e.g.*, [Ch]Cl–formic acid) weaken lignin's interaction with cellulose as compared to [Ch]Cl–EG.[56] Further, reactive force field MD simulations were performed to understand the depolymerization mechanism of LCC in the DES environment. Notably, the decarboxylation reaction of the *p*-coumaric acid (*p*CA) ester occurred, resulting in the dissociation of *p*CA along with lignin. Further investigation demonstrated that various DES adducts were formed through etherification and acetylation reactions, and the reaction pathways and quantities were systematically simulated.[211] Miao *et al.*[291] investigated the dissolution mechanism of lignin (guaiacylglycerol-*β*-guaiacyl ether (GG) dimer as a model structure for lignin) in [Ch]Cl-based DESs using MD simulations and reported that the difference between interaction energies of lignin-[Ch]Cl/OA and lignin-[Ch]Cl/OA/EG systems was not significant. Further, diffusion coefficients were positively correlated with biomass pretreatment efficacy: faster lignin diffusion indicated better solubilization, aligning well with experimental biomass pretreatment.

Further MD simulations and DFT calculations have been performed to understand lignin dissolution and *β*-O-4 bond preservation in DESs.[292,293] The molecular simulation results confirmed that ethylene glycol (EG) and 1,2-butanediol (1,2-BD) protect the β-O-4 linkages in lignin by forming ether bonds at the α-position of lignin chains.[40] These nucleophilic attacks by diols inhibit condensation and stabilize lignin structures. DFT calculations showed that such α-etherification increases the energy barrier for unwanted condensation reactions. This helps in preserving native lignin that is suitable for valorization. This mechanistic insight was supported by NMR analysis and correlated with a 74.7% lignin removal and 91.6% cellulose digestibility. Wang *et al.* performed MD and DFT calculations, and the simulation results revealed that DESs disrupt the hydrogen bonding network within lignocellulosic biomass and form new hydrogen bonds with DES components.[294] [Ch]Cl–urea was an effective solvent in disrupting up to 78.4% of native hydrogen bonds between cellulose

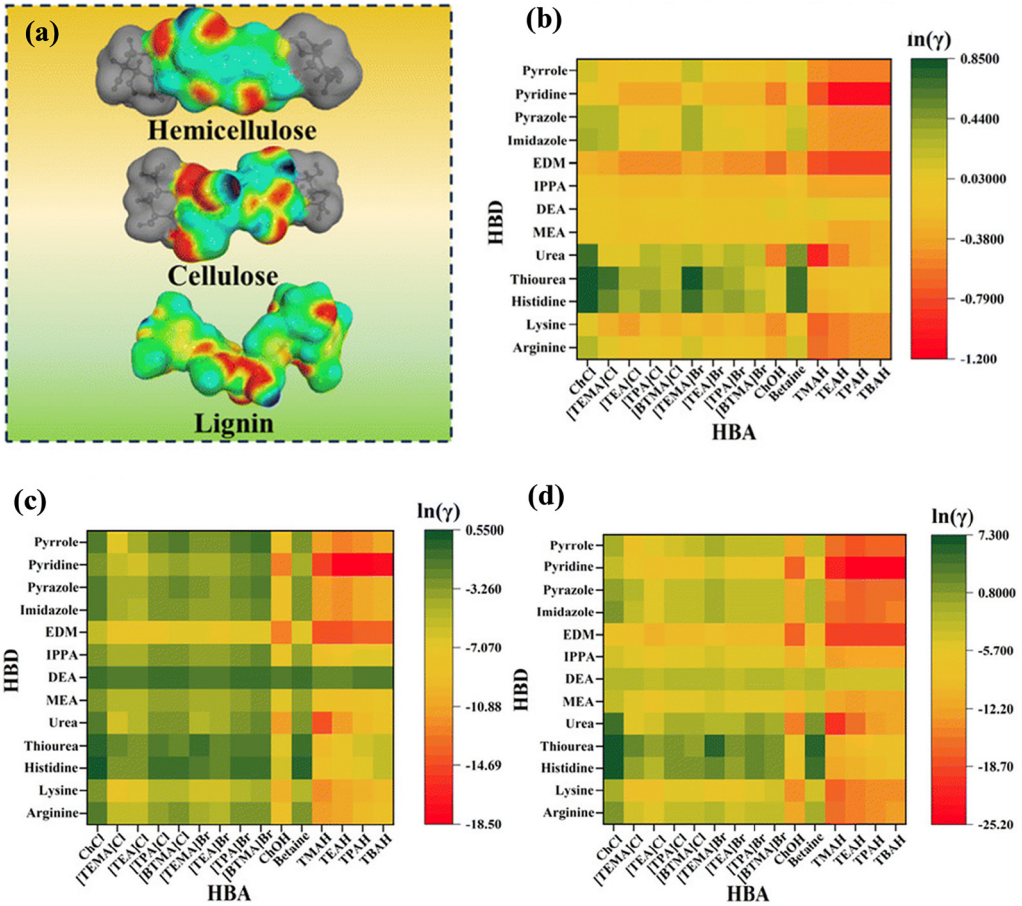

Fig. 10 (a) 3D-representation of cellulose (mid-dimer of glucotetrose), hemicellulose (mid-dimer of xylotetrose), and lignin (dimer) structures along with their COSMO cavities. The COSMO-RS calculated ln(γ) of (b) cellulose, (c) hemicellulose and (d) lignin model in different solvent systems. Reproduced with permission from ref. 329. Copyright 2025, Royal society of chemistry.

and lignin/hemicellulose. Further, in systems like [Ch]Cl/DEA/EG DES, ethylene glycol as the primary HBD, competing for –OH sites on the lignin surface, weakened hemicellulose–solvent interactions, thus preserving hemicellulose and promoting lignin removal. The structural integrity of glycosidic bonds was preserved due to weaker interaction energies between hemicellulose and DES.[295]

Ma *et al.*[296] combined MD simulations and reduced density gradient (RDG) analysis to show that [Ch]Cl–urea–ethylenediamine ([Ch]Cl–U–EDA) forms strong hydrogen bonds with lignin and the facilitated lignin retains β-O-4 bonds. The extracted lignin was further utilized in hydrogels for yeast immobilization, demonstrating a holistic approach for sustainable biomass conversion. However, the molecular simulations performed for only 10 ns, which is not sufficient for full convergence of lignin polymer dynamics. Moreover, the simulations were conducted only once without replicate runs, thereby lacking the statistical robustness necessary to validate the reported observations. Further, Zhang *et al.*[297] performed MD simulations to compare [Ch]Cl–glyoxylic acid (GA) DES with conventional [Ch]Cl–lactic acid. The [Ch]Cl–GA system showed higher binding energy to lignin, enhancing lignin solubility and preventing C–C condensation. The stabilized lignin retained 69.4% β-O-4 content, enabling further transformation into bio-oil and functional materials. In addition, electrostatic interactions were found to be the primary contributors to total interaction energy.[298] Pan *et al.*[299] implemented MD and DFT to reveal the role of bio-acid tailored ternary DESs (*e.g.*, [Ch]Cl–citric acid–butanediol) in lignin valorization. The simulations showed enhanced carboxylation and lignin–DES interactions that promoted self-assembly into nanospheres, while preserving cellulose structure for nanomaterial fabrication. Wu *et al.*[300] explored the formation of lignin nanoparticles (LNPs) using sulfamic acid–urea DES. Classical MD simulations revealed that hydrogen bonds and π-π stacking interactions drive the self-assembly of lignin. The study also demonstrated that DES breaks internal lignin H-bonding, aiding solubilization and nanoparticle formation while preserving the aromatic core.

Ji and Lv[301] conducted a comparative MD and quantum chemistry study of organic acid, DESs ([Ch]Cl–lactic acid), and ionic liquid ([Amim]Cl). The strongest lignin–solvent interaction energy (ΔE = −15.11 kcal mol^{-1}) was observed for organic acid (*p*-TsOH), attributed to a combination of C–H···π

and strong H-bonding with lignin, explaining superior delignification performance. *p*-TsOH can be utilized as an HBD for DES preparation. Zhou *et al.* performed MD simulations to understand the interactions of acidic DES (citric acid–water–[Ch]Cl) and cellulose. The results demonstrated that DESs disrupt the intra- and inter-molecular hydrogen bonding networks within cellulose chains and increase solvent-accessible surface area (SASA), resulting in the reduction in cellulose crystallinity and aiding in biomass deconstruction. Yan Yu and coworkers[210] performed multiscale molecular simulations, combining *ab initio* MD and DFT to uncover how a [Ch]Cl–oxalic acid DES pretreatment acts on wheat straw biomass. They demonstrated that oxalic acid-enabled acidolysis preferentially cleaves ether linkages in LCCs, removing high hemicellulose (with a 35.6 kJ mol^{-1} barrier and favorable −43.5 kJ mol^{-1} reaction energy; see Fig. 11). Once hemicellulose is removed, the lignin adapts a coil-like structure (confirmed *via* classical MD) strengthening intermolecular lignin–lignin contacts. This structural expansion and rearrangement increase lignin binding in the fiber matrix, which experiments showed leads to improved porosity, densified pellet formation, enhanced mechanical strength, lower moisture uptake, and superior combustion properties. In recent studies, Mohan *et al.*[124] calculated the Hansen solubility parameters (HSP) of lignin and different solvents to understand the correlation between solubility parameters and the solubility of lignin. The solubility parameters (SPs) quantify the affinity between solute and solvents based on the 'like-seeks-like' principle, which is used in chemistry to rapidly screen solvents for dissolution. The closer the values of solubility parameters, the higher the affinity between solute and solvents. Mohan *et al.*[124] modelled the SPs of different lignin types and reported that the SPs range between 24.3–25.5 $MPa^{1/2}$. Metal-based DESs have gained significant attention as solvents for the deconstruction of lignocellulosic biomass and high delignification. The SP of lignin is close to $ZnCl_2$–EG as compared to $ZnCl_2$–glycerol, indicating that lignin has a high affinity with $ZnCl_2$–EG.

8.1. Challenges and critical gaps in molecular simulations

COSMO-RS, DFT, and MD are powerful tools for high-throughput solvent screening and understanding molecular interactions. Studies investigating biomass/DES molecular simulations have predominantly focused on lignin rather than on cellulose and hemicellulose. However, the researchers predominantly used lignin dimers or trimers with the ether (β-O-4) linkage as the model compound for molecular simulations. As discussed above, lignin is a complex, heterogeneous biopolymer primarily composed of three phenylpropanoid units (G, H, and S). These phenylpropane monomers are bonded together by C–O–C ether (β-O-4, α-O-4, and 4-O-5) and C–C interunit (β–β, β-5, β-1, and 5–5) bonds. Simple dimeric or trimeric lignin model structures fail to capture the full diversity of these linkages and monomeric units. For example, the linkage distribution in hardwood lignin typically includes β-O-4 (50–65%), α-O-4 (4–8%), 4-O-5 (6–7%), β–β (3–7%), 5–5 (4–10%), and β-1 (5–7%).[302] The monomeric composition generally consists of G units (25–50%), S units (45–75%), and H units (0–8%).[303] Several computational tools have been developed to generate lignin model structures with defined monomeric units and linkage compositions, including LigninBuilder,[304] Lignin-KMC,[305] LigninGraphs,[306] and SPRIG[307] (Simple Polydisperse Residue Input Generator). These tools enable building lignin polymers with varying degrees of polymerization and polydispersity, facilitating their use in molecular simulations.

Another significant challenge in the field is the limited number of studies that have employed molecular simulations to investigate the interactions of cellulose and hemicellulose with DESs. Despite the growing interest in DESs for biomass pretreatment, most computational efforts have primarily focused on [Ch]Cl-based DESs, particularly those combined with non-ionic hydrogen bond donors (type III DESs). While these systems have provided valuable insights, they represent only a subset of the broader chemical space of DESs. Other DES types, including those involving ionic hydrogen bond donors, metal salts, or alternative hydrogen bond acceptors remain largely unexplored in simulation studies. Expanding molecular simulation efforts to include these underrepresented DES categories is crucial for a more comprehensive understanding of solvent–biomass interactions and for guiding the rational design of next-generation solvents for efficient lignocellulosic biomass deconstruction.

9. Machine learning for predicting biomass pretreatment efficacy in DESs

Molecular simulation studies require substantial computational costs and are, for now, best applied to elucidate underlying molecular mechanisms in the context of using lignocellulosic biomass. As an alternative, machine learning (ML), a sub-field of artificial intelligence (AI), has shown promise as a potential high-throughput screening framework for designing optimal solvents and processing condition optimization. Unlike molecular simulation approaches, ML has the capability to automatically learn and identify patterns and, when coupled with feature importance techniques, can assist in generating mechanistic hypotheses for rigorous testing. AI/ML presents great potential in handling scientific tasks associated with high-dimensional complexity associated with these systems and generates accurate predictive models.[308,309]

Recently, there has been a surge in AI/ML applications for biomass pretreatment and solvent property predictions.[151,310] Several studies have attempted to develop AI/ML models for predicting physicochemical properties of DESs, such as viscosity,[151,311,312] density,[311,313] melting temperatures,[311] ionic conductivity,[314] solvatochromic parameters,[133] *etc.*[107] These physicochemical properties are critical in designing solvents for biomass pretreatment. For example, a solvent with lower viscosity, liquid at room temperature, and has higher hydrogen bonding basicity is a better solvent for biomass deconstruction.[315] Recent advancements in ML have significantly

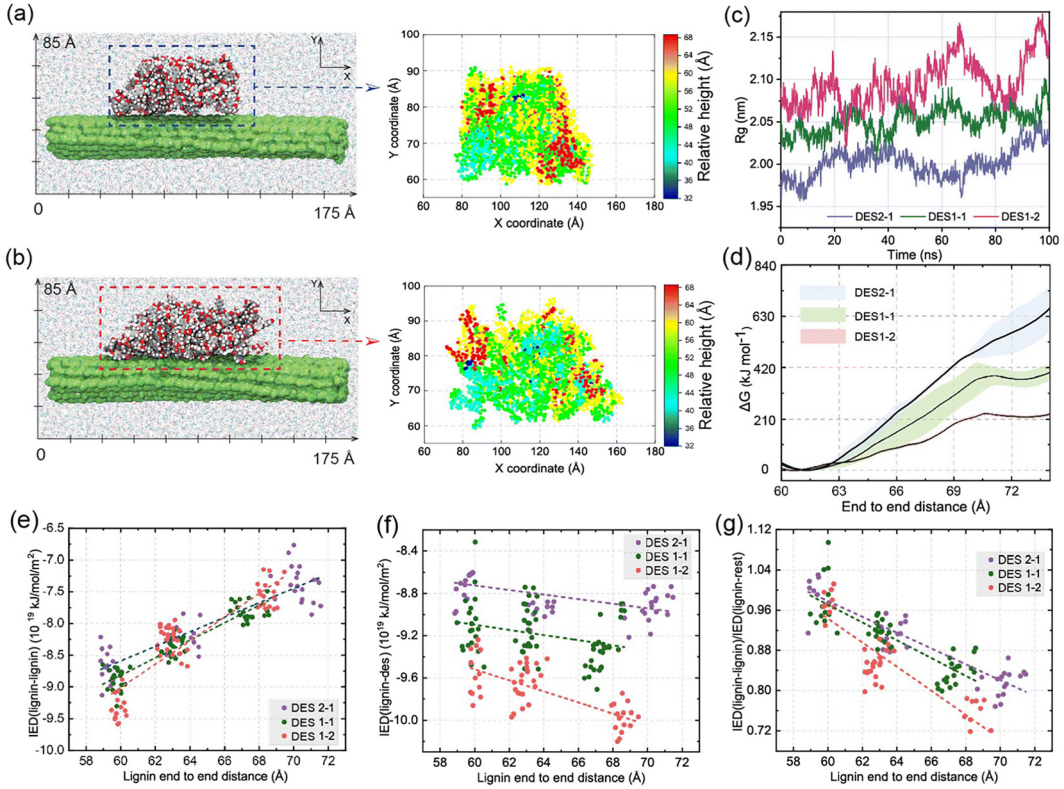

Fig. 11 Lignin–cellulose systems in (a) DES2-1 and (b) DES1-2 from MD simulations. (c) Radius of gyration of lignin in DESs; (d) free energy profiles for three DES systems. Interaction energy density of (e) lignin–lignin; (f) lignin–DES; (g) normalized ratio of interaction energy density for intra-lignin interactions and of lignin with the rest of the system. Reproduced from ref. 210. Copyright 2024, Royal Society of Chemistry.

enhanced the predictive and optimization capabilities for lignocellulosic biomass pretreatment using DESs. A range of ML methods, including random forest (RF), extreme gradient boosting (XGBoost), artificial neural networks (ANN), and partial least squares (PLS) has been employed to predict biomass targets such as lignin removal, cellulose retention, and sugar yields.[316,317] These ML models were trained on the diverse input features such as physicochemical properties of DESs (*e.g.*, melting point, surface tension, pK_a, molar ratio, surface area of HBA/HBD, *etc.*), reaction conditions (biomass particle size, liquid/solid ratio, severity factor, reaction time, and temperature), and biomass composition (cellulose, hemicellulose, and lignin contents) as key features influencing pretreatment efficiency. Notably, XGBoost achieved higher predictive accuracy (R^2 > 0.9) than other ML models. Further, feature importance analysis was performed to understand the importance of input features on the ML model predictions, and the features such as hydrophilicity of DES, temperature, and hemicellulose content, were identified as key predictors for lignin removal.

Sumer and Van Lehn[318] have presented an integrated molecular simulation and ML framework to predict lignin solubility in DESs. The authors performed classical MD simulations to extract key interaction descriptors, such as hydrogen bonding, radial distribution functions, and solvation shell properties for various lignin fragments in different DES environments. These simulation-derived descriptors were then used as input features for training an ANN model, which was capable of accurately capturing nonlinear relationships between lignin structure, solvent interactions, and solubility (Fig. 12). The ANN model successfully predicted the solubility trends of lignin fragments in diverse DESs and revealed the critical role of specific lignin linkages (*e.g.*, β-O-4, β–β) and solvent characteristics in determining solubility. The study emphasizes that solubility is not solely dictated by bulk solvent parameters but is significantly influenced by molecular-level interactions, including π–π stacking and hydrogen bonding. Recently, Zhong *et al.*[319] developed an interpretable and explainable ML model for predicting lignin removal efficacy in DESs. They compiled a dataset of 467 data points comprising 19 different herbaceous biomass types, 27 HBAs, and 36 HBDs with varied molar ratios under different operating conditions. The study evaluated several ML algorithms, including Categorical Boosting (CatBoost), RF, SVR, ANN, and XGBoost. Among these, XGBoost exhibited the best predictive performance, achieving an R^2 value of 0.82 and RMSE of 0.095. Importantly, the dataset used in the ML was predominantly composed of Type III DESs, with only limited representation of other DES classes. Consequently, the ML model is most reliable for predicting the performance of solvents residing within this relatively narrow chemical space (Type III DES systems) and may not give accurate results for other DES types.

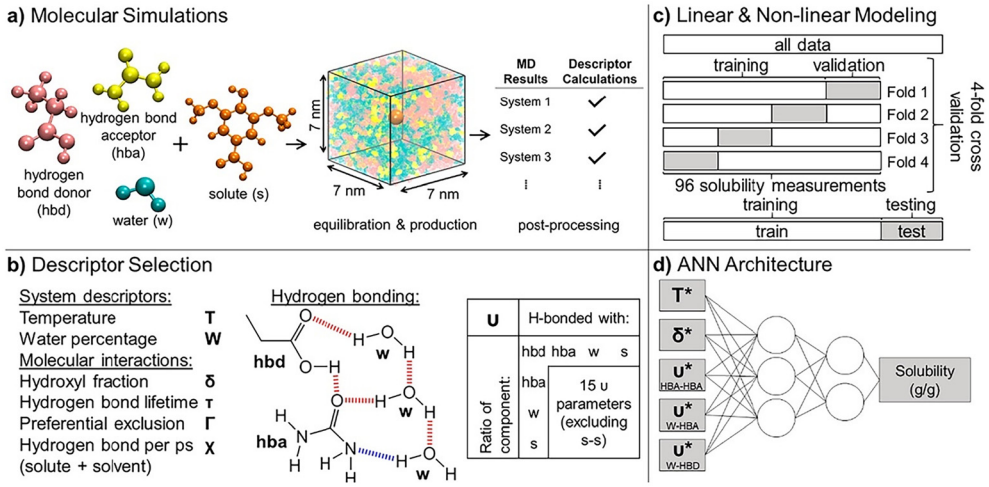

Fig. 12 Schematic representation of (a) DES, water, and lignin model compounds in a periodic simulation box and how MD results for different systems were used to calculate descriptors, (b) example descriptors and corresponding symbols, and (c) 4-fold cross validation applied to both linear and nonlinear models. (d) Architecture of the shallow artificial neural network (ANN) used for nonlinear regression. Reproduced with permission from ref. 318. Copyright 2022, American Chemical Society.

More experimental work is needed to include other DES classes and make the model more general and reliable.

Featurization techniques have included not only traditional cheminformatics descriptors but also spectroscopic and structural parameters. Gao *et al.*[320] and Kartal & Özveren[321] demonstrated that features derived from Raman spectroscopy and proximate analysis can be leveraged by ML models such as XGBoost and ANN to accurately predict lignin content and composition in biomass with R^2 values ranging from 0.94 and 0.96, respectively. Additionally, studies have combined DFT calculations with ML to derive solvent-specific descriptors for DES screening. For instance, Ge *et al.*[322] trained a range of ML models to predict cellulose retention and biomass delignification in 104 DESs using DFT-derived electronic properties, experimental pretreatment conditions, and Kamlet–Taft parameters as inputs. The authors have developed accurate ML models for both cellulose retention and delignification, and identified that initial cellulose, lignin, and solid loadings were the most effective features for ML. However, the data sets used in the ML models are very small.[320–322]

In terms of structural modeling, Xu *et al.* introduced a deep learning framework (LigninGen) capable of constructing lignin molecular structures from IR and NMR data, providing an avenue for rational design of lignin model molecules for molecular simulations (Fig. 13).[323] Other efforts, such as those by Löfgren *et al.*[324] and Castro Garcia *et al.*,[325] utilized Bayesian optimization and RF to model lignin depolymerization and optimize biorefinery conditions for desirable lignin properties (*e.g.*, β-O-4 linkage content, molecular weight) with minimal experimental data. These studies underscore the growing role of ML not only in predicting pretreatment outcomes but also in guiding solvent design and biomass valorization strategies across the lignocellulosic bioeconomy. Furthermore, Mohan *et al.* developed ML models to predict the viscosity[151] and Kamlet–Taft parameters[133] of DESs, establishing strong correlations between these solvent properties and their effectiveness in lignin removal from biomass. Their findings revealed that DESs with lower viscosities facilitate more efficient delignification. Conversely, an increase in hydrogen bond basicity (β) of the DESs was positively correlated with high lignin removal, indicating the critical role of solvent transport properties and polarity in biomass pretreatment.

9.1 Challenges for AI/ML models

Overall, ML has proven effective in accelerating solvent screening, improving process design, and revealing mechanistic insights into DES–biomass interactions. These approaches reduce reliance on time- and cost-intensive trial-and-error experiments while enabling data-driven solvent selection and lignin valorization strategies. However, several challenges must be addressed to explore the full potential of AI/ML in solvent design and optimize reaction conditions. One of the key challenges in implementing AI/ML to bioprocessing is the limited availability of high-quality and well-labeled datasets, such as biomass categories, DESs types, molar ratio, HBA, and HBDs. The performance of AI/ML methods is strongly dependent on the quality of datasets and having precise and diverse datasets is essential for building accurate and generalizable models.

To advance AI/ML-driven innovations, collaboration among institutions, national laboratories, and industries is critical to generate and share comprehensive datasets. Furthermore, another potential challenge for AI/ML models in bioprocessing is small dataset availability. Small data often brings challenges such as data imbalance and risk of overfitting or underfitting due to limited sample sizes and complex, high-dimensional input features. In small data scenarios, careful feature selection and engineering become particularly important. To address the data imbalance and prevent the risk of overfitting,

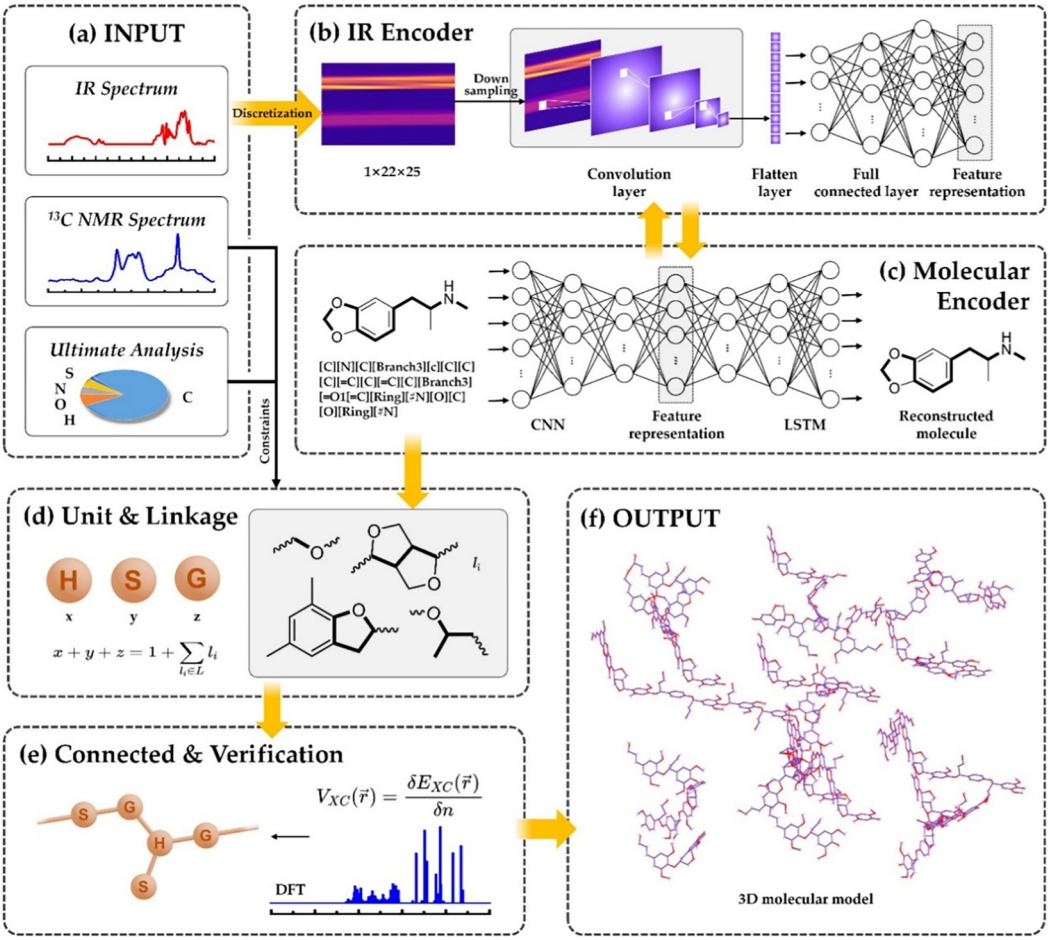

Fig. 13 Flow diagram of the lignin molecule generation from the data of IR, ^{13}C NMR and ultimate analysis by LigninGen. Reproduced with permission from ref. 323. Copyright 2025, Elsevier.

strategies such as chemical space analysis can be used to identify similar, dissimilar, and stratified subsets of compounds. In addition, when working with limited data, it is important to implement tools for evaluating model robustness and transferability. Techniques such as applicability domain (AD), bias-variance analysis, and learning curve analysis provide better insight into a model's ability to generalize and the transferability of ML models.

9.2 Data standardization guidelines for AI/ML

To address the limitations associated with small and heterogeneous datasets, it is imperative to establish rigorous data standardization practices in DES-based biomass pretreatment studies. First, the experimental methodology must be described in sufficient detail to ensure reproducibility, including clear documentation of solvent preparation, biomass preprocessing, and reaction protocols. Second, all reported data should include statistical analysis such as standard deviation, error bars, and uncertainty measurements for both tabulated results and graphical representations. Third, complete reporting of experimental conditions, encompassing DES composition, water content, biomass particle size, biomass composition, temperature, reaction time, pressure, and solid-to-liquid ratio is essential to enable meaningful cross-study comparisons.

Furthermore, consistency in units, definitions, and reporting formats must be maintained across studies to facilitate data integration and machine readability. Importantly, the reporting of negative or low-performance data (*e.g.*, low lignin removal, poor sugar yields, or inefficient DES systems) should be encouraged, as such data are critical for reducing bias and improving the robustness and generalizability of ML models. Expanding dataset diversity by systematically exploring broader chemical space, including novel DES formulations, ternary systems, and diverse biomass feedstocks is also necessary to improve model transferability. Finally, adherence to FAIR (Findable, Accessible, Interoperable, and Reusable) data principles should be prioritized to support the development of open, high-quality datasets that can accelerate AI/ML-driven discovery in sustainable solvent design. To address these critical challenges of limited and non-standardized datasets, we propose a comprehensive reporting framework to guide future DES-based biomass pretreatment studies. This framework integrates experimental, computational, and data-centric parameters to ensure reproducibility, improve data interoperability,

and enable the development of robust and generalizable machine learning models. The recommended minimum experimental reporting standards are summarized in Table 9.

10. Outlook

To accelerate the transition of DES-based biomass pretreatment from laboratory-scale to industrial implementation, future research must move beyond descriptive investigations toward clearly defined and coordinated research priorities. First, a critical priority is the development of standardized experimental protocols and open-access databases encompassing DES composition, physicochemical properties, biomass characteristics, and pretreatment results (delignification, biomass composition after pretreatment, sugar yields, *etc.*). The current lack of standardized datasets limits reproducibility and hinders the development of generalizable predictive models. Establishing benchmarking frameworks for evaluating lignin removal, cellulose retention, solvent recyclability, and energy efficiency is essential for cross-study comparison and data-driven optimization.

In this context, the development of a centralized, community-accessible digital infrastructure is urgently needed. A dedicated DES database platform (*e.g.*, a web-based repository or integrated software ecosystem) should be established to systematically curate physicochemical properties, compositional information (HBA/HBD types and molar ratios), biomass-specific pretreatment metrics, and process conditions. Such a platform should be continuously updated on a regular basis (*e.g.*, quarterly or half year) to ensure that newly generated experimental and computational data are rapidly disseminated. In addition, adopting rigorous data standardization and transparency practices across the DES research community is essential. Researchers should follow the FAIR principles to ensure that datasets are accessible, well-annotated, and reusable across studies. Standardized reporting should include detailed DES compositions, synthesis procedures, physicochemical properties, and pretreatment conditions. In addition, the systematic reporting of negative or non-ideal results should be strongly encouraged. Inclusion of such data will reduce publication bias, improve the robustness and generalizability of AI/ML models, and provide a more realistic representation of the DES design space, ultimately enabling more reliable predictive modeling and process optimization.

Second, methodological advancements are required to integrate multiscale modeling with experimental validation. DFT, MD, and COSMO-RS approaches provide molecular-level insights, their predictive capability remains limited by simplified model systems and restricted chemical space exploration. Future efforts should focus on coupling these methods with physics-informed ML and high-throughput screening to enable inverse design of DES systems tailored for specific biomass types. Additionally, expanding computational studies to include realistic lignin polymer models and underexplored DES classes will improve mechanistic understanding and predictive accuracy. Third, process-level innovations and scalability considerations must be prioritized, particularly in DES recovery and recycling. Although techniques such as antisolvent precipitation, membrane separation, and electrodialysis show promise, their energy consumption, solvent loss, and long-term stability remain key challenges. Systematic comparison and optimization of these recovery methods, combined with closed-loop solvent reuse strategies, are essential for improving economic feasibility and reducing environmental impact.

Fourth, existing datasets are typically small, heterogeneous, and lack standardized reporting, further limiting model robustness and transferability. These limitations indicate that the current experimental database is insufficient for developing broadly generalized ML models. Most models are therefore restricted to interpolation within the training domain rather than reliable extrapolation to new DES systems. To overcome these challenges, future work should focus on generating large, diverse, and standardized datasets spanning all DES classes. Integration of high-throughput experiments with computational screening methods (*e.g.*, COSMO-RS and molecular simulations) can accelerate data generation. Furthermore, incorporating physics-informed descriptors and implementing rigorous validation strategies, such as applicability domain analysis and uncertainty quantification, will be essential to improve model reliability. Overall, ML provides a powerful framework for accelerating DES design and biomass pretreatment optimization, its current application should be viewed as complementary to experimental and computational approaches, rather than a standalone predictive tool. Fifth, systematic toxicological data for eutectic mixtures remains scarce, and most assessments rely on extrapolations from individual components, which may not accurately reflect the synergistic or antagonistic effects within DES formulations. Leaching of metal ions during biomass processing or DES recycling poses additional risks, particularly in applications where solvent loss into effluent streams is unavoidable. Therefore, a balanced perspective is essential. Metal-based DESs offer high pretreatment efficiency and recyclability, but these advantages must be weighed against potential environmental hazards, especially for large-scale industrial deployment. Future research should prioritize standardized ecotoxicity assays (*e.g.*, using aquatic organisms, soil microbes, and plant models), biodegradability studies, and life cycle impact assessments that explicitly include toxicity categories.

Sixth, early integration of TEA and LCA analysis should become a standard practice in DES research. Current studies demonstrate promising economic and environmental potential; however, inconsistencies in system boundaries, assumptions, and datasets limit their comparability. Developing standardized TEA/LCA frameworks and incorporating renewable energy inputs, solvent recyclability, and process intensification strategies will provide a more accurate assessment of sustainability. Finally, strategic directions for advancing sustainability should emphasize the design of bio-derived and low-toxicity DES components, circular biorefinery integration, and hybrid

Table 9 Recommended standardized reporting framework for DES-based biomass pretreatment studies to enable robust AI/ML development

Category	Parameter	Details to report	Rationale for AI/ML
DES composition	HBA and HBD	Full chemical names, structures (SMILES/InChI), and purity	Enables molecular-level descriptor generation and molecular simulations
	Molar ratio	Exact HBA to HBD molar ratio	Critical for structure–property relationships
	Water content	wt% or mol% water	Strongly affects DES physicochemical properties
	DES preparation conditions	Temperature, time, and mixing procedure	Ensures reproducibility across datasets
DES properties	Physicochemical properties	Viscosity, melting temperature, polarity (*e.g.*, Kamlet–Taft), pK_a, conductivity, and surface tension	Key parameters in controlling biomass pretreatment efficiency and also ML input features
Biomass characteristics	Biomass type	Source and species (herbaceous/hardwood/softwood)	Captures variability across feedstocks
	Composition	Cellulose, hemicellulose, and lignin (wt%)	Essential for defining biomass types in AI/ML
	Particle size	Distribution or average size with method	Influences mass transfer and reaction kinetics
	Monolignol	Lignin composition (H, G, and S units)	Captures lignin variability in biomass types
	Preprocessing	Drying, milling, and extractives removal	Affects accessibility and reproducibility
Pretreatment conditions	Operating conditions	Temperature, time, and pressure	Core process variables
	Solid–liquid ratio	g biomass per g DES or g biomass per mL DES	Govern reaction severity and mass transfer
	Severity factor	Severity ($\log R_0$) as a function of time and temperature	Standard comparison across studies
	Mixing/reactor details	Stirring rate and reactor type (batch/flow/microwave)	Impacts heat and mass transfer
	Additives	Water, catalysts, and co-solvents	Alters reaction pathways and efficiency
Targets	Lignin removal	Delignification, %	Primary target for ML prediction
	Cellulose retention	Cellulose retained, %	Indicates selectivity
	Hemicellulose removal	Hemicellulose removed, %	Complement fractionation analysis
	Sugar yields	Glucose/xylose yield (%) after hydrolysis	Key downstream performance indicator
	Mass balance	Closure across phases (%)	Ensures data reliability
Best practices & data quality	Replicates and error	Mean ± standard deviation, number of repeats	Required for uncertainty-aware ML
	Measurement methods	Analytical protocols (*e.g.*, NREL, spectroscopy)	Ensures cross-study comparability
	Negative results	Report low/failed performance cases	Reduces bias and improves model robustness
	Unit consistency	Maintain consistent units and reporting standards across studies	Avoids data preprocessing inconsistencies
	Data diversity	Explore broader chemical space (new DESs, biomass types, compositions)	Enhances model robustness and extrapolation
	FAIR principles	Ensure data is findable, accessible, interoperable, and reusable	Facilitates database creation and AI/ML integration

pretreatment approaches. Combining DES systems with complementary techniques such as microwave-assisted processing, hydrothermal treatment, or biological methods offers significant opportunities to enhance efficiency and reduce processing severity. Furthermore, leveraging AI/ML-driven design frameworks can enable the rapid identification of optimal solvent systems with minimal environmental footprint. Collectively, these research priorities and strategic directions provide a roadmap for advancing DES-based biomass pretreatment toward scalable, economically viable, and environmentally sustainable biorefinery technologies.

11. Conclusion

In conclusion, this comprehensive review emphasizes DESs as a versatile and sustainable solvents and catalyst for lignocellulosic biomass pretreatment, integrating experimental advancements, computational modeling, and emerging ML perspectives. The composition of DES systems—dictated by pK_a, molecular complexity, and HBA/HBD combinations, which influences their physicochemical properties. DESs demonstrate selective lignin dissolution across diverse biomass types, with hardwood and softwood exhibiting different solubilities due to structural and compositional disparities. Herbaceous feedstocks, in particular, benefit from the ability of DESs to effectively disrupt hemicellulose–lignin interfaces, facilitating fractionation. Studies on the pretreatment of hardwoods such as poplar using ternary DESs remain relatively limited compared to their binary DESs. Future research should prioritize the design and evaluation of ternary DES formulations with enhanced pretreatment performance.

Computational studies, including MD simulations and quantum chemical calculations, have elucidated solvation mechanisms of lignin in DESs, revealing how HBA/HBD interactions weaken lignin polymer networks. Anions of HBA and HBD play an important role in the dissolution of lignin by forming strong hydrogen bonds with hydroxyl groups of lignin and show greater interactions. Further, DES recovery technologies, ranging from antisolvent precipitation to membrane

separation, offer pathways for sustainable solvent recycling, although scalability remains a significant challenge. TEA and LCA underscore the potential of DES-based pretreatment for cost-effective biofuel and biochemical production.

Despite recent advances, the fundamental mechanisms underlying DES-mediated lignocellulose depolymerization remain incompletely understood. This knowledge gap presents a significant barrier to the industrial-scale implementation of DES-based biomass pretreatment technologies. Future research could employ interdisciplinary approaches to elucidate the underlying mechanisms, enabling the rational design of DES components for enhanced functionality. Ternary DES systems exhibit greater compositional and mechanistic complexity than their binary counterparts, necessitating more systematic investigation. Three critical research gaps must be addressed: (1) systematic comparison of recycling methodologies, (2) rigorous TEA, and (3) comprehensive LCA, representing essential directions for future research to evaluate practical viability and environmental impacts. Furthermore, integrating DES pretreatment with complementary physical or chemical methods presents a promising approach to enhancing lignocellulosic separation efficiency. Potential synergistic strategies include combining DES with conventional steam explosion, microwave-assisted treatment, surfactant addition, or biological processes. These combinatorial approaches warrant systematic investigation to optimize their effectiveness. Despite their advantages, several practical challenges remain for the large-scale deployment of DESs. The cost and availability of certain HBA/HBD components, particularly specialty chemicals, may limit scalability. In addition, many DES systems require specific operating conditions (*e.g.*, elevated temperature, controlled water content) to achieve optimal performance, which can increase process complexity. However, recent advances in DES recyclability, development of bio-derived and low-cost components, and process integration strategies are helping to mitigate these limitations and improve overall feasibility.

In addition, critical gaps persist, particularly in leveraging ML for predicting pretreatment outcomes. Current AI/ML models face challenges in handling the high-dimensional complexity of DES–composition–property–efficacy relationships, compounded by limited standardized datasets and interpretability issues. Future research must prioritize interdisciplinary approaches that merge experimental design with advanced ML algorithms, enabling data-driven optimization of DES formulations and pretreatment protocols. By bridging these gaps, DES technology can transition from laboratory promise to industrial reality, unlocking the full potential of lignocellulosic biomass as a renewable resource for a circular bioeconomy.

Author contributions

K. H., K. S., C. G., Y. C., X. X., Y. C., J. G.: conceptualization, data collections, formal analysis, writing original draft, and visualization. M. M.: conceptualization, data collections, formal analysis, computational and ML data analysis, writing original draft, supervision, editing, and finalizing all content. Y. X., X. Z., and J. C. S.: supervision, editing, and funding. All authors reviewed the manuscript and accepted the content.

Conflicts of interest

The authors declare no conflicts of interest.

Data availability

No new primary data were generated or analyzed in this review. The data supporting the results and analysis presented in this article are derived from previously published works, which have been duly cited in the reference section.

Acknowledgements

The work was supported by the National Key R&D Program of China (2024YFD1300804), Agricultural science and technology independent innovation project of Jiangsu Province (CX(24) 1009), the Research Startup Foundation of Yancheng Teachers University (204070022), and the International Innovation Center for Forest Chemicals and Materials (cxgd20220208). The authors also acknowledge the Undergraduate Students' Innovation and Entrepreneurship Training Program Project (S202510324009) and Postgraduate Research & Practice Innovation Program of Jiangsu Province (KYCX25_1378) for supporting the work presented in this paper. This work was also supported by the US Department of Energy (DOE), Office of Science, through the Genomic Science Program, Office of Biological and Environmental Research (contract no. FWP ERKP752).

References

1 A. Hu, H. Wang and J. Ding, *ACS Omega*, 2022, **7**, 33192–33198.
2 E. L. Smith, A. P. Abbott and K. S. Ryder, *Chem. Rev.*, 2014, **114**, 11060–11082.
3 D. O. Abranches and J. A. P. Coutinho, *Annu. Rev. Chem. Biomol. Eng.*, 2023, **14**, 141–163.
4 N. Özel and M. Elibol, *Carbohydr. Polym.*, 2021, **262**, 117942.
5 A. P. Abbott, G. Capper, D. L. Davies, R. K. Rasheed and V. Tambyrajah, *Chem. Commun.*, 2003, 70–71.
6 B. B. Hansen, S. Spittle, B. Chen, D. Poe, Y. Zhang, J. M. Klein, A. Horton, L. Adhikari, T. Zelovich and B. W. Doherty, *Chem. Rev.*, 2021, **121**, 1232–1285.
7 M. Wang, X. Fu, Y. Chang, J. Wei and H. Cui, *Ind. Crops Prod.*, 2025, **229**, 121028.
8 Q.-G. Zhang, Y. Wei, S.-S. Sun, C. Wang, M. Yang, Q.-S. Liu and Y.-A. Gao, *J. Chem. Eng. Data*, 2012, **57**, 2185–2190.

9 A. P. Abbott, G. Capper, D. L. Davies and R. Rasheed, *Inorg. Chem.*, 2004, **43**, 3447–3452.
10 S. Khandelwal, Y. K. Tailor and M. Kumar, *J. Mol. Liq.*, 2016, **215**, 345–386.
11 Y. T. Tan, A. S. M. Chua and G. C. Ngoh, *Bioresour. Technol.*, 2020, **297**, 122522.
12 M. Zhou, O. A. Fakayode, A. E. A. Yagoub, Q. Ji and C. Zhou, *Renewable Sustainable Energy Rev.*, 2022, **156**, 111986.
13 Y. Liu, J. B. Friesen, J. B. McAlpine, D. C. Lankin, S.-N. Chen and G. F. Pauli, *J. Nat. Prod.*, 2018, **81**, 679–690.
14 D. O. Abranches and J. A. P. Coutinho, *Curr. Opin. Green Sustainable Chem.*, 2022, **35**, 100612.
15 Q. Liu, H. Mou, W. Chen, X. Zhao, H. Yu, Z. Xue and T. Mu, *Ind. Eng. Chem. Res.*, 2019, **58**, 23438–23444.
16 M. P. Gundupalli, K. Cheenkachorn, S. Chuetor, S. Kirdponpattara, S. P. Gundupalli, P.-L. Show and M. Sriariyanun, *Carbohydr. Polym.*, 2023, **306**, 120599.
17 D. Huo, Y. Sun, Q. Yang, F. Zhang, G. Fang, H. Zhu and Y. Liu, *Bioresour. Technol.*, 2023, **376**, 128937.
18 K. Huang, J. Song, K. Su, X. Xu, K. D. Jetti, Y. Xu, X. Zhou, M. K. Kidder, J. C. Smith and M. Mohan, *npj Mater. Sustainability*, 2026, **4**, 7.
19 K. D. Jetti and N. S. Kishore, *Sugar Tech*, 2024, **26**, 562–572.
20 K. D. Jetti, R. R. Gns, D. Garlapati and S. K. Nammi, *Int. Microbiol.*, 2019, **22**, 247–254.
21 D. R. Lobato-Peralta, E. Duque-Brito, H. I. Villafán-Vidales, A. Longoria, P. J. Sebastian, A. K. Cuentas-Gallegos, C. A. Arancibia-Bulnes and P. U. Okoye, *J. Cleaner Prod.*, 2021, **293**, 126123.
22 A. Wagle, M. J. Angove, A. Mahara, A. Wagle, B. Mainali, M. Martins, R. Goldbeck and S. R. Paudel, *Sustain. Energy Technol. Assess.*, 2022, **49**, 101702.
23 M. Vohra, J. Manwar, R. Manmode, S. Padgilwar and S. Patil, *J. Environ. Chem. Eng.*, 2014, **2**, 573–584.
24 J. C. Solarte-Toro, Y. Chacón-Pérez and C. A. Cardona-Alzate, *Electron. J. Biotechnol.*, 2018, **33**, 52–62.
25 J. Xu, C. Li, L. Dai, C. Xu, Y. Zhong, F. Yu and C. Si, *ChemSusChem*, 2020, **13**, 4284–4295.
26 K. Zhang, Z. Pei and D. Wang, *Bioresour. Technol.*, 2016, **199**, 21–33.
27 Z. Yang, Z. Xu, M. Feng, J. R. Cort, R. Gieleciak, J. Heyne and B. Yang, *Fuel*, 2022, **321**, 124040.
28 M. J. John, M. C. Lefatle and B. Sithole, *Sustainable Chem. Pharm.*, 2022, **25**, 100594.
29 S. Yao, S. Nie, Y. Yuan, S. Wang and C. Qin, *Bioresour. Technol.*, 2015, **185**, 21–27.
30 M. J. Hülsey, H. Yang and N. Yan, *ACS Sustainable Chem. Eng.*, 2018, **6**, 5694–5707.
31 K. Chen, J. Sang, Z. Wang, U.-K. Ibrahim, W. Xia, A. Guo, J. Zhang and D. Hou, *Fuel*, 2021, **286**, 119401.
32 M. Si, M. Sillanpää, S. Zhuo, J. Zhang, M. Liu, S. Wang, C. Gao, L. Chai, F. Zhao and Y. Shi, *Ind. Crops Prod.*, 2020, **152**, 112469.
33 T. Mori, Y. Tsuboi, N. Ishida, N. Nishikubo, T. Demura and J. Kikuchi, *Sci. Rep.*, 2015, **5**, 11848.
34 A. Barhoum, J. Jeevanandam, A. Rastogi, P. Samyn, Y. Boluk, A. Dufresne, M. K. Danquah and M. Bechelany, *Nanoscale*, 2020, **12**, 22845–22890.
35 D. Tocco, C. Carucci, M. Monduzzi, A. Salis and E. Sanjust, *ACS Sustainable Chem. Eng.*, 2021, **9**, 2412–2432.
36 M. Zhou, Y. Feng, H. Li and X. Tian, *Carbohydr. Polym.*, 2024, **326**, 121593.
37 X. Yang, Y. Zhang, P. Sun and C. Peng, *Smart Mol.*, 2024, **2**, e20240019.
38 D. Ji, Y. Wang, J. Peng, D. Yuan, Z. Li, D. Ji and H. Wu, *Ind. Eng. Chem. Res.*, 2024, **63**, 19916–19935.
39 U. M. Ahmad, N. Ji, H. Li, Q. Wu, C. Song, Q. Liu, D. Ma and X. Lu, *Ind. Crops Prod.*, 2021, **170**, 113646.
40 M. Zhang, C. Ren, X. Song, R. Zhang, X. Shi, H. Zhang, D. Ji and L. Zang, *Biomass Bioenergy*, 2025, **197**, 107836.
41 H. Deng, S. Wang, J. Shi, D. Zhang and W. Xu, *Int. J. Biol. Macromol.*, 2025, **306**, 141613.
42 Z. Yao, G. Chong and H. Guo, *Appl. Sci.*, 2024, **14**, 7662.
43 E. Novaes, M. Kirst, V. Chiang, H. Winter-Sederoff and R. Sederoff, *Plant Physiol.*, 2010, **154**, 555–561.
44 S.-J. Jung, S.-H. Kim and I.-M. Chung, *Biomass Bioenergy*, 2015, **83**, 322–327.
45 X. Zhang, A. Liu, X. Li, W. Xu, X. Duan, J. Shi and X. Li, *Cellulose*, 2025, **32**, 4637–4650.
46 Y.-L. Loow, E. K. New, G. H. Yang, L. Y. Ang, L. Y. W. Foo and T. Y. Wu, *Cellulose*, 2017, **24**, 3591–3618.
47 H. Xu, J. Peng, Y. Kong, Y. Liu, Z. Su, B. Li, X. Song, S. Liu and W. Tian, *Bioresour. Technol.*, 2020, **310**, 123416.
48 F. O. Farias, J. F. B. Pereira, J. A. P. Coutinho, L. Igarashi-Mafra and M. R. Mafra, *Fluid Phase Equilib.*, 2020, **503**, 112319.
49 Q. Wang, K. Cao, F. Yan, X. Duan and J. Shi, *Biomass Convers. Biorefin.*, 2025, **15**, 1–18.
50 F. Baraka, M. M. Langari, I. Beitia, I. Dávila, J. Labidi, A. Morales and L. Sillero, *J. Environ. Chem. Eng.*, 2025, **13**, 117087.
51 Y. Zhu, T.-X. Yang, B.-K. Qi, H. Li, Q.-S. Zhao and B. Zhao, *Int. J. Biol. Macromol.*, 2023, **236**, 123977.
52 P. Li, W. Qian, S. Wu and Y. Liu, *ACS Sustainable Chem. Eng.*, 2025, **13**, 9987–10018.
53 A. M. da Costa Lopes, J. R. B. Gomes, J. A. P. Coutinho and A. J. D. Silvestre, *Green Chem.*, 2020, **22**, 2474–2487.
54 W.-X. Li, W.-Z. Xiao, Y.-Q. Yang, Q. Wang, X. Chen, L.-P. Xiao and R.-C. Sun, *Ind. Crops Prod.*, 2021, **170**, 113692.
55 H. Xu, Y. Kong, J. Peng, W. Wang and B. Li, *ACS Sustainable Chem. Eng.*, 2021, **9**, 7101–7111.
56 Q. Li, Y. Dong, K. D. Hammond and C. Wan, *J. Mol. Liq.*, 2021, **344**, 117779.
57 Z. Chen, Y. Wang, H. Cheng and H. Zhou, *Ind. Crops Prod.*, 2022, **187**, 115335.
58 C. Alvarez-Vasco, R. Ma, M. Quintero, M. Guo, S. Geleynse, K. K. Ramasamy, M. Wolcott and X. Zhang, *Green Chem.*, 2016, **18**, 5133–5141.

59 A. L. Sazali, N. AlMasoud, S. K. Amran, T. S. Alomar, K. F. Pa'ee, Z. M. El-Bahy, T. K. Yong, D. J. Dailin and L. F. Chuah, *Chemosphere*, 2023, **338**, 139485.
60 R. S. B. Ferreira, A. M. Ferreira, J. A. P. Coutinho and E. A. C. Batista, *ACS Sustainable Chem. Eng.*, 2024, **12**, 15893–15900.
61 R. Alcalde, M. Atilhan and S. Aparicio, *J. Mol. Liq.*, 2018, **272**, 815–820.
62 Y. Liu, N. Deak, Z. Wang, H. Yu, L. Hameleers, E. Jurak, P. J. Deuss and K. Barta, *Nat. Commun.*, 2021, **12**, 5424.
63 N. Arshad, E. J. Panakkal, A. Chantarasiri, P. Pornwongthong, H. El Bari, W. Fatriasari, P. Tantayotai and M. Sriariyanun, *Bioresour. Technol. Rep.*, 2025, **31**, 102190.
64 T. Sathasivam, T. Wu, U. A. Weerasinghe, P. Y. M. Yew, X. L. Quek, Y. J. Eng and D. Kai, *Bioresour. Technol.*, 2026, **442**, 133753.
65 Q. Xia, Y. Liu, J. Meng, W. Cheng, W. Chen, S. Liu, Y. Liu, J. Li and H. Yu, *Green Chem.*, 2018, **20**, 2711–2721.
66 S. Han, R. Wang, K. Wang, J. Jiang and J. Xu, *Bioresour. Technol.*, 2022, **363**, 127905.
67 P. Panyamao, S. Charumanee, J. Ruangsuriya and C. Saenjum, *ACS Sustainable Chem. Eng.*, 2023, **11**, 13962–13973.
68 S. Hong, X.-J. Shen, Z. Xue, Z. Sun and T.-Q. Yuan, *Green Chem.*, 2020, **22**, 7219–7232.
69 A. P. Abbott, G. Capper, D. L. Davies, K. J. McKenzie and S. U. Obi, *J. Chem. Eng. Data*, 2006, **51**, 1280–1282.
70 Y. Bao, Y. Wang, C. Yan and Z. Xue, *Green Chem. Eng.*, 2025, **6**, 21–35.
71 N. R. Mirza, N. J. Nicholas, Y. Wu, K. A. Mumford, S. E. Kentish and G. W. Stevens, *J. Chem. Eng. Data*, 2015, **60**, 3246–3252.
72 M. Mohan, J. D. Keasling, B. A. Simmons and S. Singh, *Green Chem.*, 2022, **24**, 4140–4152.
73 M. Mohan, P. Viswanath, T. Banerjee and V. V. Goud, *Mol. Phys.*, 2018, **116**, 2108–2128.
74 M. Gambino and J. P. Bros, *Thermochim. Acta*, 1988, **127**, 223–236.
75 A. P. Abbott, G. Capper, D. L. Davies, H. L. Munro, R. K. Rasheed and V. Tambyrajah, *Chem. Commun.*, 2001, 2010–2011.
76 D. O. Abranches, M. A. R. Martins, L. P. Silva, N. Schaeffer, S. P. Pinho and J. A. P. Coutinho, *Chem. Commun.*, 2019, **55**, 10253–10256.
77 N. Schaeffer, D. O. Abranches, L. P. Silva, M. A. R. Martins, P. J. Carvalho, O. Russina, A. Triolo, L. Paccou, Y. Guinet, A. Hedoux and J. A. P. Coutinho, *ACS Sustainable Chem. Eng.*, 2021, **9**, 2203–2211.
78 E. Zhu, J. Cheng, L. Huang, H. Shen, J. Meng, S. Wang, Z. Shi, M. W. Ullah, J. Ma, L. Zhang and Z. Wang, *Chem. Eng. J.*, 2026, **527**, 171882.
79 I. Juneidi, M. Hayyan and M. A. Hashim, *RSC Adv.*, 2015, **5**, 83636–83647.
80 M. Bisht, M. Martins, A. C. R. V. Dias, S. P. M. Ventura and J. A. P. Coutinho, *Green Chem.*, 2021, **23**, 8940–8948.
81 J. Tan, D. Yu, J. Yuan, H. Wu, H. Luo, H. Zhang, X. Li, H. Li and S. Yang, *Fuel*, 2023, **347**, 128485.
82 L. Carbonell-Rozas, R. Canales, R. Romero-González, M. F. Silva and A. G. Frenich, *Anal. Bioanal. Chem.*, 2025, **417**, 183–197.
83 D. Ren, Y. Yang, M. Fang, T. Xie, K. Li, J. Zhang, Y. Zhuang and L. Yi, *Chem. Eng. J.*, 2026, **533**, 174811.
84 S. Sharma, P. Nargotra, V. Sharma, R. Bangotra, M. Kaur, N. Kapoor, S. Paul and B. K. Bajaj, *Bioresour. Technol.*, 2021, **333**, 125191.
85 R. K. Sarangal, M. Nargotra and R. Singh, *Int. J. Bus. Data Anal.*, 2020, **1**, 293–317.
86 C. Florindo, M. M. Oliveira, L. C. Branco and I. M. Marrucho, *J. Mol. Liq.*, 2017, **247**, 441–447.
87 E. K. New, T. Y. Wu, K. S. Voon, A. Procentese, K. P. Y. Shak, W. H. Teoh, J. W. Lim and J. Md. Jahim, *Ind. Eng. Chem. Res.*, 2021, **60**, 2011–2026.
88 T. Lemaoui, A. S. Darwish, N. E. H. Hammoudi, F. Abu Hatab, A. Attoui, I. M. Alnashef and Y. Benguerba, *Ind. Eng. Chem. Res.*, 2020, **59**, 13343–13354.
89 L. F. Grantham and S. J. Yosim, *J. Phys. Chem.*, 1963, **67**, 2506–2507.
90 A. Berlin, F. Ménès, S. Forcheri and C. Monfrini, *J. Phys. Chem.*, 1963, **67**, 2505–2506.
91 Q. Zhang, K. De Oliveira Vigier, S. Royer and F. Jérôme, *Chem. Soc. Rev.*, 2012, **41**, 7108–7146.
92 J. Vila, B. Fernández-Castro, E. Rilo, J. Carrete, M. Domínguez-Pérez, J. R. Rodríguez, M. García, L. M. Varela and O. Cabeza, *Fluid Phase Equilib.*, 2012, **320**, 1–10.
93 A. P. Abbott, *ChemPhysChem*, 2005, **6**, 2502–2505.
94 H. Z. Su, J. M. Yin, Q. S. Liu and C. P. Li, *Acta Phys.-Chim. Sin.*, 2015, **31**, 1468–1473.
95 R. K. Ibrahim, M. Hayyan, M. A. AlSaadi, S. Ibrahim, A. Hayyan and M. A. Hashim, *J. Mol. Liq.*, 2019, **276**, 794–800.
96 T. El Achkar, H. Greige-Gerges and S. Fourmentin, *Environ. Chem. Lett.*, 2021, **19**, 3397–3408.
97 A. P. Abbott, D. Boothby, G. Capper, D. L. Davies and R. K. Rasheed, *J. Am. Chem. Soc.*, 2004, **126**, 9142–9147.
98 A. P. Abbott, G. Capper and S. Gray, *ChemPhysChem*, 2006, **7**, 803–806.
99 M. Li, Y. Pu and A. Ragauskas, *Front. Chem.*, 2016, **4**, 45.
100 F. Gabriele, M. Chiarini, R. Germani, M. Tiecco and N. Spreti, *J. Mol. Liq.*, 2019, **291**, 111301.
101 P. J. Smith, C. B. Arroyo, F. Lopez Hernandez and J. C. Goeltz, *J. Phys. Chem. B*, 2019, **123**, 5302–5306.
102 M. Petrowsky and R. Frech, *J. Phys. Chem. B*, 2009, **113**, 5996–6000.
103 F. S. Mjalli and H. Mousa, *Chin. J. Chem. Eng.*, 2017, **25**, 1877–1883.
104 V. Vorobyova, M. Skiba, K. Vinnichuk, O. Linyucheva and G. Vasyliev, *J. Mol. Struct.*, 2025, **1323**, 140743.
105 S. Spittle, D. Poe, B. Doherty, C. Kolodziej, L. Heroux, M. A. Haque, H. Squire, T. Cosby, Y. Zhang, C. Fraenza, S. Bhattacharyya, M. Tyagi, J. Peng, R. A. Elgammal, T. Zawodzinski, M. Tuckerman, S. Greenbaum, B. Gurkan, C. Burda, M. Dadmun, E. J. Maginn and J. Sangoro, *Nat. Commun.*, 2022, **13**, 219.

106 R. Dikki, V. Khokhar, M. Zeeshan, S. Bhattacharjee, O. K. Coskun, R. Getman and B. Gurkan, *Green Chem.*, 2024, **26**, 3441–3452.
107 F. J. López-Flores, C. Ramírez-Márquez, J. B. González-Campos and J. M. Ponce-Ortega, *Ind. Eng. Chem. Res.*, 2025, **64**, 3103–3117.
108 G. García, S. Aparicio, R. Ullah and M. Atilhan, *Energy Fuels*, 2015, **29**, 2616–2644.
109 A. A. M. Elgharbawy, M. Hayyan, A. Hayyan, W. J. Basirun, H. M. Salleh and M. E. S. Mirghani, *Biomass Bioenergy*, 2020, **137**, 105550.
110 M. Zhang, X. Zhang, Y. Liu, K. Wu, Y. Zhu, H. Lu and B. Liang, *Environ. Sci. Pollut. Res.*, 2021, **28**, 35537–35563.
111 Y. Gao, M. Fan, X. Cheng, X. Liu, H. Yang, W. Ma, M. Guo and L. Li, *Int. J. Biol. Macromol.*, 2024, **278**, 134593.
112 M. A. Sedghamiz and S. Raeissi, *J. Mol. Liq.*, 2018, **269**, 694–702.
113 B. Tang and K. H. Row, *Monatsh. Chem.*, 2013, **144**, 1427–1454.
114 M. H. Shafie, R. Yusof and C.-Y. Gan, *J. Mol. Liq.*, 2019, **288**, 111081.
115 Z. Chen, X. Bai and L. A, *ACS Sustainable Chem. Eng.*, 2018, **6**, 12205–12216.
116 E. Smith, A. Abbott and K. Ryder, *Chem. Rev.*, 2014, **114**, 11060–11082.
117 S. P. Ijardar, V. Singh and R. L. Gardas, *Molecules*, 2022, **27**, 1368.
118 A. Khajeh, M. Shakourian-Fard and K. Parvaneh, *J. Mol. Liq.*, 2021, **321**, 114744.
119 Urvika, R. Gaba and R. Kataria, in *Deep Eutectic Solvents*, American Chemical Society, 2025, vol. 1504, ch. 1, pp. 1–29.
120 K. A. Omar and R. Sadeghi, *J. Mol. Liq.*, 2022, **360**, 119524.
121 I. Bashir, A. H. Dar, K. K. Dash, V. K. Pandey, U. Fayaz, R. Shams, S. Srivastava and R. Singh, *Sustainable Chem. Pharm.*, 2023, **33**, 101102.
122 C.-X. Zeng, S.-J. Qi, R.-P. Xin, B. Yang and Y.-H. Wang, *J. Mol. Liq.*, 2016, **219**, 74–78.
123 K. Haraźna, K. Walas, P. Urbańska, T. Witko, W. Snoch, A. Siemek, B. Jachimska, M. Krzan, B. D. Napruszewska, M. Witko, S. Bednarz and M. Guzik, *Green Chem.*, 2019, **21**, 3116–3126.
124 M. Mohan, K. Huang, V. R. Pidatala, B. A. Simmons, S. Singh, K. L. Sale and J. M. Gladden, *Green Chem.*, 2022, **24**, 1165–1176.
125 R. Verma, M. Mohan, V. V. Goud and T. Banerjee, *ACS Sustainable Chem. Eng.*, 2018, **6**, 16920–16932.
126 A. K. Lavrinenko, I. Y. Chernyshov and E. A. Pidko, *ACS Sustainable Chem. Eng.*, 2023, **11**, 15492–15502.
127 L. B. Ayres, M. Bandara, C. D. McMillen, W. T. Pennington and C. D. Garcia, *ACS Sustainable Chem. Eng.*, 2024, **12**, 11260–11273.
128 T. Wu, P. Zhan, W. Chen, M. Lin, Q. Qiu, Y. Hu, J. Song and X. Lin, *Comput. Chem. Eng.*, 2025, **196**, 109065.
129 S. Momeni, K. Craplewe, M. Safder, S. Luz, D. Sauvageau and A. Elias, *ACS Sustainable Chem. Eng.*, 2023, **11**, 15146–15170.
130 K. Shahbaz, F. S. G. Bagh, F. S. Mjalli, I. M. AlNashef and M. A. Hashim, *Fluid Phase Equilib.*, 2013, **354**, 304–311.
131 C. Florindo, A. J. S. McIntosh, T. Welton, L. C. Branco and I. M. Marrucho, *Phys. Chem. Chem. Phys.*, 2018, **20**, 206–213.
132 A. Pandey, R. Rai, M. Pal and S. Pandey, *Phys. Chem. Chem. Phys.*, 2014, **16**, 1559–1568.
133 M. Mohan, N. Gugulothu, S. Guggilam, T. R. Rajitha, M. K. Kidder and J. C. Smith, *Green Chem. Eng.*, 2025, **6**, 275–287.
134 W. Chen, X. Bai, Z. Xue, H. Mou, J. Chen, Z. Liu and T. Mu, *New J. Chem.*, 2019, **43**, 8804–8810.
135 Y. Chen, W. Chen, L. Fu, Y. Yang, Y. Wang, X. Hu, F. Wang and T. Mu, *Ind. Eng. Chem. Res.*, 2019, **58**, 12741–12750.
136 Y.-L. Chen, X. Zhang, T.-T. You and F. Xu, *Cellulose*, 2019, **26**, 205–213.
137 N. Gugulothu, M. Mohan, M. R. Marland, J. C. Smith and M. K. Kidder, *J. Chem. Inf. Model.*, 2025, **65**, 5856–5867.
138 M. Mohan, M. D. Smith, O. N. Demerdash, B. A. Simmons, S. Singh, M. K. Kidder and J. C. Smith, *ACS Sustainable Chem. Eng.*, 2023, **11**, 7809–7821.
139 M. Mohan, M. D. Smith, O. Demerdash, M. K. Kidder and J. C. Smith, *J. Chem. Phys.*, 2023, **158**, 214502.
140 H. Ghaedi, M. Ayoub, S. Sufian, A. M. Shariff and B. Lal, *J. Mol. Liq.*, 2017, **241**, 500–510.
141 M. Mohan, M. D. Smith, O. Demerdash, M. K. Kidder and J. C. Smith, *J. Chem. Phys.*, 2023, **158**, 214502.
142 Y. Chen, L. Fu, Z. Liu, F. Dai, Z. Dong, D. Li, H. Liu, D. Zhao and Y. Lou, *J. Mol. Liq.*, 2020, **318**, 114042.
143 H. Qin, X. Hu, J. Wang, H. Cheng, L. Chen and Z. Qi, *Green Energy Environ.*, 2020, **5**, 8–21.
144 A. Hayyan, F. S. Mjalli, I. M. AlNashef, Y. M. Al-Wahaibi, T. Al-Wahaibi and M. A. Hashim, *J. Mol. Liq.*, 2013, **178**, 137–141.
145 A. Hayyan, F. S. Mjalli, I. M. AlNashef, T. Al-Wahaibi, Y. M. Al-Wahaibi and M. A. Hashim, *Thermochim. Acta*, 2012, **541**, 70–75.
146 P. Kashyap, S. Gahlyan, M. Rani, D. P. Tiwari and S. Maken, *J. Mol. Liq.*, 2020, **319**, 114219.
147 M. Gholami, B. Schuur and Y. Roy, *Sep. Purif. Technol.*, 2022, **302**, 122097.
148 A. Bhattarai, M. A. Rub and D. Kumar, *J. Mol. Liq.*, 2022, **350**, 118587.
149 T. Lemaoui, A. Boublia, A. S. Darwish, M. Alam, S. Park, B. H. Jeon, F. Banat, Y. Benguerba and I. M. AlNashef, *ACS Omega*, 2022, **7**, 32194–32207.
150 L. Zhou, X. Meng, W. Li, J. Yu, C. O. Kemefa, S. Y. Dai, A. J. Ragauskas and J. S. Yuan, *Green Chem.*, 2025, **27**, 6260–6271.
151 M. Mohan, K. D. Jetti, M. D. Smith, O. N. Demerdash, M. K. Kidder and J. C. Smith, *J. Chem. Theory Comput.*, 2024, **20**, 3911–3926.
152 G. Gygli, X. Xu and J. Pleiss, *Sci. Rep.*, 2020, **10**, 21395.
153 J. N. Al-Dawsari, A. Bessadok-Jemai, I. Wazeer, S. Mokraoui, M. A. AlMansour and M. K. Hadj-Kali, *J. Mol. Liq.*, 2020, **310**, 113127.

154 M. Mohan, K. D. Jetti, M. D. Smith, O. N. Demerdash, M. K. Kidder and J. C. Smith, *J. Chem. Theory Comput.*, 2024, **20**, 3911–3926.
155 R. Haghbakhsh, M. Taherzadeh, A. R. C. Duarte and S. Raeissi, *J. Mol. Liq.*, 2020, **307**, 112972.
156 M. del Mar Contreras-Gámez, Á. Galán-Martín, N. Seixas, A. M. da Costa Lopes, A. Silvestre and E. Castro, *Bioresour. Technol.*, 2023, **369**, 128396.
157 H. Zhu, X. He, Z. Xu and L. Dai, *Green Chem.*, 2025, **27**, 1278–1299.
158 F. A. Vicente, N. Tkalec and B. Likozar, *Chem. Commun.*, 2024, **61**, 1002–1013.
159 F. Oyoun, A. Toncheva, L. C. Henríquez, R. Grougnet, F. Laoutid, N. Mignet, K. Alhareth and Y. Corvis, *ChemSusChem*, 2023, **16**, e202300669.
160 Y. Guo, J. Zhang, C. Wang, M. Liu, J. You, L. Yin and M. Shi, *Sustainable Chem. Pharm.*, 2024, **39**, 101569.
161 X. Zhou, T. Huang, J. Liu, H. Gao, H. Bian, R. Wang, C. Huang, J. Sha and H. Dai, *Bioresour. Technol.*, 2021, **320**, 124327.
162 Y. Zhi, X. Lu, L. Pang, L. Jiang, H. Tian, X. Chen and B. Xia, *Chem. Eng. J.*, 2025, **519**, 165477.
163 A. Satlewal, R. Agrawal, P. Das, S. Bhagia, Y. Pu, S. K. Puri, S. S. V. Ramakumar and A. J. Ragauskas, *ACS Sustainable Chem. Eng.*, 2019, **7**, 1095–1104.
164 M. G. Morán-Aguilar, M. Calderón-Santoyo, R. P. de Souza Oliveira, M. G. Aguilar-Uscanga and J. M. Domínguez, *Carbohydr. Polym.*, 2022, **298**, 120097.
165 P. Luan, X. Zhao, K. Copenhaver, S. Ozcan and H. Zhu, *Adv. Fiber Mater.*, 2022, **4**, 736–757.
166 D. Smink, A. Juan, B. Schuur and S. R. A. Kersten, *Ind. Eng. Chem. Res.*, 2019, **58**, 16348–16357.
167 W. Zhang, P. Xu, Z. Chen, Q. Liu, G. Li and P. Cui, *Fuel*, 2024, **378**, 132975.
168 J.-j. Li, H. Xiao, X.-d. Tang and M. Zhou, *Energy Fuels*, 2016, **30**, 5411–5418.
169 Q. Liu, T. Yuan, Q.-j. Fu, Y.-y. Bai, F. Peng and C.-l. Yao, *Cellulose*, 2019, **26**, 9447–9462.
170 Z.-K. Wang, S. Hong, J.-l. Wen, C.-Y. Ma, L. Tang, H. Jiang, J.-J. Chen, S. Li, X.-J. Shen and T.-Q. Yuan, *ACS Sustainable Chem. Eng.*, 2020, **8**, 1050–1057.
171 S. Li, Y. Wang, Q. Dong, Z. Yuan, T. Mu, Z. Xue and L. Cao, *Carbohydr. Polym.*, 2024, **346**, 122628.
172 K. H. Kim, T. Dutta, J. Sun, B. Simmons and S. Singh, *Green Chem.*, 2018, **20**, 809–815.
173 C.-W. Zhang, S.-Q. Xia and P.-S. Ma, *Bioresour. Technol.*, 2016, **219**, 1–5.
174 J. Guo, G. Yu and J. Wang, *J. Environ. Chem. Eng.*, 2025, 118256.
175 Z. Zhang, J. Xu, J. Xie, S. Zhu, B. Wang, J. Li and K. Chen, *Carbohydr. Polym.*, 2022, **290**, 119472.
176 Z. Guo, Q. Zhang, T. You, X. Zhang, F. Xu and Y. Wu, *Green Chem.*, 2019, **21**, 3099–3108.
177 C. Kundu, S. P. Samudrala, M. A. Kibria and S. Bhattacharya, *Sci. Rep.*, 2021, **11**, 11183.
178 D. Díez, A. Urueña, R. Piñero, A. Barrio and T. Tamminen, *Processes*, 2020, **8**, 1048.
179 C. E. Okonkwo, S. Z. Hussain, S. Manzoor, B. Naseer, A. E. Taiwo, M. Ayyash, A. H. Al-Marzouqi and A. Kamal-Eldin, *Bioresour. Technol. Rep.*, 2023, **23**, 101577.
180 X. Long, M. Yao, S. Wang, C. Ren, X. Zhao, C. Qin, C. Liang, C. Huang and S. Yao, *ChemSusChem*, 2025, **18**, e202402345.
181 Y. Wang, X. Meng, K. Jeong, S. Li, G. Leem, K. H. Kim, Y. Pu, A. J. Ragauskas and C. G. Yoo, *ACS Sustainable Chem. Eng.*, 2020, **8**, 12542–12553.
182 X. Zhao, G. Lyu, X. Meng, Y. Liu, Z. Wang and C. G. Yoo, *Bioresour. Technol.*, 2024, **407**, 131148.
183 L. Zhang, C. Zhang, Y. Ma, X. Zhao and X. Zhang, *Ind. Crops Prod.*, 2024, **211**, 118257.
184 L.-L. Sun, S.-N. Sun, X.-F. Cao and S.-Q. Yao, *Carbohydr. Polym.*, 2024, **343**, 122420.
185 Y. Ma, Q. Xia, Y. Liu, W. Chen, S. Liu, Q. Wang, Y. Liu, J. Li and H. Yu, *ACS Omega*, 2019, **4**, 8539–8547.
186 B. Shen, S. Hou, Y. Jia, C. Yang, Y. Su, Z. Ling, C. Huang, C. Lai and Q. Yong, *Bioresour. Technol.*, 2021, **341**, 125787.
187 G. van Erven, V. J. P. Boerkamp, J. W. van Groenestijn and R. J. A. Gosselink, *Green Chem.*, 2024, **26**, 7101–7112.
188 M. Mohan, H. Choudhary, A. George, B. A. Simmons, K. Sale and J. M. Gladden, *Green Chem.*, 2021, **23**, 6020–6035.
189 M. Mohan, B. A. Simmons, K. L. Sale and S. Singh, *Sci. Rep.*, 2023, **13**, 271.
190 M. Mohan, K. L. Sale, R. S. Kalb, B. A. Simmons, J. M. Gladden and S. Singh, *ACS Sustainable Chem. Eng.*, 2022, **10**, 11016–11029.
191 T. Xiao, M. Hou, X. Guo, X. Cao, C. Li, Q. Zhang, W. Jia, Y. Sun, Y. Guo and H. Shi, *Renewable Sustainable Energy Rev.*, 2024, **192**, 114243.
192 J. A. Sirviö, M. Mikola, J. Ahola, J. P. Heiskanen, S. Filonenko and A. Ämmälä, *Carbohydr. Polym.*, 2023, **312**, 120815.
193 J. Xie, J. Chen, Z. Cheng, S. Zhu and J. Xu, *Carbohydr. Polym.*, 2021, **269**, 118321.
194 J. Jiang, N. C. Carrillo-Enríquez, H. Oguzlu, X. Han, R. Bi, J. N. Saddler, R.-C. Sun and F. Jiang, *Carbohydr. Polym.*, 2020, **247**, 116727.
195 D. Pradhan, A. K. Jaiswal and S. Jaiswal, *Carbohydr. Polym.*, 2022, **285**, 119258.
196 S. B. Jamaldheen, M. B. Kurade, B. Basak, C. G. Yoo, K. K. Oh, B.-H. Jeon and T. H. Kim, *Bioresour. Technol.*, 2022, **346**, 126591.
197 M. Hu, X. Lv, Y. Wang, L. Ma, Y. Zhang and H. Dai, *Carbohydr. Polym.*, 2024, **343**, 122460.
198 S. Sugiarto, U. A. Weerasinghe, J. K. Muiruri, A. Y. Q. Chai, J. C. C. Yeo, G. Wang, Q. Zhu, X. J. Loh, Z. Li and D. Kai, *Chem. Eng. J.*, 2024, **499**, 156177.
199 J. Cheng, C. Huang, X. Liu, X. Zhou, Y. Zhan, T. Chen, C. Huang, X. Meng, G. Fang and A. J. Ragauskas, *ACS Sustainable Chem. Eng.*, 2023, **11**, 10158–10163.

200 O. M. Terrett and P. Dupree, *Curr. Opin. Biotechnol.*, 2019, **56**, 97–104.
201 S. Pang, X. Wang, J. Pu, C. Liang, S. Yao and C. Qin, *Polymers*, 2024, **16**, 1403.
202 S. F. Ahmed, M. Mofijur, S. N. Chowdhury, M. Nahrin, N. Rafa, A. T. Chowdhury, S. Nuzhat and H. C. Ong, *Fuel*, 2022, **318**, 123618.
203 W. Song, J. Jiang, H. Jiang, C. Liu, Y. Dong, X. Chen and L.-P. Xiao, *Fuel*, 2023, **348**, 128521.
204 C. G. Yoo and A. J. Ragauskas, in *Lignin Utilization Strategies: From Processing to Applications*, American Chemical Society, 2021, vol. 1377, ch. 1, pp. 1–12.
205 X. Kang, A. Kirui, M. C. Dickwella Widanage, F. Mentink-Vigier, D. J. Cosgrove and T. Wang, *Nat. Commun.*, 2019, **10**, 347.
206 J. Ralph, C. Lapierre and W. Boerjan, *Curr. Opin. Biotechnol.*, 2019, **56**, 240–249.
207 P. Li, Z. Zhang, X. Zhang, K. Li, Y. Jin and W. Wu, *RSC Adv.*, 2023, **13**, 3241–3254.
208 X. Yue, J. Lin, O. Mankinen, T. Suopajärvi, M. Mikola, A. Mikkelson, H. Huttunen, L. Chen, J. Ahola, V.-V. Telkki, S. Sun and H. Liimatainen, *Angew. Chem., Int. Ed.*, 2025, **64**, e202505975.
209 D. Raikwar, K. Van Aelst, T. Vangeel, S. Corderi, J. Van Aelst, S. Van den Bosch, K. Servaes, K. Vanbroekhoven, K. Elst and B. F. Sels, *Chem. Eng. J.*, 2023, **461**, 141999.
210 Y. Yu, Z. Wan, J. M. Parks, S. Sokhansanj, O. J. Rojas and J. C. Smith, *Green Chem.*, 2024, **26**, 9142–9155.
211 S. Wang, Y. Li, X. Wen, Z. Fang, X. Zheng, J. Di, H. Li, C. Li and J. Fang, *Ind. Crops Prod.*, 2022, **177**, 114430.
212 C. Liu, M. Lei, Y. Fan, X. Kong, H. Zhang and R. Xiao, *J. Anal. Appl. Pyrolysis*, 2023, **176**, 106262.
213 J. Li, Y.-N. Zha, H.-M. Wang, J.-N. Tian and Q.-X. Hou, *Ind. Crops Prod.*, 2025, **229**, 121004.
214 H. Ramzan, M. Usman, F. Nadeem, M. Shahzaib, M. U. Rahman, R. R. Singhania, F. Jabeen, A. K. Patel, C. Qing, S. Liu, G. Piechota and N. Tahir, *Bioresour. Technol.*, 2023, **386**, 129492.
215 W.-l. Xie, B. Hu, Y. Liu, H. Fu, J. Liu, B. Zhang and Q. Lu, *Proc. Combust. Inst.*, 2023, **39**, 3303–3311.
216 J. Lu, M. Wang, X. Zhang, A. Heyden and F. Wang, *ACS Catal.*, 2016, **6**, 5589–5598.
217 E. S. Morais, A. M. Da Costa Lopes, M. G. Freire, C. S. R. Freire and A. J. D. Silvestre, *ChemSusChem*, 2021, **14**, 686–698.
218 Y. Zhao, U. Shakeel, M. S. U. Rehman, H. Li, X. Xu and J. Xu, *J. Cleaner Prod.*, 2020, **253**, 120076.
219 D. Tarasov, M. Leitch and P. Fatehi, *Biotechnol. Biofuels*, 2018, **11**, 269.
220 Z. Liu, Y. Hou and S. Hu, *Ind. Crops Prod.*, 2024, **212**, 118297.
221 C. He, F. Shen, D. Tian, M. Huang, L. Zhao, Q. Yu and F. Shen, *Int. J. Biol. Macromol.*, 2024, **254**, 127853.
222 G. Song, W. Hu, Q. Liu, Z. Deng, H. Zhang, C. Shi, M. Madadi, C. Sun and F. Sun, *Int. J. Biol. Macromol.*, 2025, **316**, 144709.
223 N. Wang, B. Xu, X. Wang, J. Lang and H. Zhang, *J. Mol. Liq.*, 2022, **366**, 120294.
224 Y. Liu and Y. Ma, *ISA Trans.*, 2021, **117**, 1–15.
225 Y. T. Tan, G. C. Ngoh and A. S. M. Chua, *Bioresour. Technol.*, 2019, **281**, 359–366.
226 A. Procentese, E. Johnson, V. Orr, A. G. Campanile, J. A. Wood, A. Marzocchella and L. Rehmann, *Bioresour. Technol.*, 2015, **192**, 31–36.
227 Z. Guo, Z. Ling, C. Wang, X. Zhang and F. Xu, *Bioresour. Technol.*, 2018, **265**, 334–339.
228 A. P. Abbott, D. Boothby, G. Capper, D. L. Davies and R. K. Rasheed, *J. Am. Chem. Soc.*, 2004, **126**, 9142–9147.
229 A. Prabhune and R. Dey, *J. Mol. Liq.*, 2023, **379**, 121676.
230 A. Isci and M. Kaltschmitt, *Biomass Convers. Biorefin.*, 2022, **12**, 197–226.
231 M. Mohan, T. Banerjee and V. V. Goud, *ACS Omega*, 2018, **3**, 7358–7370.
232 P. Weerachanchai and J.-M. Lee, *Bioresour. Technol.*, 2014, **169**, 336–343.
233 J. Xu, B. Liu, H. Hou and J. Hu, *Bioresour. Technol.*, 2017, **234**, 406–414.
234 J. Cheng, C. Huang, Y. Zhan, S. Han, J. Wang, X. Meng, C. G. Yoo, G. Fang and A. J. Ragauskas, *Chem. Eng. J.*, 2022, **443**, 136395.
235 G. Yan, Y. Zhou, L. Zhao, W. Wang, Y. Yang, X. Zhao, Y. Chen and X. Yao, *Ind. Crops Prod.*, 2022, **183**, 115005.
236 H. Zhang, Z. Yu, T. Gu, L. Xiang, M. Shang, C. Shen and Y. Su, *Chem. Eng. J.*, 2020, **391**, 123580.
237 T. Wang, J. Jiao, Q.-Y. Gai, P. Wang, N. Guo, L.-L. Niu and Y.-J. Fu, *J. Pharm. Biomed. Anal.*, 2017, **145**, 339–345.
238 L.-X. Zhang, H. Yu, H.-B. Yu, Z. Chen and L. Yang, *Chin. Chem. Lett.*, 2014, **25**, 1132–1136.
239 M. Panić, V. Gunjević, G. Cravotto and I. R. Redovniković, *Food Chem.*, 2019, **300**, 125185.
240 M. Gholami, J. M. Tijburg and B. Schuur, *Sep. Purif. Technol.*, 2024, **338**, 126526.
241 P. K. Naik, M. Mohan, T. Banerjee, S. Paul and V. V. Goud, *J. Phys. Chem. B*, 2018, **122**, 4006–4015.
242 Y. Liu, J. Li, R. Fu, L. Zhang, D. Wang and S. Wang, *Ind. Crops Prod.*, 2019, **140**, 111620.
243 K. Le, M. Zuo, X. Song, X. Zeng, X. Tang, Y. Sun, T. Lei and L. Lin, *J. Chem. Technol. Biotechnol.*, 2017, **92**, 2929–2933.
244 P. H. Tran and P. V. Tran, *Fuel*, 2019, **246**, 18–23.
245 M.-Z. Gao, Q. Cui, L.-T. Wang, Y. Meng, L. Yu, Y.-Y. Li and Y.-J. Fu, *Microchem. J.*, 2020, **154**, 104598.
246 G. Grillo, V. Gunjević, K. Radošević, I. R. Redovniković and G. Cravotto, *Antioxidants*, 2020, **9**, 1069.
247 J. Li and H. A. Chase, *Nat. Prod. Rep.*, 2010, **27**, 1493–1510.
248 J. Lang, J. Lu, P. Lan, N. Wang, H. Yang and H. Zhang, *Catalysts*, 2020, **10**, 636.
249 P. T. P. Aryanti, F. A. Nugroho, G. Lugito and K. Khoiruddin, *Sep. Purif. Technol.*, 2025, **367**, 132892.
250 X. Liang, Y. Fu and J. Chang, *Sep. Purif. Technol.*, 2019, **210**, 409–416.

251 X. Liang and Y. Guo, *Bioresour. Technol.*, 2022, **362**, 127805.
252 X. Liang, J. Zhang, Z. Huang and Y. Guo, *Ind. Crops Prod.*, 2023, **194**, 116351.
253 Y. Zhang, Z. Zhang, K. Guo and X. Liang, *Bioresour. Technol.*, 2022, **365**, 128175.
254 M. Gholami, B. Middelkamp, Y. Roy, W. M. de Vos and B. Schuur, *Chem. Eng. Res. Des.*, 2024, **202**, 468–479.
255 J. Li, J. Lu, H. Sang, Y. Zhang, B. Qi, J. Luo, Y. Wan and Y. Zhuang, *ACS Appl. Polym. Mater.*, 2023, **5**, 5641–5649.
256 D. Lu, Z. Yao, L. Jiao, M. Waheed, Z. Sun and L. Zhang, *Adv. Membr.*, 2022, **2**, 100032.
257 J. C. Kasper and W. Friess, *Eur. J. Pharm. Biopharm.*, 2011, **78**, 248–263.
258 K. M. Jeong, M. S. Lee, M. W. Nam, J. Zhao, Y. Jin, D.-K. Lee, S. W. Kwon, J. H. Jeong and J. Lee, *J. Chromatogr., A*, 2015, **1424**, 10–17.
259 A. Satlewal, R. Agrawal, S. Bhagia, J. Sangoro and A. J. Ragauskas, *Biotechnol. Adv.*, 2018, **36**, 2032–2050.
260 O. M. E. Sada, I. S. A. Hiemstra, N. Chorhirankul, M. Eppink, R. H. Wijffels, A. E. M. Janssen and A. Kazbar, *Biotechnol. Rep.*, 2024, **43**, e00849.
261 R. Mahmud, S. M. Moni, K. High and M. Carbajales-Dale, *J. Cleaner Prod.*, 2021, **317**, 128247.
262 H. Rajapakse, R. Raviadaran and D. Chandran, *Results Eng.*, 2025, **26**, 105188.
263 C. L. Yiin, Z. Y. Lai, B. L. F. Chin, S. S. M. Lock, K. W. Cheah, M. J. Taylor, A. Al-Gailani, B. W. Kolosz and Y. H. Chan, *J. Cleaner Prod.*, 2024, **470**, 143248.
264 G. Zang, A. Shah and C. Wan, *Biofuels, Bioprod. Biorefin.*, 2020, **14**, 326–343.
265 L. Tao, X. Chen, A. Aden, E. Kuhn, M. E. Himmel, M. Tucker, M. A. A. Franden, M. Zhang, D. K. Johnson, N. Dowe and R. T. Elander, *Biotechnol. Biofuels*, 2012, **5**, 69.
266 A. K. Kumar, S. Sharma, G. Dixit, E. Shah, A. Patel and G. Boczkaj, *Biofuels, Bioprod. Biorefin.*, 2020, **14**, 746–763.
267 K. R. Kumar, B. Anusha and B. Satyavathi, *Biomass Convers. Biorefin.*, 2024, **14**, 26371–26385.
268 J. Zhao, J. Lee and D. Wang, *Bioresour. Technol.*, 2022, **356**, 127277.
269 D. Humbird, R. Davis, L. Tao, C. Kinchin, D. Hsu, A. Aden, P. Schoen, J. Lukas, B. Olthof, M. Worley, D. Sexton and D. Dudgeon, *Process Design and Economics for Biochemical Conversion of Lignocellulosic Biomass to Ethanol: Dilute-Acid Pretreatment and Enzymatic Hydrolysis of Corn Stover*, 2011.
270 Z.-J. Huang, G.-J. Feng, K.-P. Lin, F.-L. Pu, Y.-M. Tan, W.-C. Tu, Y.-L. Han, X.-D. Hou, H.-M. Zhang and Y. Zhang, *Ind. Crops Prod.*, 2020, **152**, 112515.
271 S. Ma, Shiva, H. Tao, J. Dempsey, X. Chen, J. Yuan, J. Y. Zhu, J. S. Yuan, L. Zhou and B. Yang, *Bioresour. Technol.*, 2025, **427**, 132402.
272 J. Peng, H. Xu, W. Wang, Y. Kong, Z. Su and B. Li, *Ind. Crops Prod.*, 2021, **172**, 114036.
273 C. He, L. Zhang, X. Zhao, J. Xin, C. Li, C. Li and X. Zhang, *Renewable Energy*, 2024, **229**, 120745.
274 A. R. G. da Silva, A. Giuliano, M. Errico, B. G. Rong and D. Barletta, *Clean Technol. Environ. Policy*, 2019, **21**, 637–654.
275 J. N. Ntihuga, T. Senn, P. Gschwind and R. Kohlus, *Energies*, 2013, **6**, 2065–2083.
276 J. B. Guinée, R. Heijungs, G. Huppes, A. Zamagni, P. Masoni, R. Buonamici, T. Ekvall and T. Rydberg, *Environ. Sci. Technol.*, 2011, **45**, 90–96.
277 X. Sun, Q. Yu, H. Yang, X. Wang, Z. Yang, Y. Li and C. Wang, *J. Environ. Chem. Eng.*, 2022, **10**, 108446.
278 Q. Zaib, M. J. Eckelman, Y. Yang and D. Kyung, *Green Chem.*, 2022, **24**, 7924–7930.
279 T. Guo, Y. Yu, Z. Wan, S. Zargar, J. Wu, R. Bi, S. Sokhansanj, Q. Tu and O. J. Rojas, *Renewable Energy*, 2022, **194**, 902–911.
280 W. Song, Y. He, R. Huang, J. Li, Y. Yu and P. Xia, *Appl. Energy*, 2023, **335**, 120758.
281 Y. Wang, H. Gao, J. Xiao, Y. Yu, Y. Yi, J. Wu, A. Manzardo, J. Zhang, Z. Wang and Q. Luo, *Environ. Sci. Technol.*, 2025, **59**, 24368–24379.
282 A. W. Putranto, S. Suhartini, Y. Wibisono, N. Masruchin, A. S. M. Chua and G. C. Ngoh, *Green Chem. Lett. Rev.*, 2025, **18**, 2507283.
283 M. Hayyan, *J. Mol. Liq.*, 2025, **439**, 128928.
284 R. Meyer, D. A. F. Paredes, M. Fuentes, A. Amelio, B. Morero, P. Luis, B. Van der Bruggen and J. Espinosa, *Sep. Purif. Technol.*, 2016, **158**, 238–249.
285 J. Puhar, R. Pučnik, F. A. Vicente, L. Čuček, B. Likozar and A. Vujanović, *Results Eng.*, 2026, 110774.
286 R. S. Payal and S. Balasubramanian, *Phys. Chem. Chem. Phys.*, 2014, **16**, 17458–17465.
287 M. Mohan, C. Balaji, V. V. Goud and T. Banerjee, *J. Solution Chem.*, 2015, **44**, 538–557.
288 K. M. Gupta and J. Jiang, *Chem. Eng. Sci.*, 2015, **121**, 180–189.
289 C. He, X. Li, F. Luo, C. Mi, A. Zhan, R. Ou, J. Fan, J. H. Clark and Q. Yu, *ACS Sustainable Chem. Eng.*, 2024, **12**, 11327–11337.
290 C. He, F. Luo, Y. Zhu, A. Zhan, J. Fan, J. H. Clark, J. Lv and Q. Yu, *Green Chem.*, 2025, **27**, 2019–2034.
291 G. Miao, J. L. Wong, J. J. Chew, D. S. Khaerudini, J. Sunarso and F. Xu, *Int. J. Biol. Macromol.*, 2025, **293**, 138847.
292 X. Pan, Y. Liu, Z. Ma, Y. Qin, X. Lu, X. Feng, Q. Shao and Y. Zhu, *J. Mol. Liq.*, 2024, **406**, 125123.
293 B. Zhu, H. Ge, J. Wei, Y. Xu, S. Wang, B. Li and H. Xu, *Ind. Crops Prod.*, 2024, **222**, 119736.
294 W. Wang, Y. Xu, B. Zhu, H. Ge, S. Wang, B. Li and H. Xu, *Bioresour. Technol.*, 2023, **385**, 129401.
295 S. Chen, F. Li, Z. Ma, H. Guo, J. Yang, M. Qiu and F. Shen, *Bioresour. Technol.*, 2025, **430**, 132571.
296 J. Ma, N. L. Ma, W. Zhang, Y. Wu, Y. Ma, G. Chen, Y. Sun, J. Wang and C. Sun, *Ind. Crops Prod.*, 2025, **230**, 121091.

297 Z. Zhang, P. Lv, H. Ji, X. Ji, Z. Tian and J. Chen, *Green Chem.*, 2024, **26**, 3453–3465.
298 S. Zhou and S. Wu, *ACS Sustainable Chem. Eng.*, 2023, **11**, 2416–2426.
299 Z. Pan, X. Liu, A. Ashori, F. Xu, K. Barta and X. Zhang, *Chem. Eng. J.*, 2024, **496**, 153952.
300 X. Wu, H. Lian, X. Li and J. Xiao, *Int. J. Biol. Macromol.*, 2023, **253**, 126664.
301 H. Ji and P. Lv, *Green Chem.*, 2020, **22**, 1378–1387.
302 Z. Ahmad, W. W. A. Dajani, M. Paleologou and C. C. Xu, *Molecules*, 2020, **25**, 2329.
303 W. Schutyser, T. Renders, G. Van den Bossche, S. Van den Bosch, S.-F. Koelewijn, T. Ennaert and B. F. Sels, in *Nanotechnology in Catalysis*, 2017, pp. 537–584.
304 J. V. Vermaas, L. D. Dellon, L. J. Broadbelt, G. T. Beckham and M. F. Crowley, *ACS Sustainable Chem. Eng.*, 2019, **7**, 3443–3453.
305 M. J. Orella, T. Z. H. Gani, J. V. Vermaas, M. L. Stone, E. M. Anderson, G. T. Beckham, F. R. Brushett and Y. Román-Leshkov, *ACS Sustainable Chem. Eng.*, 2019, **7**, 18313–18322.
306 Y. Wang, J. Kalscheur, E. Ebikade, Q. Li and D. G. Vlachos, *J. Cheminf.*, 2022, **14**, 43.
307 V. Sethuraman, J. V. Vermaas, L. Liang, A. J. Ragauskas, J. C. Smith and L. Petridis, *Biomacromolecules*, 2024, **25**, 767–777.
308 M. Mohan, S. Guggilam, D. Bhowmik, M. K. Kidder and J. C. Smith, *ACS Sustainable Chem. Eng.*, 2025, **13**, 20737–20753.
309 M. Mohan, M. K. Kidder and J. C. Smith, *Green Chem.*, 2025, **27**, 15106–15123.
310 A. Pyka, G. Cardellini, H. van Meijl and P. J. Verkerk, *J. Cleaner Prod.*, 2022, **330**, 129801.
311 V. Odegova, A. Lavrinenko, T. Rakhmanov, G. Sysuev, A. Dmitrenko and V. Vinogradov, *Green Chem.*, 2024, **26**, 3958–3967.
312 D. Shi, F. Zhou, W. Mu, C. Ling, T. Mu, G. Yu and R. Li, *Phys. Chem. Chem. Phys.*, 2022, **24**, 26029–26036.
313 M. Abdollahzadeh, M. Khosravi, B. H. K. Masjidi, A. S. Behbahan, A. Bagherzadeh, A. Shahkar and F. T. Shahdost, *Sci. Rep.*, 2022, **12**, 4954.
314 A. Boublia, T. Lemaoui, F. A. Hatab, A. S. Darwish, F. Banat, Y. Benguerba and I. M. AlNashef, *J. Mol. Liq.*, 2022, **366**, 120225.
315 K. N. Marsh, J. A. Boxall and R. Lichtenthaler, *Fluid Phase Equilib.*, 2004, **219**, 93–98.
316 H. Xu, C. Dong, W. Wang, Y. Liu, B. Li and F. Liu, *Ind. Crops Prod.*, 2023, **196**, 116431.
317 H. Ge, Y. Liu, B. Zhu, Y. Xu, R. Zhou, H. Xu and B. Li, *Ind. Crops Prod.*, 2023, **203**, 117138.
318 Z. Sumer and R. C. Van Lehn, *ACS Sustainable Chem. Eng.*, 2022, **10**, 10144–10156.
319 Z. Zhong, B. M. T. Gorish, Y. Bai, W. I. Y. Abdelmula, W. Dang and D. Zhu, *Green Chem.*, 2025, **27**, 11036–11054.
320 W. Gao, L. Zhou, S. Liu, Y. Guan, H. Gao and B. Hui, *Bioresour. Technol.*, 2022, **348**, 126812.
321 F. Kartal and U. Özveren, *Carbohydr. Polym. Technol. Appl.*, 2021, **2**, 100148.
322 H. Ge, Y. Bai, R. Zhou, Y. Liu, J. Wei, S. Wang, B. Li and H. Xu, *ACS Sustainable Chem. Eng.*, 2024, **12**, 7578–7590.
323 C. Xu, H.-D. Liu, T. Lu, R. Guo, G.-Y. Li and H. Zhang, *Chem. Phys. Lett.*, 2025, **864**, 141934.
324 J. Löfgren, D. Tarasov, T. Koitto, P. Rinke, M. Balakshin and M. Todorović, *ACS Sustainable Chem. Eng.*, 2022, **10**, 9469–9479.
325 A. C. Garcia, C. Shuo and J. S. Cross, *Bioresour. Technol.*, 2022, **345**, 126503.
326 M. Pätzold, S. Siebenhaller, S. Kara, A. Liese, C. Syldatk and D. Holtmann, *Trends Biotechnol.*, 2019, **37**, 943–959.
327 J. Rao, Z. Lv, G. Chen and F. Peng, *Prog. Polym. Sci.*, 2023, **140**, 101675.
328 P. Verdía Barbará, H. Choudhary, P. S. Nakasu, A. Al-Ghatta, Y. Han, C. Hopson, R. I. Aravena, D. K. Mishra, A. Ovejero-Pérez, B. A. Simmons and J. P. Hallett, *Chem. Rev.*, 2025, **125**, 5461–5583.
329 C. He, F. Luo, Y. Zhu, A. Zhan, J. Fan, J. H. Clark, J. Lv and Q. Yu, *Green Chem.*, 2025, **27**, 2019–2034.
330 Y.-h. Ci, F. Yu, C.-x. Zhou, H.-e. Mo, Z.-y. Li, Y.-q. Ma and L.-h. Zang, *Green Chem.*, 2020, **22**, 8713–8720.
331 A. A. Oun and J.-W. Rhim, *Carbohydr. Polym.*, 2016, **150**, 187–200.
332 Z. Wang, J. Zhou, Y. Yin, M. Mu, Y. Liu, D. Zhou, W. Wang, X. Zuo and J. Yang, *Green Chem.*, 2024, **26**, 2300–2312.
333 A. M. Asim, M. Uroos, N. Muhammad and J. P. Hallett, *ACS Sustainable Chem. Eng.*, 2021, **9**, 8080–8089.
334 J. Cheng, C. Huang, Y. Zhan, X. Liu, J. Wang, X. Meng, C. G. Yoo, G. Fang and A. J. Ragauskas, *Green Chem.*, 2023, **25**, 1571–1581.
335 P. J. Piedade, M. M. Nowotarski, G. Dudek and R. M. Lukasik, *New J. Chem.*, 2024, **48**, 16015–16025.
336 E. Gbenga and A. Sam, *Am. J. Mech. Mater. Eng.*, 2019, **3**, 1–10.
337 C. J. Pelegrín, M. Ramos, A. Jiménez and M. C. Garrigós, *Front. Nutr.*, 2022, **9**, 944830.
338 B. N. Jaffur, G. Kumar and P. Khadoo-Jeetah, *Int. J. Biol. Macromol.*, 2024, **269**, 131888.
339 G. Parsai, P. Patel, P. A. Parikh and J. K. Parikh, *Bioresour. Technol. Rep.*, 2024, **26**, 101849.
340 A. Meraj, M. Jawaid, S. P. Singh, M. M. Nasef, H. Ariffin, H. Fouad and B. Abu-Jdayil, *Sci. Rep.*, 2024, **14**, 8672.
341 Z. Zhang, P. Lv, H. Ji, X. Ji, Z. Tian and J. Chen, *Green Chem.*, 2024, **26**, 3453–3465.
342 S. Han, R. Wang, K. Wang, J. Jiang and J. Xu, *Bioresour. Technol.*, 2022, **363**, 127905.
343 S. Magalhães, A. Moreira, R. Almeida, P. F. Cruz, L. Alves, C. Costa, C. Mendes, B. Medronho, A. Romano, M. d. G. Carvalho, J. A. F. Gamelas and M. d. G. Rasteiro, *ACS Omega*, 2022, **7**, 26005–26014.
344 Y. Ohashi and T. Watanabe, *ACS Omega*, 2018, **3**, 16271–16280.

345 L. Das, E. C. Achinivu, C. A. Barcelos, E. Sundstrom, B. Amer, E. E. K. Baidoo, B. A. Simmons, N. Sun and J. M. Gladden, *ACS Sustainable Chem. Eng.*, 2021, **9**, 4422–4432.
346 C. Nitsos, R. Stoklosa, A. Karnaouri, D. Vörös, H. Lange, D. Hodge, C. Crestini, U. Rova and P. Christakopoulos, *ACS Sustainable Chem. Eng.*, 2016, **4**, 5181–5193.
347 A. Requejo, A. Rodríguez, Z. González, F. Vargas and L. Jiménez, *BioResources*, 2012, **7**, 3142–3159.
348 W. Liu, H. Du, K. Liu, H. Liu, H. Xie, C. Si, B. Pang and X. Zhang, *Carbohydr. Polym.*, 2021, **267**, 118220.
349 A. V. Belesov, D. A. Lvova, V. V. Pishchevskaya, I. I. Pikovskoi, A. V. Faleva, N. V. Shkaeva, A. V. Malkov and D. S. Kosyakov, *Biomass Convers. Biorefin.*, 2025, **15**, 20657–20669.
350 N. Jacquet, G. Maniet, C. Vanderghem, F. Delvigne and A. Richel, *Ind. Eng. Chem. Res.*, 2015, **54**, 2593–2598.
351 A. Procentese, F. Raganati, G. Olivieri, M. E. Russo, L. Rehmann and A. Marzocchella, *Bioresour. Technol.*, 2017, **243**, 464–473.
352 Y. Niu, T. Hemashini and C. P. Leh, *Cellulose*, 2026, **33**, 571–605.
353 J. Shi, M. A. Ebrik and C. E. Wyman, *Bioresour. Technol.*, 2011, **102**, 8930–8938.
354 N. R. Baral and A. Shah, *Biofuels, Bioprod. Biorefin.*, 2016, **10**, 70–88.
355 J. Xu, J. J. Cheng, R. R. Sharma-Shivappa and J. C. Burns, *Energy Fuels*, 2010, **24**, 2113–2119.
356 A. Brandt-Talbot, F. J. V. Gschwend, P. S. Fennell, T. M. Lammens, B. Tan, J. Weale and J. P. Hallett, *Green Chem.*, 2017, **19**, 3078–3102.
357 F. J. V. Gschwend, C. L. Chambon, M. Biedka, A. Brandt-Talbot, P. S. Fennell and J. P. Hallett, *Green Chem.*, 2019, **21**, 692–703.
358 M. M. Rahman, H. Choudhary, B. A. Simmons, J. M. Gladden and A. Rodriguez, *Green Chem.*, 2025, **27**, 15338–15373.
359 D. Smink, S. R. A. Kersten and B. Schuur, *Chem. Eng. Res. Des.*, 2020, **164**, 86–101.
360 A.-L. Li, X.-D. Hou, K.-P. Lin, X. Zhang and M.-H. Fu, *J. Biosci. Bioeng.*, 2018, **126**, 346–354.
361 F. Rodríguez-Rebelo, B. Rodríguez-Martínez, P. G. Del-Río, M. N. Collins, G. Garrote and B. Gullón, *Ind. Crops Prod.*, 2024, **216**, 118761.
362 N. Wittner, K. Vasilakou, W. Broos, S. E. Vlaeminck, P. Nimmegeers and I. Cornet, *Ind. Eng. Chem. Res.*, 2023, **62**, 18292–18302.
363 J. Vasco-Correa and A. Shah, *Fermentation*, 2019, **5**, 30.
364 C. Fernandes, E. Melro, S. Magalhães, L. Alves, R. Craveiro, A. Filipe, A. J. M. Valente, G. Martins, F. E. Antunes, A. Romano and B. Medronho, *Int. J. Biol. Macromol.*, 2021, **177**, 294–305.
365 F. Bergua, I. Delso, J. Muñoz-Embid, C. Lafuente and M. Artal, *Food Chem.*, 2021, **336**, 127717.
366 M. Francisco, A. van den Bruinhorst and M. C. Kroon, *Green Chem.*, 2012, **14**, 2153–2157.
367 D. J. G. P. van Osch, L. J. B. M. Kollau, A. van den Bruinhorst, S. Asikainen, M. A. A. Rocha and M. C. Kroon, *Phys. Chem. Chem. Phys.*, 2017, **19**, 2636–2665.
368 Y. Dai, J. van Spronsen, G.-J. Witkamp, R. Verpoorte and Y. H. Choi, *Anal. Chim. Acta*, 2013, **766**, 61–68.
369 A. Paiva, R. Craveiro, I. Aroso, M. Martins, R. L. Reis and A. R. C. Duarte, *ACS Sustainable Chem. Eng.*, 2014, **2**, 1063–1071.
370 T. El Achkar, S. Fourmentin and H. Greige-Gerges, *J. Mol. Liq.*, 2019, **288**, 111028.
371 D. J. G. P. van Osch, C. H. J. T. Dietz, S. E. E. Warrag and M. C. Kroon, *ACS Sustainable Chem. Eng.*, 2020, **8**, 10591–10612.
372 Y. Song, R. P. Chandra, X. Zhang, T. Tan and J. N. Saddler, *Sustainable Energy Fuels*, 2019, **3**, 1329–1337.
373 J. Xie, J. Xu, Z. Cheng, S. Zhu and B. Wang, *Ind. Crops Prod.*, 2021, **172**, 114058.
374 X. Chen, J. Zhu, Y. Tian, Z. Wang, J. Pan, Y. Zhan and W. Song, *Ind. Crops Prod.*, 2025, **229**, 120976.
375 L. Ma, S. Zhang, S. Zhang, P. Li, J. Li, S. Lei, W. Sun and G. Zheng, *Int. J. Hydrogen Energy*, 2025, **106**, 1233–1242.
376 Y. Liu, J. Zheng, J. Xiao, X. He, K. Zhang, S. Yuan, Z. Peng, Z. Chen and X. Lin, *ACS Omega*, 2019, **4**, 19829–19839.
377 G. Wu, Y. Cheng, C. Huang, C. Yong and Y. Fu, *Green Chem.*, 2025, **27**, 1556–1569.
378 J. Guo, G. Yu and J. Wang, *J. Environ. Chem. Eng.*, 2025, **13**, 118256.
379 A. W. Putranto, S. Dutta, C. W. Priananda, H. A. Illias, Q. Syafiqoh, N. Masruchin, Y. Wibisono, S. Suhartini, A. S. M. Chua and G. C. Ngoh, *Biomass Bioenergy*, 2025, **196**, 107672.
380 H. Gao, J. Xiao, Y. Wang, Y. Yu, J. Wu, J. Zhang, Z. Wang, S. Wang and Q. Luo, *Ind. Crops Prod.*, 2025, **226**, 120673.
381 Z. Tang, C. Zhang, J. Yin, B. Fan, Y.-C. He and C. Ma, *Int. J. Biol. Macromol.*, 2025, **301**, 140151.
382 P.-R. Zhou, X.-P. Zheng, Y.-P. Du, Y. Chai, Y.-C. Zhang and Y.-Z. Zheng, *Int. J. Biol. Macromol.*, 2025, **297**, 139922.
383 J. Xu, P. Zhou, X. Liu, L. Yuan, C. Zhang and L. Dai, *ChemSusChem*, 2021, **14**, 2740–2748.
384 Q. Zhang, J. Meng, Q. Tian, L. Zhang, J. Shen, Y. Ni and Z. Wang, *Bioresour. Technol.*, 2025, **430**, 132545.
385 Y. Bai, X.-F. Zhang, J. Ma, M. Yu, L. Shu, X. Gu and J. Yao, *Int. J. Biol. Macromol.*, 2025, **308**, 142657.
386 X.-J. Shen, J.-L. Wen, Q.-Q. Mei, X. Chen, D. Sun, T.-Q. Yuan and R.-C. Sun, *Green Chem.*, 2019, **21**, 275–283.
387 Y. Zheng, P. Xue, R. Guo, J. Gong, G. Qian, C. Chen, D. Min, Y. Tong and M. Lu, *Int. J. Biol. Macromol.*, 2025, **298**, 140070.
388 L.-L. Sun, L.-J. Zhao, S.-Q. Yao, Y. Han, J.-L. Wen, T.-Q. Yuan, S.-N. Sun and X.-F. Cao, *Ind. Crops Prod.*, 2025, **229**, 120982.
389 C. Ji, R. Weng, C. Yu, Y. Fan and J. Ouyang, *Ind. Crops Prod.*, 2025, **227**, 120779.
390 V. Provost, S. Dumarcay, I. Ziegler-Devin, M. Boltoeva, D. Trébouet and M. Villain-Gambier, *Bioresour. Technol.*, 2022, **349**, 126837.
391 R. Ceaser, S. Rosa, D. Montané, M. Constantí and F. Medina, *Bioresour. Technol.*, 2023, **369**, 128470.

392 V. Ippolitov, I. Anugwom, M. Mänttäri and M. Kallioinen-Mänttäri, *Ind. Crops Prod.*, 2025, **226**, 120755.
393 J. Vladić, S. Kovačević, K. Aladić, S. Rebocho, S. Jokić, S. Podunavac-Kuzmanović, A. R. C. Duarte and I. Jerković, *Food Bioprocess Technol.*, 2024, **17**, 1215–1230.
394 K. H. Kim, Y. Mottiar, K. Jeong, P. H. N. Tran, N. T. Tran, J. Zhuang, C. S. Kim, H. Lee, G. Gong, J. K. Ko, S.-M. Lee, S. Y. Kim, J. Y. Shin, H. Jeong, H. K. Song, C. G. Yoo, N.-K. Kim and S. D. Mansfield, *Green Chem.*, 2022, **24**, 9055–9068.